Journal of Petroleum Science and Engineering 208 (2022) 109438

Contents lists available at ScienceDirect

Journal of Petroleum Science and Engineering

journal homepage: www.elsevier.com/locate/petrol

Application of iron oxide nanoparticles in oil recovery – A critical review of the properties, formulation, recent advances and prospects

Faruk Yakasai [a,c], Mohd Zaidi Jaafar [a,b,*], Sulalit Bandyopadhyay [d], Augustine Agi [a,b], Mohd Akhmal Sidek [a,b]

[a] Department of Petroleum Engineering, School of Chemical and Energy Engineering, Faculty of Engineering, Universiti Teknologi Malaysia, 81310, Johor Bahru, Malaysia
[b] Institute for Oil and Gas (IFOG), Universiti Teknologi Malaysia, 81310, Johor Bahru, Malaysia
[c] Department of Chemical and Petroleum Engineering, Faculty of Engineering, Bayero University, Kano, PMB 3011, Nigeria
[d] Department of Chemical Engineering, Faculty of Natural Sciences, Norwegian University of Science and Technology, N-7491, Trondheim, Norway

ARTICLE INFO

Keywords:
Iron oxide nanoparticles
Synthesis
Interfacial tension
Wettability
Oilfield application
Enhanced oil recovery

ABSTRACT

Iron oxide nanoparticles (IONPs) are of particular interest in multiple fields and in enhanced oil recovery (EOR) due to their unique advantages and characteristics. Albeit several laboratory research articles on IONPs in EOR are available, a critical review is still elusive in literature. Herein, critical information on the properties, formulation and application of IONPs in oil recovery is depicted. The basic physical, structural and physicochemical properties of IONPs were introduced. Thereafter, the preparation of iron oxide nanofluids (IONFs) was discussed. Likewise, potential application of IONPs, in petroleum industry was elucidated. Subsequently, effectiveness of IONPs in EOR was compared with other nanoparticles and the efficacy of surface coatings were reviewed. Finally, the main challenges hindering the applications of IONPs in oil field reservoir were identified and solutions proffered. Experimental results from the literature indicate that the effectiveness of IONPs in reservoir applications is directly related to their surface coatings. The coatings are used to enhance stability and transportation, minimise rock adsorption, and target specific oil recovery mechanisms, resulting in incremental oil recovery. Hence, surface treatment is a necessity for reservoir condition applications.

1. Introduction

In the recent years, an unprecedented amount of research, development and application of nanotechnology in biological, environmental, and technological fields has surfaced. This is largely related to the special features in nanoparticles (NPs) and how they can be tailored to fit desired applications. The special features are that their physical, structural, thermal, electrical, and magnetic properties differ from the properties of the bulk material. NPs are defined as submicron moieties with diameters ranging from 1 to 100 nm, made of inorganic or organic materials (Srivastava et al., 2020; Dolai et al., 2021; Faudzi and Hamzah, 2021). However, several examples of particles with diameters >100 nm which have novel properties compared to the bulk materials are also referred to as NPs in the literature (Wu et al., 2008; Jeevanandam et al., 2018; Ngouangna et al., 2020). These attractive characteristics have been widely recognised in medical and biomedical fields, and numerous works on the subject can be found in the literature (Arias et al., 2018; Cotin et al., 2018; Sangaiya and Jayaprakash, 2018). Cross disciplinary research over the past decade has revealed that nanotechnology possesses considerable promise for oilfield applications, especially reservoir applications. Nanomaterials in reservoir applications can simultaneously offer more than one function and have tuneable characteristic to meet operational, environmental, and technical requirements. The ultra-fine particles can easily be transported through reservoir pores to reach target location as they are smaller than the rock pores and only required in low concentrations (Xi et al., 2016).

In several oil reservoirs, more than two thirds of the original oil in place is trapped and cannot be recovered using convectional oil recovery methods. Hence, enhanced oil recovery (EOR) techniques are utilized to improve oil recovery. The emerging application of nanotechnology in EOR has focused on the application of nanomaterials to improve oil production. Till date, several reviews have been published on the

* Corresponding author. Department of Petroleum Engineering, School of Chemical and Energy Engineering, Faculty of Engineering, Universiti Teknologi Malaysia, 81310, Johor Bahru, Malaysia.
E-mail address: mzaidi@utm.my (M.Z. Jaafar).

https://doi.org/10.1016/j.petrol.2021.109438
Received 18 May 2021; Received in revised form 3 August 2021; Accepted 24 August 2021
Available online 2 September 2021

potential of nanomaterials in EOR. However, previous reviews have mostly focused on the general governing mechanism and behaviour of the nanomaterials in reservoir applications (Negin et al., 2016; Kamal et al., 2017; Sun et al., 2017; Agi et al., 2018; Druetta et al., 2018; Eltoum et al., 2020; Foroozesh & Kumar, 2020; Yakasai et al., 2021). Nevertheless, Gbadamosi et al. (2018) presented the application of polymer coated NPs in EOR. They stated that polymeric coatings reduce particle adsorption, improve stability and improve oil recovery mechanisms. Specifically, polymeric coatings can improve injection fluids viscosity and improve sweep efficiency. Sikiru et al. (2020) presented insights into the application of graphene NPs in EOR. Their review analysed the synthesis methods and the role of graphene NPs in oil recovery. Graphene NPs can substantially decrease oil viscosity and alter rock wettability. Alnarabiji and Husein (2020) presented the current state and future prospects of bare silica (SiO_2) nanofluids in EOR. Their review introduced the advantages of SiO_2 NPs and the influence of reservoir parameters such as high temperature, pH, and salinity on oil recovery. SiO_2 NPs have been the most widely used NPs in EOR due to their high stability, easy surface modification routes and environmentally chemical nature. Recently, the focus has been more on magnetic NPs (MNPs) owing to their higher magnetization, higher stability in organic solvent, acid and basic solutions, narrow size distribution and high adsorption ability. Iron oxide NPs (IONPs) are of particular interest in multiple fields due to their unique advantages and characteristics. They are eco-friendly and utilized by living organism ranging from bacteria to plants and mammals. For instance, Magnetotactic bacteria and bees synthesize magnetic iron particles that function as compasses, allowing them to navigate using the Earth's geomagnetic field (Moura and Unterlass, 2020). Iron oxide and other MNPs are steadily gaining traction in EOR due to their peculiar characteristics in the presence of a magnetic field. This is reflected in the number of original research papers on MNPs in EOR (Gomaa et al., 2018a; Kazemzadeh et al., 2018; Rezvani et al., 2018; Izadi et al., 2019; Pereira et al., 2020). Rezvani et al. (2018) stated that the interfacial viscosity measurement showed that IONPs adsorbed more asphaltene molecules, which improved the stability of the emulsion formed. Likewise, Pereira et al. (2020) revealed that IONPs selectively removed asphaltene molecules, improved wettability modification and prevented scale formation, which contributed to flow assurance during nanofluid flooding. Albeit several laboratory research articles on IONPs in EOR are available, a critical review on synthesis and tuning of surface properties to understand their EOR mechanisms is still elusive in literature. Hence, the scope of this review.

Herein, a critical review on the application of IONPs targeting oil recovery mechanisms is presented. It is expected that the present review will provide guidance and contribute towards wider adoption of iron oxide nanofluid (IONF) in material science, chemistry, pharmaceutical, chemical engineering, drilling and well completion. Here, the basic physical, structural and physicochemical properties of IONPs was introduced. Thereafter, the preparation of IONFs was discussed. Likewise, potential application of IONPs in petroleum industry was elucidated. Subsequently, application of IONPs in EOR and comparison of the effectiveness of IONPs against other NPs and the effectiveness of surface coatings was reviewed. Finally, the main challenges hindering the applications of IONPs in oil field reservoir were identified and solutions proffered.

The first part focuses on the characterisation of IONPs. The synthesis methods, dispersion, homogenization and stabilization techniques were explained in the second part. The third part was devoted to the oil recovery application of IONFs. The oil recovery mechanisms of IONFs and the comparison of IONFs with other nanofluid used in EOR were critically discussed in the fourth part. The fifth part summarize the transport and retention of IONP in porous media. The final part elaborates on the challenges and prospects for IONPs field applications.

2. Characteristics iron oxide nanoparticles

Iron oxides are natural compounds which can also be synthesised in the laboratory. Iron oxides consist of cations of iron (II) (Fe^{2+}) and/or iron (III) (Fe^{3+}) and certain oxygen containing anions (Kharisov et al., 2012). Iron oxide is a collective term used to describe iron oxides, hydroxides or oxide-hydroxides. Although they are all made up of various ferrous and ferric compounds and have the basic composition of Fe, O, and/or hydroxide (OH), they differ in valency and crystal structure. Hence, they are differentiated based on the composition of O^{2-} and/or OH^- anions within the crystal structure (Rochelle and Cornell, 2006). Up to sixteen different phases of iron oxide have been recognised (Table 1). Amongst them, magnetite (Fe_3O_4) followed by hematite (α-Fe2O3), and maghemite (γ-Fe2O3) are the most extensively studied for oil and gas applications (Fig. 1).

Magnetite consists of an inverse spinel structure which has 32 oxygen atoms close packed in a face centred cubic (FCC) orientation with iron ions located within 16 of the 32 octahedral holes and 8 of the 64 tetrahedral holes. The inverse spinel crystal structure has eight Fe^{2+} and eight Fe^{3+} ions in the octahedral vacancies, and eight Fe^{3+} ions in the tetrahedral vacancies. Thus, magnetite has an inverse spinel formula of $Fe^{3+}(Fe^{2+}\ Fe^{3+})O_4$ or Fe_3O_4. The desirable characteristics of iron oxide for oil and gas applications are high thermal conductivity and saturation magnetization which is highly influenced by thermal effects (Nikiforov et al., 2013). Magnetization is caused by magnetic dipoles correlated with electron spin and orbital moment, and electron movement from one ion to another allows for high conductivity at temperatures above 120 K. Iron oxide has two unpaired electrons and unlike bulk Fe, which has four unpaired electrons, they are less magnetic. However, in the nanoscale domain, particle size dominates the magnetic behaviour and below a certain critical value, usually ~35 nm, the particles exhibit superparamagnetic behaviour by forming a single magnetic domain (Rahmani et al., 2014). In contrast to permanent magnets, IONPs are paramagnetic. That is, they are only magnetic in the presence of a magnetic field, by aligning themselves parallel to the applied magnetic field. As a result, when the field is withdrawn, they lose their magnetism (Fig. 2).

In a dispersion fluid, thermal agitation and random Brownian motion resulting from their small sizes prevents them from automatically aligning. However, when a magnetic field is present, the pattern of dipole moment alignment towards the magnetic field overcomes thermal agitation, and as the magnetic field strength increases, the NPs gradually align themselves depending on their magnetic properties and saturation magnetization. Generally, the magnetic properties of materials are categorised based on the amount of external energy required to reverse their magnetization (diamagnetic, paramagnetic, ferri and

Table 1
Various forms of iron oxide (Rochelle and Cornell, 2006).

i. Iron oxide		ii. Iron oxide- Hydroxide	
Mineral Name	Formula	Mineral Name	Formula
Wüstite	FeO	Goethite	α-FeOOH
Magnetite	Fe_3O_4	Akageneite	β- FeOOH
Hematite	α-Fe_2O_3	Lepidocrocite	γ- FeOOH
β-Maghemite	β-Fe_2O_3	Feroxyhyte	δ- FeOOH
Maghemite	γ-Fe_2O_3	High pressure FeOOH	FeOOH
ε-Maghemite	ε- Fe_2O_3	ferrihydrite	$Fe_5HO_8.4H_2O$ approx.
High pressure iron oxide	Fe_4O_5	Schwertmannite	$Fe_{16}O_{16}(OH)_y(SO_4)_z.nH_2O$
		Green rust	$Fe_x^{3+}Fe_y^{2+}(OH)_{3x+2y-z}$ $(A^-)_z$; $A^- = Cl^-, 1/2SO_4^{2-}, CO3^{2-}$

iii. Iron Hydroxide			
Mineral Name	**Formula**	**Mineral Name**	**Formula**
Iron (II) hydroxide	$Fe(OH)_2$	Bernalite (iron (III) hydroxide	$Fe(OH)_3$

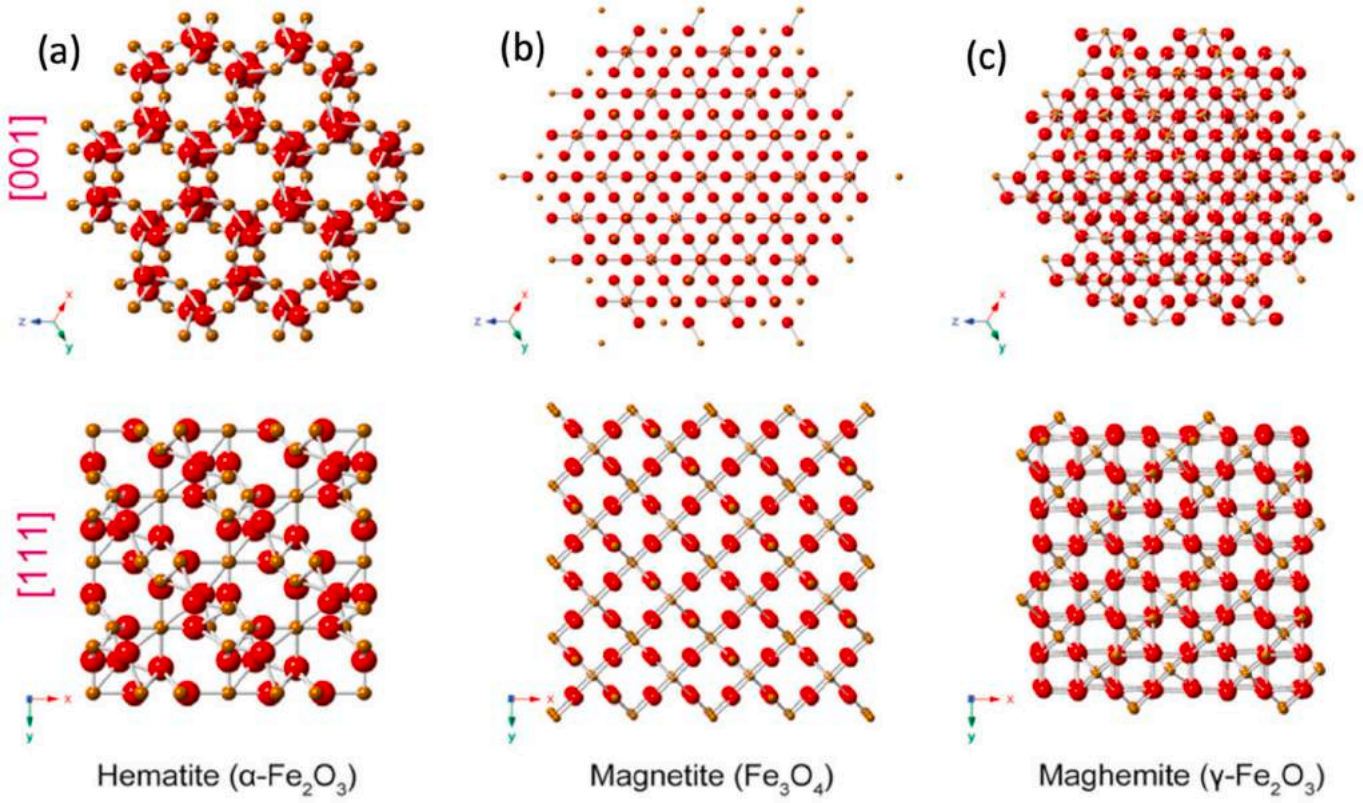

Fig. 1. (a–c) crystal structure of (a) $\alpha - Fe_2O_3$ hematite (b) Fe_3O_4 Magnetite (c) $\gamma - Fe_2O_3$ maghemite from the view of [001] and [111] (2 × 2 × 2) (Wu et al., 2016).

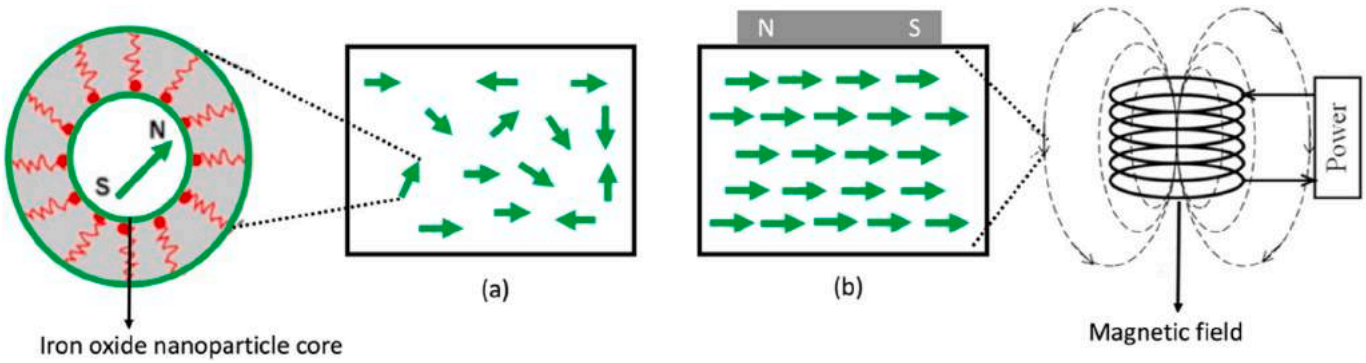

Fig. 2. Illustration of paramagnetic behaviour of IONPs (a) IONPs dispersed in a fluid showing no magnetic behaviour and moving randomly due to Brownian motion (b) IONPs completely aligned in the presence of strong magnetic field (Rahmani et al., 2014).

ferromagnetic materials). More specifically, they are quantified using magnetic susceptibility (χ). This is characterised as the ratio of induced magnetization (M) to the applied magnetic field (H) (Krahne et al., 2011), and best described using hysteresis curves showing total magnetic field (B) against applied magnetic field (H) (Fig. 3).

As illustrated in Fig. 3, H_C is coercive field, illustrating the external field needed to return magnetization to zero. This is linked to the anisotropic energy barrier that must be overcome to invert the direction of the dipoles. M_R is remanent magnetization, illustrating the residual magnetization at zero applied field. As illustrated, ferromagnets have remnant magnetizations (M) whereas paramagnetic and super-paramagnetic materials have no remnant magnetization (M) until a magnetic field is applied. M_s is saturation magnetization which is the maximum magnetization the material can attain with increasing magnetic field. For IONPs, the saturation magnetization increases with decreasing particles sizes because of disordered crystal structure caused by their high surface curvature (Bandyopadhyay, 2016). Equation (1) describes the relationship between saturation magnetization and magnetic field whereas Equation (2) describes the forces generated on the particles by quantifying the magnetic field (Macnae, 2017; Zhou et al., 2020).

$$M = M_0 L\left(\frac{\mu_p H}{k_B T}\right) + \varkappa_a H \tag{1}$$

$$F = \mu_o V M \nabla H \tag{2}$$

whereas $L(x) = coth - 1/x$ is the Langevin function, x is Langevin parameter, M_0 is particle saturation magnetization μ_p is average particle magnetic moment and χ_a is linear component, F is magnetic force, V is particle concentration, M is particle magnetization, ∇H is magnetic field

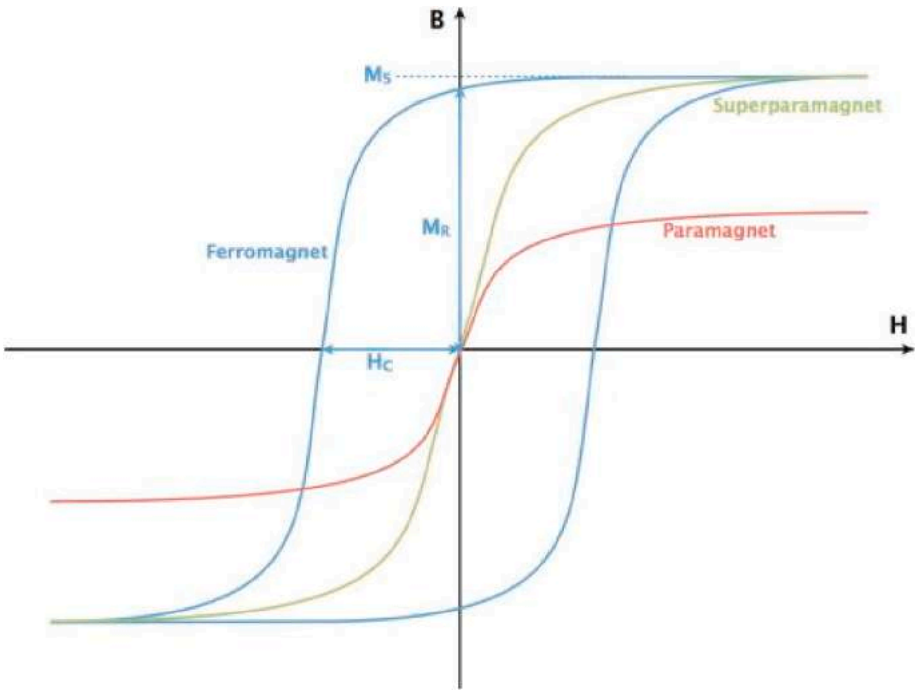

Fig. 3. Hysteresis curves of various magnetic materials showing total magnetic field (B) against applied magnetic field (H), saturation magnetization (M_s), coercivity (H_c) and remnant magnetization (M_R). Ferromagnetic material (blue) superparamagnetic (green) and paramagnetic (red) materials (Giustini et al., 2010). (For interpretation of the references to colour in this figure legend, the reader is referred to the Web version of this article.)

gradient, T is temperature and K_B is Boltzmann constant.

Furthermore, when IONPs are subjected to a particular frequency and amplitude from a magnetic field, they generate extreme localised heat known as "hyperthermia" in medicine (Vallabani and Singh, 2018). The governing mechanism behind this phenomenon has been proposed as (i) Néel relaxation losses, a function of the magnetic moments within the particles between two metastable antiparallel orientations (ii) Frictional losses due to Brownian rotation, known as Brownian friction losses and (iii) Hysteresis losses, due to magnetization irreversibility. As illustrated in Fig. 3, the areas enclosed by the hysteresis loop, identified as M_S, H_C, and M_r, reflect the amount of energy lost to the environment as H moves to and fro (H (M_S) – H (-M_S)). Theoretically, the frequency multiplied by the integral of the B–H curve over the closed loop is equal to the total power lost to heat (Dennis and Ivkov, 2013). Thus, when ferromagnetic NPs are subjected to an interchanging magnetic field, energy is emitted in the form of heat. The wider the ferromagnet's magnetic hysteresis curve, the more heat they can generate. These heating characteristics can be utilized in oil viscosity reduction, flow assurance and conformance control during oil production. Whereas the characteristics required for the creation of an induction field when exposed to a magnetic field can be utilized for detection and manipulation during transportation in oil and gas reservoirs.

3. Preparation of IONFs

The utilization of IONPs for reservoir applications closely depend on their properties such as particle sizes, morphologies and surface coating which regulate their magnetization, surface energy, aggregation rate, dispersibility and mobilization in the porous medium. These parameters are fine-tuned during synthesis. However, due to their colloidal nature, synthesis of superparamagnetic IONPS can sometimes be a complex process. Herein, the key technical challenges are (i) specifying and defining experimental conditions for the desired monodisperse size and shape (ii) selecting an appropriate reproducible method that can be industrialized without any complex purification procedure. The consensus on the synthesis of NPs allows for their synthesis via two approaches: solution-based bottom-up approaches such as chemical synthesis using a metal precursor or top-down approaches such as lithography, thermal or mechanical approaches. Regarding top-down approach, the NPs tend to have a relatively wide size distribution and uncontrollable shape. By contrast, the bottom-up approach allows more precise control and synthesis with high structural purity, diverse shapes, uniform sizes, compositions and surface properties (Wu et al., 2015). Thus, from a fundamental and functional point of view the bottom-up approach offers superior control and flexibility. The general procedures and reaction mechanism governing the synthesis of NPs using bottom-up approach can be described using the classical nucleation and growth theory (Thanh et al., 2014).

3.1. Classical nucleation and growth theory

The foremost stage towards the formation of NPs in a solution is the nucleation process, a phenomena whereby solid particles are created from the precursor solution, this may happen either in the bulk solution (homogeneous nucleation) or on solid substrates such as impurities or seeds (heterogenous nucleation) (Camargo et al., 2015). The driving force behind nucleation is supersaturation ($\Delta\mu$), defined by Equation (3) and thermodynamically described by Equations (4) and (5) (Kashchiev and van Rosmalen, 2003).

$$\Delta\mu = \mu_s\mu_c \tag{3}$$

$$\Delta\mu = kTln(S) \tag{4}$$

$$S = \frac{a_1^{n1}a_2^{n2}\ldots.a_j^{nj}}{a_{1e}^{n1}a_{2e}^{n2}\ldots.a_{ne}^{nj}} \tag{5}$$

whereas μ_s and μ_c are chemical potentials of a molecule in the solution and in the bulk of the crystal phase, respectively, k is Boltzmann's constant, T is temperature in Kelvin and S is supersaturation ratio, n_i is number of the ith ions in a crystal molecule, a_j and a_{je} are, the real and equilibrium behaviours of these ions in the solution, while the denominator is the solubility product.

Nucleation is only possible above a certain supersaturation limit, which is when the concentration of the solute in the chemical solution exceeds the concentration defined by the equilibrium solubility. The solution is considered supersaturated, saturated or undersaturated when $S > 1$, $S = 1$ or $S < 1$ respectively. Upon nucleation, the growth process begins, driven by the decreasing surface free energy until an equilibrium state of the bulk solution is reached (Agi et al., 2021). The nucleation and growth of NPs as a function of time and solute concentration is depicted in LaMer's diagram Fig. 4. As illustrated in Fig. 4, in the chemical approach, NPs are synthesised by dissolving a metal precursor in a solvent, leading to the formation monomers (building blocks) due to chemical reaction. When the monomers concentration reaches the critical super-saturation level ($\Delta\mu$), the nuclei is formed, followed by growth through either monomer attachment, aggregation of the nuclei or a combination of both (Chang and Waclawik, 2014; Zhang et al., 2015). The growth process involves the deposition of atoms, molecules, or particles onto the NPs in the saturated solution and several theories, namely – diffusion theories, surface energy theories and adsorption layer theories have been used to explain the process. According to diffusion theories, matter is continuously deposited as a result of a concentration gradient between the bulk and the surface, while the surface energy theories suggest that the shape is determined by the minimum surface energy. Adsorption layer theories suggest that crystal growth is an interrupted process that occurs layer by layer (Bandyopadhyay, 2016; Agi et al., 2021).

3.2. IONPs synthesis methods

In view of the immense interest on the application of IONPs, there are several synthesis methods. Several studies have identified effective methods to produce controlled, stable, and monodispersed particles. The most popular amongst them are co-precipitation, thermal decomposition, hydrothermal reaction, microemulsions, sol-gel syntheses and sonochemical reactions (Hassanjani-Roshan et al., 2011; Kayani et al., 2014; Ozel et al., 2015; Unni et al., 2017; Cid, 2018). Other methods found in the literature include electrochemical synthesis, laser pyrolysis techniques, microorganism or bacterial synthesis. Fig. 5 illustrates the different pathways of producing IONPS. As illustrated in Fig. 5, the co-precipitation method, solvothermal approaches and microemulsion approaches appear to be the most commonly utilized methods of synthesizing IONPs. Thus, these methods are discussed below.

3.2.1. The Co-precipitation method

The co-precipitation approach is used to synthesize IONPs by mixing an aqueous salt solution, followed by the inclusion of the base in an inert environment at high temperature. In detail, the method consists of stoichiometrically mixing ferrous (Fe^{2+}) and ferric (Fe^{3+}) salts in a 1:2 M ratio to a basic solution (such as water, ethanol and ammonium hydroxide (NH_4OH) as a catalyst) at either room or elevated temperatures under viscous stirring (Sharma et al., 2020). The ferric and ferrous ions ratio, type of salts used (such as chlorides, sulfates, nitrates, perchlorates), reaction temperature, ionic strength of the dispersion, absolute pH value, and reactions parameters (such as basic solution drop speed and stirring speed) regulates the size and shape of the IONPS produced (Campos et al., 2015). Thermodynamics of the reaction (Equation (6)) show that the surface of the particles adsorb OH- in a neutral aqueous solution to create an OH- rich surface and complete precipitation of Fe_3O_4 is usually at a pH of between 8 and 14 in a non-oxidizing oxygen environment (Jolivet et al., 2004). However, in the presence of oxygen, magnetite (Fe_3O_4) which is not very stable and susceptible to oxidation, can be converted into maghemite (γFe_2O_3) (Equation (7)). Therefore, synthesis is usually carried out using nitrogen or argon gas to create an oxygen-free atmosphere.

$$Fe^{2+} + 2Fe^{3+} + 8OH^- \rightarrow Fe_3O_4 + 4H_2O \quad (6)$$

$$Fe_3O_4 + 2H^+ \rightarrow \gamma\ Fe_3O_4 + Fe^{2+} + H_2O \quad (7)$$

The challenges associated with the coprecipitation approach include (1) Controlling reaction parameters which are the deciding variables of the final product. (2) Regulating the pH of the aqueous solution to achieve a high yield of uniform monodispersed NPs. During synthesis and purification, high pH levels need to be corrected. (3) Particles may agglomerate owing to extremely small particle size, resulting in increased specific surface area and high surface energy (Majidi et al., 2016). Shalbafan et al. (2020a) synthesised Fe_3O_4 NPs using co-precipitation method for EOR experiments. The NPs were synthesised with 0.0001 g of $FeCl_3$ and 0.9 g of $FeCl_2$ stirred at 80 ± 0.1 °C for 30 min at speeds of 1800 rpm. The NPs had particle sizes within the range of 5–12 nm. Similarly, Pereira et al. (2020) synthesised Fe_3O_4 NPs using co-precipitation method for EOR experiments. The precursors salts used were $FeCl_3$ and $FeSO_4$. 80% of the particles had an average diameter ranging from 4.3 to 8.3 nm.

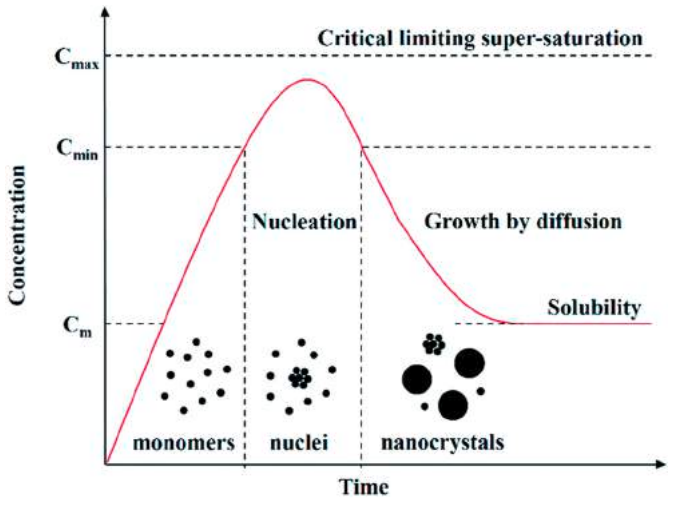

Fig. 4. Schematic illustration of the nucleation and growth process of nanoparticles in solution (Chang and Waclawik, 2014).

3.2.2. Solvothermal approaches

The solvothermal approach is also known as the hydrothermal method. It is one of the most effective and widely used methods for developing crystal growth in a variety of materials. The technique consists of several chemical methods for crystallising materials in a closed container filled with aqueous solution at temperatures ranging from 130 °C to 250 °C and high vapour pressures ranging from 0.3 to 4 MPa (Aval et al., 2016). The process entails combining Fe^{3+} salt precursors with acetates, urea, and sodium citrate in an aqueous solution or organic solvent, then transferring the mixture to an autoclave and heating it at 200 °C for 8–24 h (Hasany et al., 2012; Ali et al., 2015a,b). This method allows the control of particle size by adjusting parameters such as temperature, pressure, and reaction time to achieve particle sizes ranging from 10 to 200 nm. Solvothermal techniques can be utilized to effectively synthesis free single crystal particles, and particles synthesised in this way may have higher crystallinity than particles synthesised via other synthetic approaches (Adewunmi et al., 2021). The challenges associated with this method include (1) slow reaction kinetics at any given temperature, however, microwave heating has been reported to enhance the kinetics of crystallization (Faraji et al., 2010). (2) Difficulty in producing nanocrystals with a diameter of less than 10 nm and outstanding hydrophilic properties. However, when the precursor concentration increases, particle sizes and size distribution tend to grow fast, with only residence time having a significant influence on the mean particle size (Stojanović et al., 2013; Shen et al., 2018; Adewunmi et al., 2021). (3) In contrast to the co-precipitation approach,

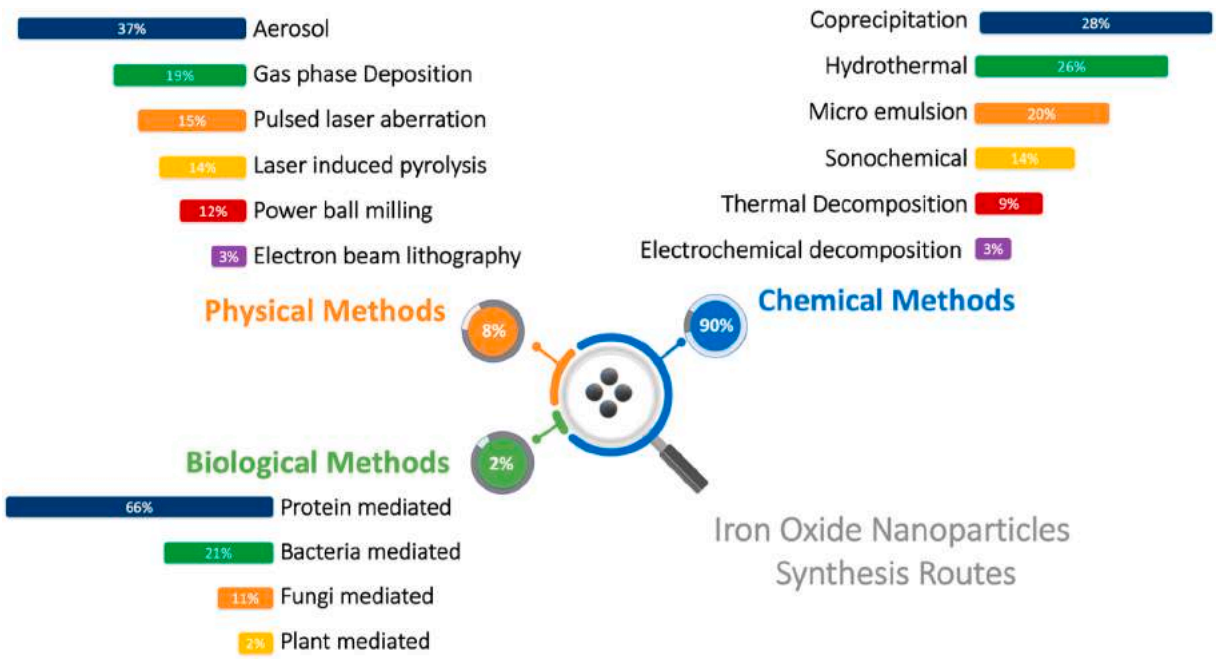

Fig. 5. Comparison of the three main routes of synthesizing IONPs. Sources: Institutes of Scientific Information (Ali et al., 2016a,b; Cotin et al., 2018; Yusoff et al., 2018).

poor yields are obtained (Frimpong and Hilt, 2010; Hernández--Hernández et al., 2020). Alvi et al. (2021) synthesised hydrophobic Fe_3O_2 using thermal decomposition to investigate their effect on drilling fluids. For this purpose, octa-decene (ODE) and oleylamine (OAm) were mixed and agitated at 120 °C for 30 min in an argon atmosphere. The temperature was subsequently raised to 180 °C, and the solution was given an injection of iron pentacarbonyl ($Fe(CO))_5$. The reaction took 20 min to complete, and the average particle size was 14.3 ± 0.60 nm. Similarly, Lü et al. (2018) used a solvothermal method to synthesize Fe_3O_4 for demulsifying oil and water emulsions, 1.62 g of $FeCl_3{\cdot}6H_2O$, 4.32 g of sodium acetate (NaAc) and 0.48 g of trisodium citrate dihydrate were combined with 60 mL ethylene glycol and agitated at room temperature for this experiment. The resultant solution was then placed in an autoclave and heated to 200 °C for 12 h for the solvothermal process. The average particle size was around 315 nm.

3.2.3. *Microemulsion approaches*

The microemulsion method, as the name implies, consists of the dispersion of two immiscible liquids (water and oil) in the presence of appropriate surfactants. Basically, the synthesis solutions consist of the polar phase (aqueous/water), nonpolar phase (oil), and surfactant. Both direct (oil dispersed in water, O/W) and reverse microemulsions (water dispersed in oil, W/O) have been utilized for the synthesis of IONPs. In this method, metal ions and other precursors are dissolved in the aqueous phase, different hydrocarbons and olefins are also dissolved in the oil phase, whilst surfactants are used to create microemulsions by forming a monolayer at the oil-water interface, with the hydrophilic head groups attracted to the aqueous phase and hydrophobic tails attracted to the oil phase. Thereon, the particles condense into nanodrops, which function as nanoreactors and the surfactants serve as particle size filters (Hernández-Hernández et al., 2020). When two identical water-in-oil microemulsions containing the specified reactants are mixed together, the microdroplets collide, consolidate, and break again, eventually forming a precipitate in the micelles. Thus, the nanodroplets of water containing chemicals undergo fast coalescence, allowing for mixing, a precipitation reaction, and an aggregation process to synthesis IONPs (Majidi et al., 2016). Particle sizes can be controlled using this method, by adjusting drop size, initial reagent concentration, and type of surfactant (Foroughi et al., 2016). The profound advantage of this method is the ease with which particle sizes and shapes can be controlled. However, yields are poor when compared to the coprecipitation method, and purification of the nanoparticles is complex due to the nature of the surfactants (Najafi and Nematipour, 2017). For EOR studies, Nguyen et al. (2016) synthesised Fe_3O_4 NPs using a mix of co-precipitation and microemulsion methods. For this, $FeCl_3$ (0.5 M, 100 ml) and $FeCl_2$ (0.5 M, 50 ml) were combined with 500 ml of water and agitated in a nitrogen atmosphere. Meanwhile, sodium dodecyl sulfate (SDS) (1 g) was dissolved in 50 mL deoxygenated distilled water, mixed with Fe^{3+} and Fe^{2+}, and heated at 80 °C for 1 h. After that, 45 mL of NH_4OH (30%) was added drop by drop. The average diameter of the NPs was 14 nm. Similarly, Hu et al. (2017) synthesised Fe_3O_4 using microemulsions comprising of 4 wt% n-hexane, 4 wt% propyl alcohol, 4 wt% SDS, and 1 wt% Span 80 as a co-surfactant. Fe^{3+} 2-ethylhexanoate was dissolved in the oil phase and utilized to make 20 mL microemulsions using optimal salinity and a known value of sodium hydroxide was dissolved in brine of comparable salinity. Sodium hydroxide (NaOH) solution was added dropwise to the solution as a precursor. The particle sizes were between 20 and 40 nm.

3.2.4. *Sol-gel synthesis method*

The Sol-gel synthesis method is a notable method of preparing NPs that has been extended to the fabrication and coating of IONPs by utilizing metallo-organic precursors (Shaker et al., 2013). This technique entails the hydrolysis and condensation of metal alkoxides or alkoxide precursors, to produce oxide particles dispersed in “sol” which is dried or gelled by eliminating solvent or chemical reaction (Yamashita et al., 2019). Herein, metal alkoxides are hydrolysed by either an acid or a base in a solvent which is usually water. The hydrolysis phase substitutes the alkoxide group with a hydroxide group derived from water and a three-dimensional metal oxide network is formed by the condensation and inorganic polymerization of the solvent. The final crystalline state of the NPs is obtained after heat treatments (Laurent et al., 2008). The variables which impact particles size and shape are reaction rates, temperature, type of precursor as well as pH. These parameters primarily influence the kinetics of hydrolysis and condensation reactions (Majidi et al., 2016). The sol-gel method of synthesizing IONPs offers the

advantage of high purity owning to pure amorphous phases, homogeneity and particle size control. The drawback of this technique is that it creates three-dimensional oxide networks, which limits its efficiency. There is also pollution from reaction by-products and product post-treatment is required (Majidi et al., 2016; Adewunmi et al., 2021). Shaker et al. (2013) synthesised Fe_3O_4 NPs for water treatment. For this, ferric nitrate and ethylene glycol were dissolved in appropriate ratios and agitated for 2 h at 400 °C. The produced sol was then heated to 800 °C to produce a gel. The gel was then aged at room temperature for roughly 1 h before being annealed in a furnace at 200, 300, and 4000 °C. The NPs had particle sizes of 28.9 nm, 88.7 nm and 67.6 nm for annealed temperatures of 200, 300, and 4000 °C, respectively. To explore EOR processes, Kazemzadeh et al. (2019) synthesised Fe_3O_4@SiO_2 nanocomposites using a sol-gel synthesis method. For this purpose, 1 g Fe_3O_4 was mixed with 100 ml distilled (DI) water and 500 ml ethanol (in a combination of 100 ml DI water and 500 ml ethanol). After that, 12 mL of ammonia solution and 54.1 g of tetraethyl ortho-silicate were added to the mixture and agitated for 5 h. The nanocomposites were around 30 nm in size. Detailed description and comparison of various alternative techniques for synthetizing IONPs can be found in literature (Hasany et al., 2012; Alsaba et al., 2020; Adewunmi et al., 2021). However, studies comparing the different synthesis methods suggest that the co-precipitation method may be the optimum method for reservoir applications owing to its simplicity, minimal energy requirement, and ease of large-scale reproducibility(Ali et al., 2016a,b; Cotin et al., 2018; Yusoff et al., 2018).

3.3. Dispersion and stability of IONPs

Effective application of nanofluids (suspension of NPs in a base fluid) intended for EOR applications need to be stable over the period of reservoir travel time which could take up to up to 3 years. For stable nanofluids, the NPs should not form large aggregates leading to sedimentation and separation from the base fluid. Agglomeration negates the beneficial size properties, while as sedimentation contributes to clogging and potential damage to the reservoir. With regard to IONPs, their intrinsic instability over a period of time is manifested either when the particles agglomerate to minimise surface energy or oxidize in air due to their high chemical activity (Wu et al., 2015a,b). Nanofluid stability depends on the balance of interparticle activity due to Brownian motion resulting from intermolecular and surface forces such as van der Waals forces, and repulsive electrostatic double layer (EDL). Attractive van der Waals forces, resulting from interactions induced by instantaneous or permanent dipoles within the interatomic bonds of the NPs destabilize dispersion stability. Whereas a cloud of counter ions around the particles (EDL) resulting from the ionization/dissociation of surface groups and/or the adsorption of charged molecules counteract the attractive van der Waals forces to balance the net charge of the dispersion. The surrounding cloud is composed of the stern and diffuse layer, the former comprises of counterions adsorbed onto the particles charged surface, while the latter is an atmosphere of oppositely charged ions. Thus, particle surface charge is usually characterized using zeta potential (ZP), which is the electrostatic potential of the particles measured at the distance from the surface where ions are not bound to the particle (Moore et al., 2015). The surface of the IONPs particles is surrounded with iron atoms which behave like Lewis acids and coordinate with other molecules to donate single pair electrons. When IONPs are dispersed in an aqueous solution, water is dissociated from the surface and it becomes hydroxyl functionalized. These hydroxyl groups are amphoteric and therefore may react with either acids or bases (Soares et al., 2015; Li et al., 2020). Accordingly, the surface charge of the particle depends on the pH of the suspension. Hence, the surface charge maybe either negative or positive depending on the pH of the medium. At pH values away from the isoelectric point (IEP), the magnitude of the surface charges increases whereas at pH values close to the IEP the surface charge approaches zero, favouring attractive van dan Waals forces and promoting aggregation. The IEP for magnetite has been reported to be around pH 6.8. Fig. 6 shows the variation of surface charge from various studies found in the literature. The Derjaguin–Landau–Verwey–Overbeek (DLVO) theory is a classical theoretical approach which uses the superposition of attractive van der Waals and repulsive forces induced by the EDL to predict nanofluid stability. It implies that the net interaction energy between two particles is a function of their distance from each other and increasing the net surface charge increases the stability of nanofluids. Agglomeration is therefore a function of distance between the particles. Fig. 7 illustrates the schematic concept of DLVO theory. The sum of van der Waals attraction (V_A) and electrostatic repulsion (V_R) equals to the net interaction energy between two particles (V_T). The area beneath the curve is the energy barrier particles need to overcome in order not to agglomerate. The higher the energy barrier, the more resistant the particles are to agglomeration. Fig. 7A shows high energy barrier resulting to substantial distance between the particles to overcome agglomeration. Fig. 7 (B) shows low energy barrier resulting from compressed EDL, the particle moving towards each other favoring agglomeration (Aurand, 2017). The EDL is also influenced by the ionic strength of the suspension. High ion concentrations or ions with higher valence numbers, such as divalent and trivalent ions, shorten the distance between particles by compressing the EDL resulting in a lower threshold for agglomeration. Furthermore, application of magnetic field speeds up aggregation (Medvedeva et al., 2012; Lim et al., 2014; Bakhteeva et al., 2016). IONPS used for reservoir applications are therefore usually modified using polymers, surfactants or other organic materials to improve dispersion stability.

3.4. Homogenization and stabilization techniques

Homogenization and stabilization techniques for proper dispersion of IONPS can be classified as mechanical and chemical stabilization techniques. In mechanical stabilization, such as ultrasonic vibration, particle aggregation is broken down prior to use. Whereas in chemical stabilization, stabilizers are added into the solution or onto the surface of the NPs to prevent aggregation by counteracting van der Waals attractive force. Chemical stabilization techniques have been broadly classified as electrostatic, steric and electro steric stabilization. Electrostatic stabilization utilizes electric repulsive forces to counteract van der Waals forces, steric stabilization utilizes a physical barrier to prevent particle cluster and electro steric stabilization utilizes both electrostatic forces and a physical barrier (Chakraborty and Panigrahi, 2020). Fig. 8 illustrates the different routes towards homogenization and stabilization of nanofluids. Particle aggregation leading in unstable nanofluids can be investigated using (a) sedimentation analysis, (b) ZP measurements, (c) spectral absorbance and transmittance measurements, (d) transmission electron microscopy, and (e) dynamic light scattering (Chakraborty and Panigrahi, 2020). Amongst these techniques, ZP is the most common metric gauge used to predict nanofluid stability resulting from electrostatic and van der Waals forces (±10 mV = highly unstable, ± 10 - 20 mV = relatively stable, ± 20–30 mV = moderately stable, ± 30 mV = highly stable. However, in the presence of steric stabilizers, ZP measurements may not accurately dissipate nanofluid stability due to steric interactions. Table 2 shows a summary of different IONPs zeta potential measurements utilizing different modifiers.

3.5. Functionalization of IONPs

Similar to chemical stabilization techniques, functionalization is the adsorption, anchoring or conjugation of chemical molecules onto the surface of NPs in order to boost their properties or achieve a specific target with high precision. Four major types of IONP based functionalization morphologies have been identified from the literature. These are (i) core–shell structure (ii) matrix dispersed structure (iii) Janus-type hetero-structures and (iv) shell–core–shell structure (Wu et al., 2015a,

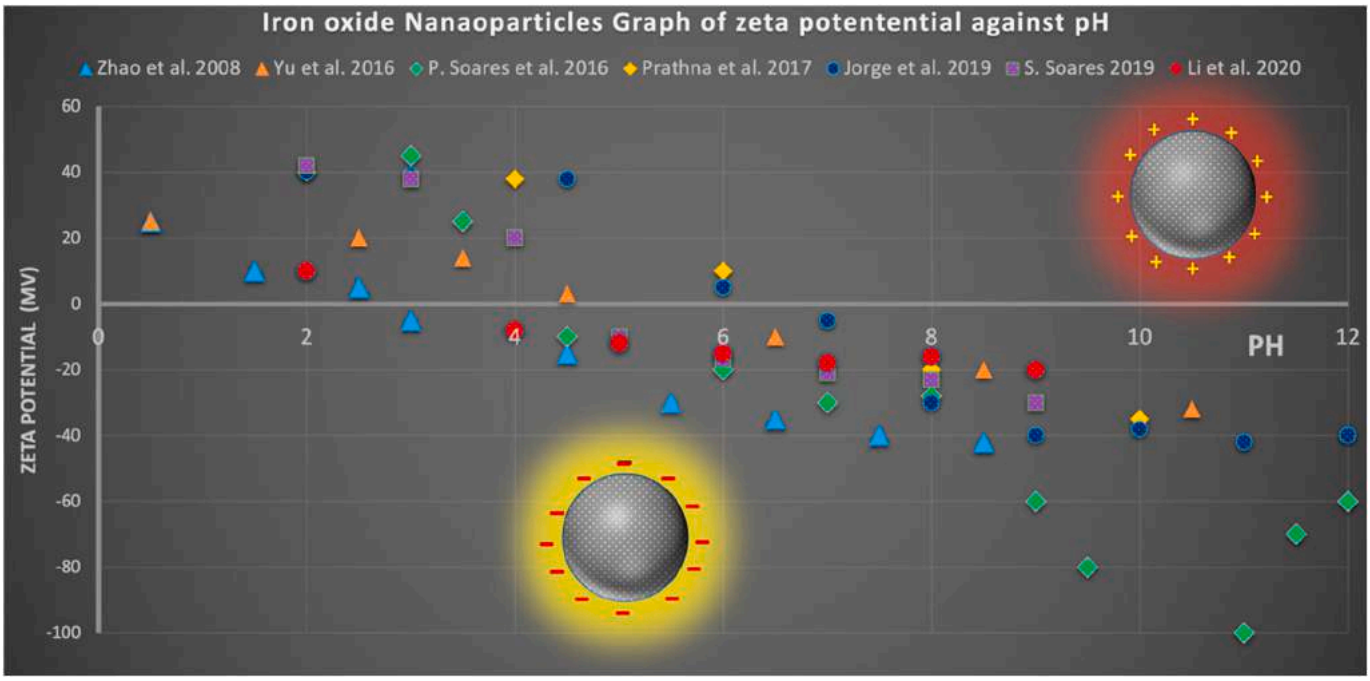

Fig. 6. The influence of pH on surface charge of IONPs from selected publications (Zhao et al., 2008; Yu et al., 2016; Soares et al., 2016, 2019bib_Soares_et_al_2016; Prathna et al., 2017bib_Soares_et_al_2019; Jorge et al., 2019; Keran Li et al., 2020).

b). With regard to reservoir applications, functionalization has enabled the tailoring of the IONPs to improve reservoir transportation and oil recovery mechanism such as asphaltene adsorption to prevent asphaltene precipitation, rock adsorption to improve wettability alteration, adsorption at the oil-water interface to improve IFT reduction, emulsion stability or demulsification. Other functions of functionalized IONPs include encapsulation for oil taggers and tracers (Huh et al., 2014). Recent and detailed IONPs functionalization techniques using different coatings can be found in the literature (Hernández-Hernández et al., 2020).

4. Applications of IONPs in oil reservoirs

Given the aforementioned properties and advantages of IONPs, they have been investigated in several oil industry applications such as drilling and completion, flow assurance and conformance control, reservoir visualization, oil/water/polymer/salts separation, and enhanced oil recovery. The most attractive characteristics of IONPs for oilfield applications are their magnetic properties, even though other NPs such as copper and nickel, among others, have similar magnetic properties, majority of the literature points towards IONPs as the most promising, owing to low production costs, minimal toxicity, convenient synthesis/modification routes and ease of magnetic separation (Kudr et al., 2017; Simonsen et al., 2018; Ali et al., 2020a,b,c; Punia et al., 2020; Adewunmi et al., 2021).

4.1. Reservoir sensing and imaging

Experimental, theoretical and conceptual models have explored the practicality of using IONPs for reservoir sensing and imaging by adapting magnetic imaging technology similar to cross-well and borehole-to-surface imaging, but at higher frequencies, utilizing magnetic permeability. Information acquisition and fluid characterization of oil reservoirs are highly demanded in oil exploration and production. They provide information about the type of fluids, quantity and porosity of reservoir rocks. Which are all essential for decision making in all facets of reservoir engineering processes, staring from well-placement and drilling to enhanced oil recovery applications. Reservoir characterization and injection fluids monitoring are two of the most common uses of reservoir sensing and imaging.

4.1.1. Reservoir characterization

In terms of reservoir heterogeneity and/or fluid characterization, electromagnetic (EM) based mapping and more recently, nuclear magnetic resonance (NMR) spectroscopy has gained a lot of interest (Mitchell et al., 2013; Kenouche et al., 2014; Rahmani et al., 2015; An et al., 2017; Jagadeesh Babu et al., 2018). EM based mapping utilize IONPs for imaging by producing ultrasonic or acoustic signals with magnetic movement (Hassani et al., 2020). EM waves are used to create interfacial variations and sound waves when the particles are adsorbed at oil-water interface. This approach is also known as magneto-acoustic tomography (Jagadeesh Babu et al., 2018). In NMR spectroscopy, IONPS are used as contrast agents to enhance logging speed of the NMR tools and discriminate oil/brine/gas signals received from the well logged with NMR during the reservoir exploration (Park et al., 2014). This is analogous to biomedical applications where they are used to distinguish signals difference between tissue/bone and tissue/vessel, among others. Numerical simulation and experimental work by Chi et al. (2016a) showed how reservoir porosity assessment could be improved using IONPs and NMR spectroscopy. Ali et al. (2018) documented application of polyethylene glycol and oleylamine functionalization IONPs as contrast agents for water and oil phases, respectively. The results showed great contrasting ability in oil reservoirs and improved NMR logging speed resulting from the enhancement of NMR T_2-relaxation time at optimum concentration due to excellent reflexivity properties. Likewise, Zhang and Daigle (2017) demonstrated how hydrophobic IONPS could act as contrast agents to separate various reservoir fluids through NMR relaxation measurements, the results showed that the NPs were able to reduce the T_2-relaxation time of oil from 2000 ms to 20 ms. Although the application of IONPs necessitates the use of surface coatings to preserve dispersion stability and increase NMR response perception by speeding up the relaxation rates of IONPs proton spins (Cheng et al., 2014). The extent of these coatings can be critical, as they may mask and hinder the magnetic characterises of the NPs which in turn affect the NMR measurements (Chi et al., 2016b). Zhu et al. (2018) reported that increasing amounts of (APTES) decreased the surface

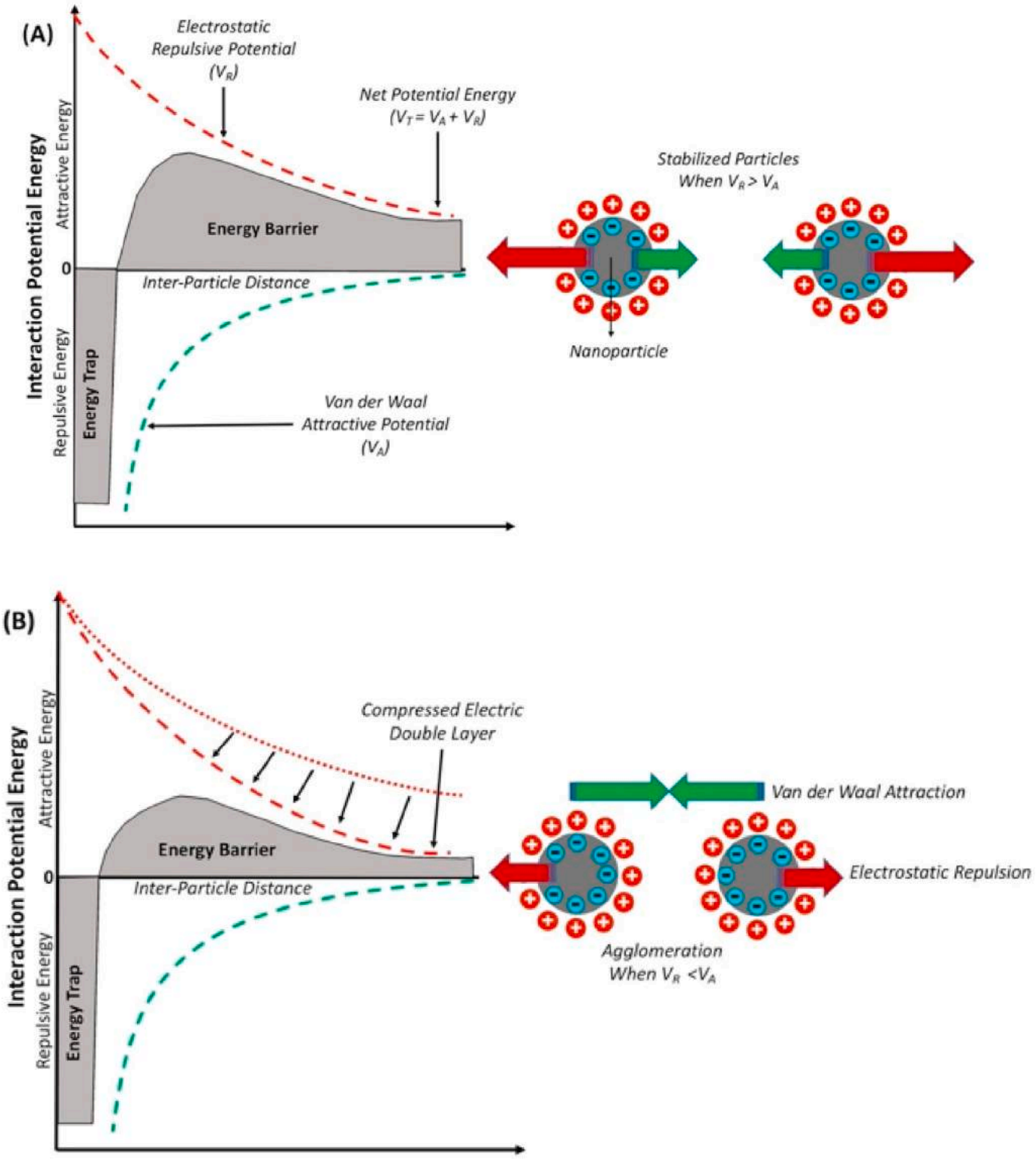

Fig. 7. Schematic concept of DLVO theory (A) High energy barrier (B) Low energy barrier (Aurand, 2017; Chakraborty and Panigrahi, 2020).

relaxivity of IONPS. According to their experiments, increasing APTES coating from 1.6 to 4.2% decreased the surface relaxivity by 26.1%. Therefore, minimum coating should be utilized for NMR application.

4.1.2. *Nanofluid flooding monitoring*

Monitoring fluid is essential for identifying bypassed oil, avoiding water fingering and proactively identifying early water breakthrough. The addition of IONPs into injection fluids during waterflood and EOR processes can allow the monitoring of fluid motion (Rahmani et al., 2013a; 2013b). Hence, existing cross-well EM induction tomography techniques are utilized to image the nanofluids and several researchers have proposed different techniques utilizing this technology. Al-Shehri et al. (2013) proposed an approach which employs EM wave travel-time tomography coupled with IONPs to enable real-time monitoring of

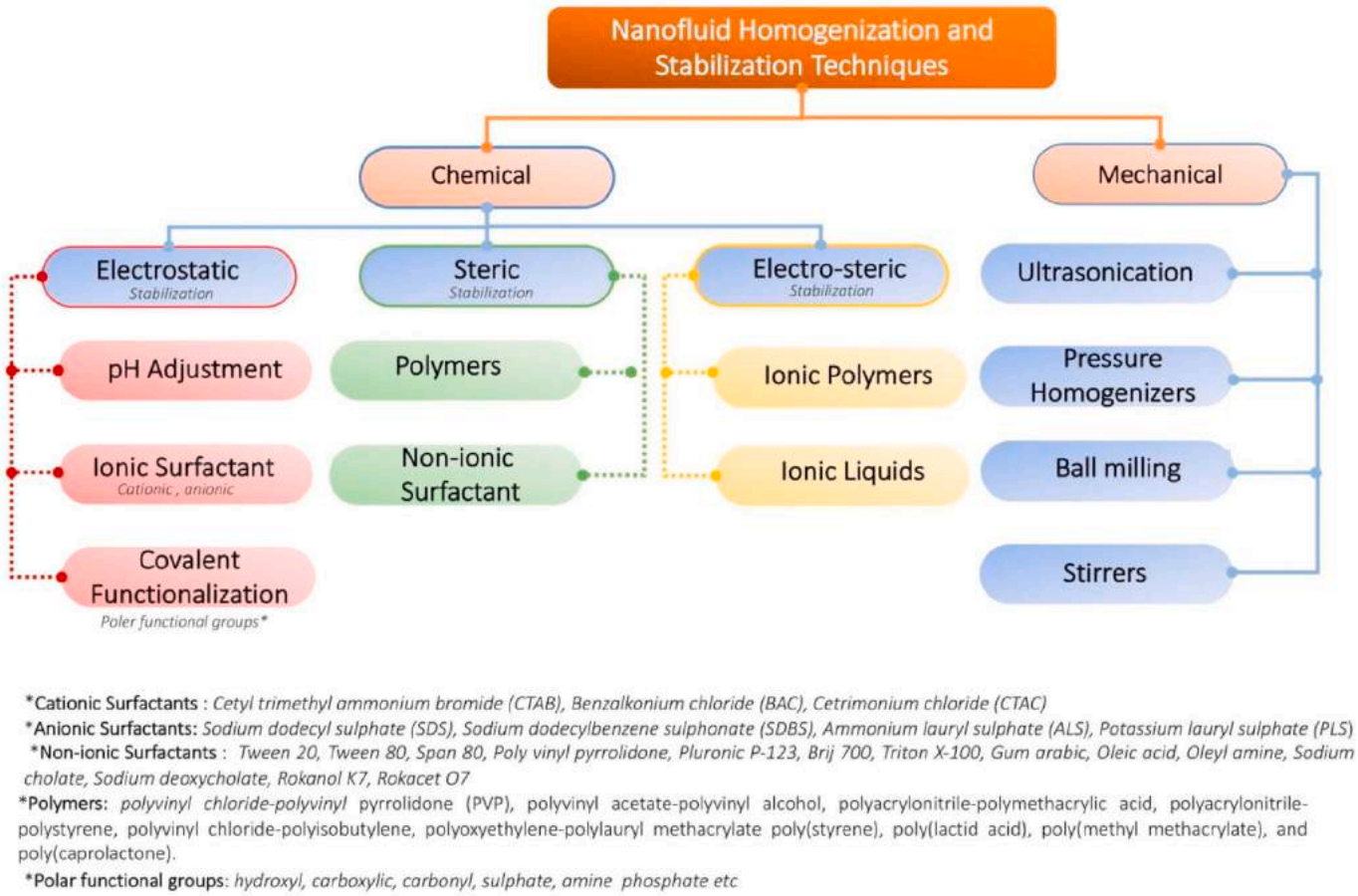

Fig. 8. Illustration of different stabilization and homogenization techniques used to stabilize NPs in a dispersion (Chakraborty and Panigrahi, 2020).

nanofluid flooding. Servin et al. (2016) proposed an approach called magnetic nanomappers (MNMs) which focuses on forward modelling and travel-time tomographic inversion software by utilizing EM waves at high frequencies. In another study the same authors Servin (2018) documented a novel approach using proximity sensing coupled with IONPS as contrast agents. The technique utilizes the presence of resistive layers between reservoirs, which act as a transmission line for EM signals, to achieve increased propagation range. For a more detailed overview of proposed techniques in reservoir sensing and imaging, the reader is directed to (Zhou et al., 2020).

4.2. Drilling and well completion improvement

In oil and gas reservoirs, drilling fluids regulate the wellbore pressure, take cuttings to the surface and seal potential fractures. However, poorly designed drilling fluids may not hold particles in suspension, allowing cuttings to build in the wellbore and result in solid-induced drill string stuck (mud cake). Differential sticking issues can also be caused by these thick mud cakes. Likewise, poorly designed drilling fluids may lead to fluid loss into the formation which increases the near wellbore pressure resulting in wellbore damage (He et al., 2016; Oseh et al., 2020a, 2020c, 2020dbib_Oseh_et_al_2020abib_Oseh_et_al_2020cbib_Oseh_et_al_2020d) Therefore, the proper design of drilling fluid is a critical element for the success of drilling and well completion. IONPs as well as other NPs are used as additives to form filter cakes that prevent the development of filtrate invasion, preserve stability under harsh reservoir conditions, improve rheological properties of drilling fluids, improve cutting lifting capacity and spacer fluids cleaning for well cementing (Al-Yasiri, 2015; Vryzas et al., 2016; Oseh et al., 2019, 2020b, 2020ebib_Oseh_et_al_2019bib_Oseh_et_al_2020b). Although several NPs can be used as additives to form filter cakes, studies have shown that filter cake formation under reservoir conditions is influenced by the type of NPs, and IONPs have been found to have superior qualities compared to SiO_2 and zinc oxide (ZnO) in this regard (Mahmoud & Nasr-El-Din, 2020). Recent studies comparing the effectiveness of IONPs to that of SiO_2 in enhancing the properties of calcium bentonite drilling fluid, showed that IONPs improved filter cake characteristics by reducing the filtrate-fluid volume, whereas SiO_2 increased the filtrate volume. According to the experiments carried out, 0.5 wt% of IONPs, SiO_2, and ZnO resulted in a disk porosity decrease of 4.7, 13.7, and 30%, respectively. In other words, IONPs had the least volume of invaded filtrate. In addition, fluids with SiO_2 additives also showed less performance at high-temperature high-pressure (HTHP) compared to IONPS which improved performance at HTHP (Mahmoud et al. 2018, 2020bib_Mahmoud_et_al_2018). Other studies have also demonstrated the high performance of IONPs at HTHP. Barry et al. (2015) evaluated the influence of IONPs clay hybrid additions into bentonite drilling fluids at both low-temperature, low-pressure (LTLP: 25 °C, 6.9 bar) and high-temperature high-pressure (HTHP: 200 °C, 70 bar) conditions. According to their findings, at very low concentrations of 0.5 wt%, IONPs reduced fluid loss by 37% and 47% in both LTLP and HTHP conditions, respectively. This was due to the formation of cross-linked and coagulated platelet networks which were even more robust at HTHP conditions. It is believed that, the superior characteristics of IONPs in the formation of filter cake at high temperature which resulted to increased filtration control is the intercalation of clay platelets, displacing complexed ions (calcium and/or sodium) (Boul and Ajayan, 2020). A key permeameter in the formation of filter cake using IONPs is particle concentration, according to computerized tomography (CT) scan analysis and scanning electron microscopy (SEM) images

Table 2
Summary of ZP measurements of IONPs and modifiers used to stabilize IONPs.

NP/Modifier	Dispersants	ZP	pH	Author
i. Fe_3O_4 ii. Fe_3O_4 @ citric acid	DI water	i. −31.3 mV ii. −45.3 mV	pH = 7	Dheyab et al. (2020)
i. Fe_3O_4 ii. Fe_3O_4 @ armoured latexes	DI water	i. −20 mV ii. −33 mV	pH = 7.08	Li et al. (2020)
i. Fe_3O_4 @ PEG polyethylene glycol ii. Fe_3O_4 @ SDS iii. Fe_3O_4 @ cetyltrimethylammonium bromide iv. Hallowed Fe_3O_4 @ SDS	DI water	i. −6.3 mV ii. −25.5 mV iii. +26.7 mV iv. −35.1 mV	pH = 7	Kim et al. (2020b)
i. Fe_3O_4@ Ethylenediaminetetraacetic ii. Fe_3O_4 @ Sodium Lauryl sulfate iii. Fe_3O_4 @ Polyvinylpyrrilidone iv. Fe_3O_4 @ SDS	1000 ppm salinity+ 0.5 wt % Tween-80	i. −46.8 mV ii. −54.2 mV iii. +119.8 mV iv. +168.3 mV	pH = 8/9	Shalbafan et al. (2019, 2020b)
i. Fe_3O_4 @ citrate ii. Fe_3O_4 @ polyelectrolyte - citrate	DI water	i. −27.4 mV ii. −30.10 mV	pH = 7.5	Izadi et al. (2019)
i. Fe_3O_4 ii. Fe_3O_4 @ oleic acid iii. Fe_3O_4 @ polyacrylamide iv. Fe_3O_4/polyacrylamide	Sodium chloride (NaCl) 500-30,000 ppm	i. −18 mV ii. −30.6 mV iii. −28.3 mV iv. −31.9 mV	–	Khalil et al., 2019
i. Fe_3O_4 ii. Fe_3O_4 @ titanium oxide (TiO_2) iii. Fe_3O_4 @ SiO_2 iv. Fe_3O_4 @ Chitosan	Seawater	i. −31.5 mV ii. −44.8 mV iii. −48.3 mV iv. −49.6 mV	–	Rezvani et al. (2018, 2019)
i. Fe_3O_4@ Tetraethyl orthosilicate ii. Fe_3O_4 @ 3-amniopropyl triethoxy trimethoxy? silane iii. Fe_3O_4 @poly (AMPS-co-AA) (poly (2-acrylamido-3-methylpropanesulfonate-co-acrylic acid)	10 mM potassium chloride (KCl) solution	i. −34.5 ± 6 ii. 28.6 ± 3 iii. −53.6 ± 1	pH = 5	Iqbal et al. (2017)
Fe_3O_4 @ Cetrimonium bromide	DI water	i. + 36.8 m ii. − 38.3 mV	i. pH = 5 ii. pH = 9	Saien and Gorji (2017)
i. Fe_3O_4@ Tetraethyl orthosilicate ii. Fe_3O_4 @ 3-amniopropyl triethoxy trimethoxy? Silane iii. Fe_3O_4 @poly (2-acrylamido-2- methyl-1-propanesulfonic acid-co-acrylic acid) (poly (AMPS-co-AA))	8% NaCl and 2% calcium chloride ($CaCl_2$)	i. −36 mV ii. +28 mV iii. −47 mV	pH = 5	Urenã-Benavides et al. (2016)
Fe_3O_4 @ SiO_2	NaCl, $CaCl_2$ 100–300 mM	−42 mV	pH = 7	Bakhteeva et al. (2016)
Fe_3O_4 + Sulfonated copolymer	1 M NaCl solution	−45 mV	pH = 8	Bagaria et al. (2013)

documented by Mahmoud et al. (2018) (Fig. 9). Low concentrations of IONPs result in the formation of two layers embedded on the cake structure, with the layer closest to the rock playing a key role in the formation of the cake microstructure of low porosity and low permeability, which effectively reduces filtrates and particle intrusion. However, at high concentrations a third layer of agglomerated particles increases the porosity and permeability of the cake structure. As a result, the filtrate efficiency is reduced. Therefore, the authors suggest the use of low concentrations between 0.3 and 0.5 wt% as the optimum concentration for effective filter cakes. These range of particle concentration is in agreement with recent findings reported by Alvi et al. (2021). Alvi et al. (2020, 2021) recently evaluated how IONPs improve the properties of water based and oil based drilling muds. According to their results, 0.5 wt% of IONPs was able to reduce the coefficient of friction and filtrate loss of hexane (oil based) by 39% and 70%, respectively. Whereas small concentrations of IONPs (0.019 wt%) was able to reduce the coefficient of friction and fluid loss of bentonite-based fluids (water based) by 47% and 20%, respectively, owning to the formation of compact and less porous structure in the cake. Furthermore, the authors observed that IONPs can improve the stability of oil-based drilling fluids by increasing the yield stress and reducing the sag factor. This effectively improves the rheological properties of the drilling mud. IONPs additivities can significantly improve the rheological properties of drilling fluids by increasing the apparent viscosity, yield stress and susceptibility to the temperature. In several experiments under reservoir conditions of HTHP, Vryzas et al. (2016, 2016b) reported considerable improvement in the yield stress, viscosity, and gel strength of bentonite-based drilling fluids when 0.5 wt% IONPs were introduced. According to their findings, IONPs provide suspension stability and connection between the bentonite particles, allowing the creation of a stiff microstructure network. Similarly, Ahmed et al. (2020a,b) reported that 3.0 wt% of IONPs improved the plastic viscosity, yield point, and 10 s gel strength of basic drilling mud by 15.0, 3.0, and 12.5%, respectively. However, the optimum concentration which reduced filtrate volume and filter cake thickness by 13.6 and 40% was 0.5 wt%. Another drilling domain that shows promise from the use IONPs is the formulation of smart drilling fluids with controllable rheological properties under a magnetic field. Thus, providing an avenue for real time in-situ control of drilling fluid rheology (K. Zhou et al., 2020). Vipulanandan et al. (2015, 2018) have demonstrated how the rheological properties of IONPs can be controlled using a magnetic field. Experiments carried out by Vryzas et al. (2017) showed that, in the presence of a magnetic field, the yield stress and viscosity of Fe_3O_4 based drilling fluids monotonously increases with increasing magnetic field, owning to the disintegration of particle chains due to Brownian random movement. More recently, Vipulanandan & Mohammed (2020) correlated the rheological

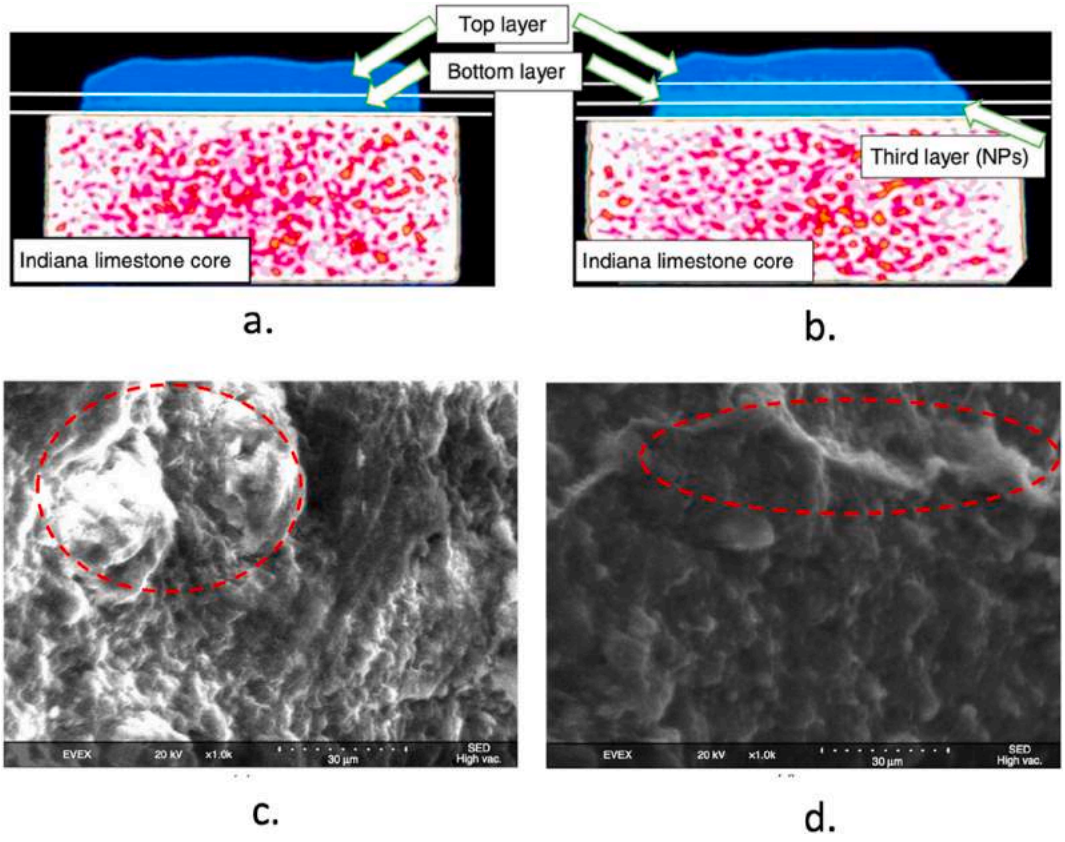

Fig. 9. (a–b) CT Scan images of filter cake samples with (a.) 0.5 wt% (b) 2.5 wt% (c–d) SEM images of the surface of the filter cakes (c.) 0.5 wt% (d) 2.5 wt% (Mahmoud et al., 2018).

properties of Fe_3O_4 drilling fluids and cement slurry with that of electrical sensitivity under different magnetic field strengths using a nonlinear resistivity and Vipulanandan property correlation model. The model can predicate the shear thinning relationship between the shear stress and shear strain rate of IONPs drilling fluids and can be used for real time field monitoring. By and large, the multiple functionalities of IONPs such as ability to formulate efficient filter cake, high stability under reservoir conditions, negligible sensitivity to HTHP, in-situ real time controllable rheological properties, and recyclability opportunities makes it an effective drilling fluid additive and superior choice over several other NPs.

4.3. *Magnetically driven separation*

Magnetitic driven separation with IONPs in the oilfield often entails demulsifying emulsions to separate oil from water. Extracted crude from reservoirs is typically accompanied by water, whereas produced water is polluted with oil or polymers. Produced oil in water or water in oil emulsions present a number of operational issues, such as corrosion in pipes and pumps, as well as catalyst poisoning in the refining process (Zolfaghari et al., 2016; Adewunmi and Kamal, 2018; Atta et al., 2018; Shehzad et al., 2018). Likewise, in order to achieve the government's water quality sustainability and discharge restrictions, oil content, polymers and large amounts of surfactants must be extracted from produced water. The most typical magnetic separation route using IONPs is demulsification through the adsorption of oil, surfactants, or polymers, followed by separation using magnetic force. Peng et al. (2012) demonstrated the use of ethyl-cellulose-grafted Fe_3O_4 (MEC) de-emulsifiers to separate water droplets from bitumen emulsion. Results showed that the settling time of the emulsions significantly decreased in the presences of a magnetic field, 1.5 wt % of MEC separated up to 25 wt % of the water, corresponding to 93% of total water in the emulsion. Peng et al. (2018) reported the demulsification of emulsions containing large amounts of surfactants and paraffin oil using IONPs. The IONPs were functionalized with amino groups ($M@NH_2$) and achieved 85–97% demulsification. According to their findings, electrostatic interactions between $M@NH_2$, surfactants, and oil were the main driving force behind demulsification. Ko et al. (2017) demonstrated the rapid separation of crude oil from water using amine functionalized Fe_3O_4. Separation occurred within seconds due to the strong adsorption of oil onto the amine coatings of Fe_3O_4. He et al. (2020b) demonstrated the effectiveness of novel Biwettable Janus IONPs coated with hydrophobic ethyl cellulose (EC) and hydrophilic sodium carboxymethyl cellulose (CMC) coated on each side of the particle surface. Compared to fully-coated EC/CMC IONPs, the Janus NPs were more effective in separating water from crude oil using a magnetic field. This was due to the stronger adsorption of the Janus particles at the oil-water interface (Liang et al., 2018). Guselnikova et al. (2020), Jamsaz et al. (2021) and khalilifard & Javadian (2021) have also reported high adsorption capabilities of IONPs coated onto polyurethane (PU) sponge to produce a hydrophobic/oleophilic magnetic nanocomposite (NC). According to their findings, the NC adsorption capacity increased under a magnetic field due to increased surface area. Thus, they are highly effective in separating surfactant stabilized emulsions. Liang et al. (2015) demonstrated the effectiveness of IONPs functionalized with oleic acid as de-emulsifiers. The authors also reported the influence of particle concentration and the role of particle wettability in demulsification. According to their results, the effectiveness of the IONPs de-emulsifiers increased with increasing particle concentration and their effectiveness was directly related to their wettability (water contact angle). Maximum demulsification of ~97% was attained when the contact angle of the NPs was at ~90°. Several other researchers have investigated the effect of particle concentration on demulsification using IONPs and the results show that the effectiveness of demulsification

increases with increasing particle concentration (He et al., 2019a; Wai et al., 2019; Guselnikova et al., 2020; Mi et al., 2020; Xiong et al., 2020; Yu et al., 2020). However, majority of the studies have used different ranges of particle concentration and an optimum concentration is desirable to keep material and infrastructure cost as low as possible. Higher concentrations require stronger magnetic fields for separation (Adewunmi et al., 2021). Magnetic IONPs have also been used for the removal of other unwanted substances such as heavy metals, and nonpolar organic contaminants. A number of studies have demonstrated the removal of cations such as calcium (Ca^{2+}) and magnesium (Mg^{2+}) and sodium (Na^{+}) using functionalized IONPs (Wang et al., 2014; Gautam et al., 2015; Prigiobbe et al., 2015; Wanna et al., 2016; Simonsen et al., 2018). This process is known as desalination and is a useful tool for improving the efficiency of oil recovery via flooding. Similar to demulsification techniques, desalination involves the use of functionalized IONPs to draw out the solutes which are then magnetically separated. Thus, the general magnetic separation mechanism of IONPs all follow a similar pattern and is merely a function of using a specific surface coating as an absorbent. Common coatings used in desalination include but not limited to triethylene glycol polyacrylic acid poly (sodium acrylate), poly (N-isopropylacrylamide), polyglycerol, dextran, citrate, and poly (ethylene glycol) (PEG) diacid (Na et al., 2014; Dey and Izake, 2015; Kim et al., 2020a). Table 3 shows a brief a summary of oilfield applications of IONPs.

5. Enhanced oil recovery

Owning to the poor production rate of waterflooding and rapid decline in the discovery of new crude oil reserves, chemical-enhanced oil recovery (CEOR) has become an important factor in oil production. However, traditional CEOR chemicals such as surfactants and polymers are compromised by high adsorption rate, precipitation/degradation at reservoir condition and high cost. Hence, a myriad of researchers have focused on utilizing nanotechnology to improve oil production (Agi et al., 2020a,2020b,2020c; Naghizadeh et al., 2020; Sagala et al., 2020; Yahya et al., 2020; Yekeen et al., 2020) Application of nanotechnology in EOR consist of nanofluid flooding, nanoemulsions with or without NPs as stabilizers and nanocatalyst for heavy oil viscosity reduction (Cardona et al., 2018). Though, the governing mechanism of oil displacement are still not fully understood and require further investigation (Agi et al., 2018; Kewen Li et al., 2018; Eltoum et al., 2020). The pathways leading to incremental oil displacement so far have been described as pore channel plugging, disjoining pressure, wettability alteration, increment of injection fluid viscosity, interfacial (IFT) reduction, asphaltene breakdown and prevention of asphaltene precipitation. Fig. 10 illustrates the schematics of the most common nanofluid EOR mechanisms. All the above mechanisms and much more can be achieved using IONPs. Pioneering work on the application of IONPs presented by Kothari et al. (2010) proposed that ferrofluids could improve oil recovery by decreasing oil viscosity owing to the dipole moment within the particles, which enables reservoir fluid molecules to align, thereby reducing the flow resistance, leading to incremental oil recovery. Using sand pack flooding and spontaneous imbibition, Ogolo et al. (2012) showed that Fe_3O_4 dispersed in DI water or diesel had significant potential in improving oil recovery. Equally significant, the study indicated that the choice of dispersion fluid and contact time between the NPs and reservoir rock had a substantial effect on oil recovery. Precisely, brine and ethanol had a negative effect on the magnitude of oil recovery. Guan et al. (2014) reported an incremental oil recovery 38% and 27% using 10–25 nm and 30–90 nm Fe_3O_4 nanofluids, respectively. The smaller NPs were more effective due to better dispersibility and higher charge density, which improved oil recovery mechanism and transportation through the porous medium.

Table 3
Summary of possible IONP applications in the oil and gas industry.

Type of IONPs	Application/Observations	Author
Drilling and Completion Improvement		
Hydrophobic Fe_3O_4	- Preventing filtrate invasion. - 0.5 wt% iron oxide dispersed in hexane reduced filtrate loss by 70% and filter cake thickness by 55%. - reduced free oil layer resulting from syneresis during aging by 16.3%.	Alvi et al. (2021)
Fe_3O_4 coated with poly (vinyl alcohol) (PVA) or Hydroxyapatite (HAp)	- Reducing condensation and imbibition rate of water near the wellbore region due to wettability alteration. - HAp is more effective in altering wettability from oil wetting to gas wetting compared to PVA.	Safaei et al. (2020)
Synergy of Fe_2O_3 & KCl–Glycol–PHPA polymer	- Reducing drilling fluid mud loss and improving rheological properties. - Mud loss was 5.9 ml after 30 min. - 3.0 wt% particle concentration improved the plastic viscosity, 10 s gel strength & yield point by 15, 12.5 3% and 12.5%, respectively. - The optimum concentration was 0.5 wt % at which filtrate volume and filter cake thickness reduced by 13.6 and 40%.	Ahmed et al. (2020a,b)
Bare Fe_2O_3	- Improving the rheological properties of the drilling mud and weight loss. - increased yield stress, shear stress and plastic viscosity by up to 200%, 175% and 105% respectively. - 1% particle concertation resulted in 91% reduction of total weight loss.	Mohammed (2017)
Bare Fe_2O_3	- Decreasing mud fluid resistivity for magnetic sensing and improving rheological behaviour using magnetic field. - Magnetic field of 0.6 T, reduced electrical resistivity by 39% and increased shear stress by 25%.	Vipulanandan et al. (2017)
Magnetic Separation		
Fe_3O_4 @ bentonite	- 0.1 wt% particle concentration adsorbed 97% of oil after 90 min. - pseudo-second-order kinetics model successfully describes the kinetic mechanism. -Langmuir isotherm model suggested a monolayer adsorption of oil onto the particle surface.	Ewis et al. (2020)
Fe_3O_4 hydrophobic EC and hydrophilic CMC	- Separation of water-in-crude oil emulsions - Janus modification improved adsorption to the oil-water interface	He et al. (2019b,c, 2020a)

(continued on next page)

Table 3 (*continued*)

Type of IONPs	Application/Observations	Author
	and also more difficult to desorb from the oil-water interface compared to EC coated magnetic nano-particles. Hence, improving demulsifica-tion speed. - Recycling test show the desirable reusability and stability of Janus Fe_3O_4	
Fe_3O_4 @ 3(Aminopropyl) triethoxysilane.	- 0.04 wt% particle concentration reduced up to 99.95% of crude O/W emulsions. - Main separation mechanism was electrostatic attraction between negatively charged O/W emulsions and positively charged modified IONPs. - Decreasing particle size increases the effect of magnetic field velocity.	Ko et al. (2016)
Fe_3O_4@poly-methylmethacrylate-acrylicacid-divinylbenzene P(MMA-AA-DVB)	- Heavy oil and water emulsion separation - P (MMA-AA-DVB) coating increased interfacial activity at oil-water inter-face leading to faster attachment and separation - 98% separation efficiency was attained after 1 h - No changes were observed on the effectiveness of NPs/ coating after 5 cycles	N. Ali et al. (2015a,b)
Reservoir Sensing, Imaging and Characterization		
Fe_3O_4 **Fe_3O_4 @ polyethylene glycol (PEG-400)** **Fe_3O_4@ oleylamine (OLA)**	- NMR logging tool to characterize fluids inside the reservoir - Spin-spin (T_2) relaxation measurements demonstrated contrasting ability of bare and both functionalized Fe_3O_4 nanofluids - Transverse relaxivity (r_2) values and stability were in the order of Fe_3O_4 @PEG, Fe_3O_4 @OLA and Fe_3O_4. - Fe_3O_4 @PEG and Fe_3O_4 @OLA relaxtivity values were 2.07 and 1.53 times greater than that of Fe_3O_4.	S. Ali et al. (2018)
Fe_3O_4 @ 3(Aminopropyl) triethoxysilane (APTES)	- Surface coating masks and hinders magnetic properties of Fe_3O_4 for NMR data interpretation. - Increasing the surface coating of APTES from 1.60 to 4.22 wt%, decreased surface reflexivity by 26.1%. - High Fe concentration (0.01 g/L) causes electron-proton in-teractions to dominate surface relaxation whereas low concentra-tions (0.002 g/L) promote proton-proton interactions.	Zhu et al. (2018)
Ferrofluids		

Table 3 (*continued*)

Type of IONPs	Application/Observations	Author
	- Proposed tracking of flood-front using cross well magnetic tomography. - NPs changed the permeability of the flooded region. - Induction effect and changes in fluid conductivities are negligible at low frequency for image contrast. - The influence of areal and vertical reservoir permeability heterogeneity on flood fronts can be detected.	Rahmani et al. (2013a, 2014, 2015)
Fe_3O_4 @ citric acid **Fe_3O_4@ PEG-grafted**	- Fe_3O_4 as nano sensors using NMR - Decreases NMR T_2 relaxation time for reservoir characterization.	Park et al. (2014)
	- Adsorption increases with increasing salt concentration thus reducing contrast agent. - Molecular theory can be used to determine interactions between IONPs sand (SiO_2) and rock ($CaCO_3$) surfaces.	
Improving Oil Recovery		
	- Reducing heavy oil viscosity - Fe_3O_4 reduced asphaltene precipitation via asphaltene adsorption - Asphaltene adsorption is a function surface coating, which may increase or decrease asphaltene adsorption - Asphaltene adsorption capacity increases with increasing pressure	Setoodeh et al. (2020)
Fe_2O_3 and Fe_3O_4 coated with citric acid.	- NPs improved macroscopic and microscopic efficiency. - Fe_2O_3 NPs did not react to the application of a magnetic field. Thus, there was no incremental oil recovery in the presence of a magnetic field.	Divandari et al. (2019)
	- Citric coated particles only responded to a magnetic field of +800 Gauss. Maximum oil recovery was 83% at 2750 Gauss. - Citric coated NPs resulted in more oil recovery in the presence of magnetic field compared to bare Fe_2O_3 and polymer solutions.	
Bare Fe_3O_4	- Magnetic field improved oil recovery owing to improved sweeping area and wettability alteration. - Water breakthrough is postponed. - Fluid front created a piston column towards	Esmaeilnezhad et al. (2018)

(*continued on next page*)

Table 3 (*continued*)

Type of IONPs	Application/Observations	Author
	the direction of the magnetic field. - Wettability modification was more pronounced in the presence of light oil than in the presence of heavy oil.	

5.1. EOR mechanisms of IONPs

To comprehend the mechanisms of IONPs and the role of interfacial tension (IFT) reduction, wettability alteration and viscosity enhancement in EOR, the connection between the capillary number and residual oil must be introduced. The capillary number (N_c) is ratio between the viscous forces and capillary forces. It is used as a metric gauge to adjudge the effectiveness of EOR mechanism and potential oil recovery. Several forms of the capillary number (Equation (8)) have been published and summarized by J.Sheng et al. (2011, 2015) The effectiveness of EOR improves by increasing the N_c, which in turn reduces the capillary force to allow oil mobilization. This can be attained by either increasing injection fluid viscosity (2) increasing the displacing fluid viscosity and/or (3) reducing the IFT (Gbadamosi et al., 2019a).

$$N_c = \frac{Viscouse\ Force}{Capillary\ Force} = \frac{\mu_{inj} \times v}{\sigma \times cos\theta} \tag{8}$$

where μ is dynamic viscosity of the displacing fluid, u is displacing viscosity, θ is contact angle, and σ is IFT between the displacing and displaced fluid.

5.1.1. Emulsion formation and stability

Emulsions is the dispersions of one liquid in an immiscible liquid, it is produced either in-situ or externally. It can increase injection fluid viscosity and assist in pore blockage, diversion of flow to towards bypassed zones, and the intrusion of oil into the moving fluid. Hence, increasing oil production (Kumar and Mandal, 2020). In CEOR, stable emulsions are formed when an amphiphilic emulsifier strongly adsorbs the oil-water interface and reduces IFT between the two phases. Adsorption of the emulsifier promotes the formation of a protective layer which can resist droplet coalescence and phase separation. The common emulsifiers used in EOR are surfactants. However, surfactant micelles dynamically adsorb and desorb easily from the oil-water interface, are susceptible to adsorption on the rock surface and prone to thermal degradation (ShamsiJazeyi et al., 2014; I. Kim et al., 2017). Thus, NPs are proposed as modifiers/alternative emulsifiers (Pei et al., 2015; Pilapil et al., 2016; Pal et al., 2019; Kumar et al., 2020; Kumar and Mandal, 2020; Pal and Mandal, 2020) Similar to pickering emulsions (emulsions stabilized by solid particles), NP stabilized emulsions exhibit enhanced stability (slow rate of droplet coalescence) resulting from improved mechanical barrier effect (Pal and Mandal, 2020). NPs irreversibly adsorb onto the oil-water interface to form rigid structures which act as a mechanical barrier against coalescence and are able to resist harsh reservoir conditions (HTHP) (Binks and Yin, 2016). Thus, NPs are thermodynamically stable. Previous studies have shown that the key parameter which determine the effectiveness of emulsions stability is the contact angle at the oil-water interface, determined by hydrophobicity/hydrophilicity of the particles. Therefore, NP emulsion stabilization is mainly a function particle surface properties (Udoetok et al., 2016). Fig. 11 illustrates the different mechanism of emulsion stability using NPs. According to the detachment energy model, particles with $\theta = 90^{\circ}$ adsorb better at the oil water interface and possess maximum desorption energy (energy required to detach particle). Thus, they are most suitable for stabilizing emulsions (Pal and Mandal, 2020). The relatively high surface area of IONPS with or without facile surface modification enables favourable adsorption at the oil-water interface. Flooding experiments carried out by Kazemzadeh et al. (2019), Izadi et al. (2019) and Rezvani et al. (2019), showed that both bare and modified Fe_3O_4 NPs generate stable in situ emulsions in the porous medium. The authors also indicated that the formation and stability of the emulsions increased with increasing particle concentration. Although, more recently, externally generated emulsions are considered as an independent technique in EOR processes (N. Kumar et al., 2017; Ahmed and Elraies, 2018; G. Kumar et al., 2020), the application of eternally generated IONP emulsions for EOR is extremely scarce in the

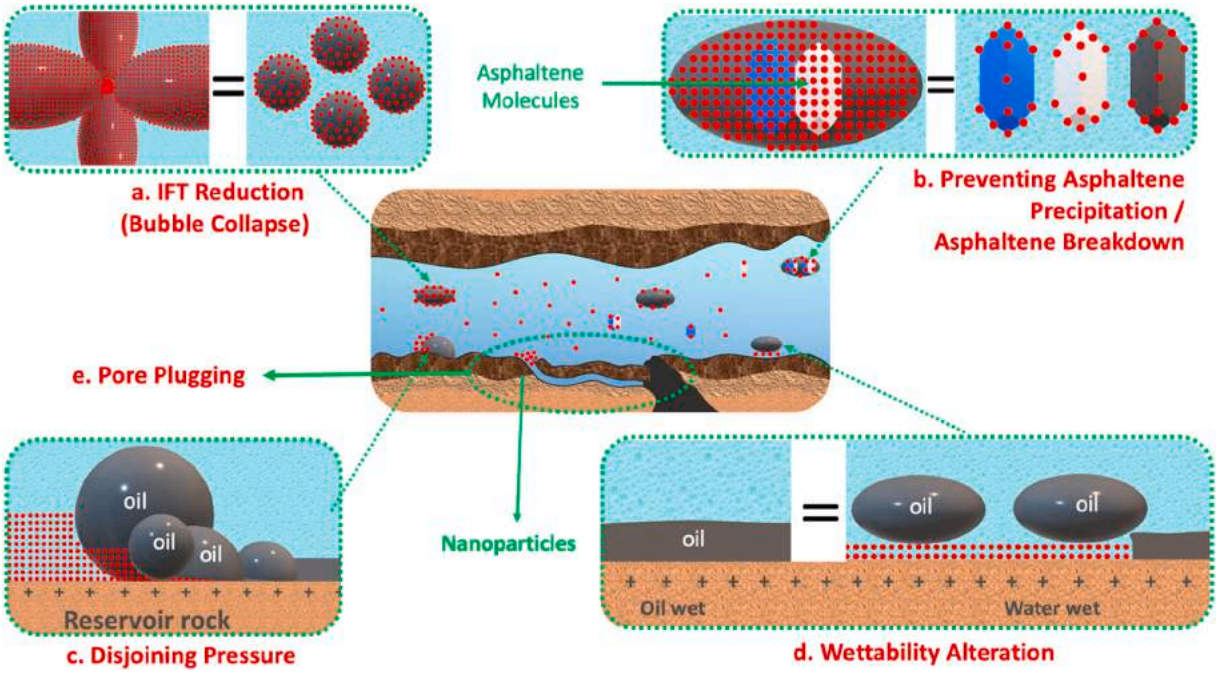

Fig. 10. Schematic illustration of various nonfluid oil recovery mechanism leading to incremental oil recovery. (a) IFT reduction (b) prevention of asphaltene precipitation and asphaltene breakdown (c) disjoining pressure (d) wettability alteration (e) pore plugging (Sun et al., 2017).

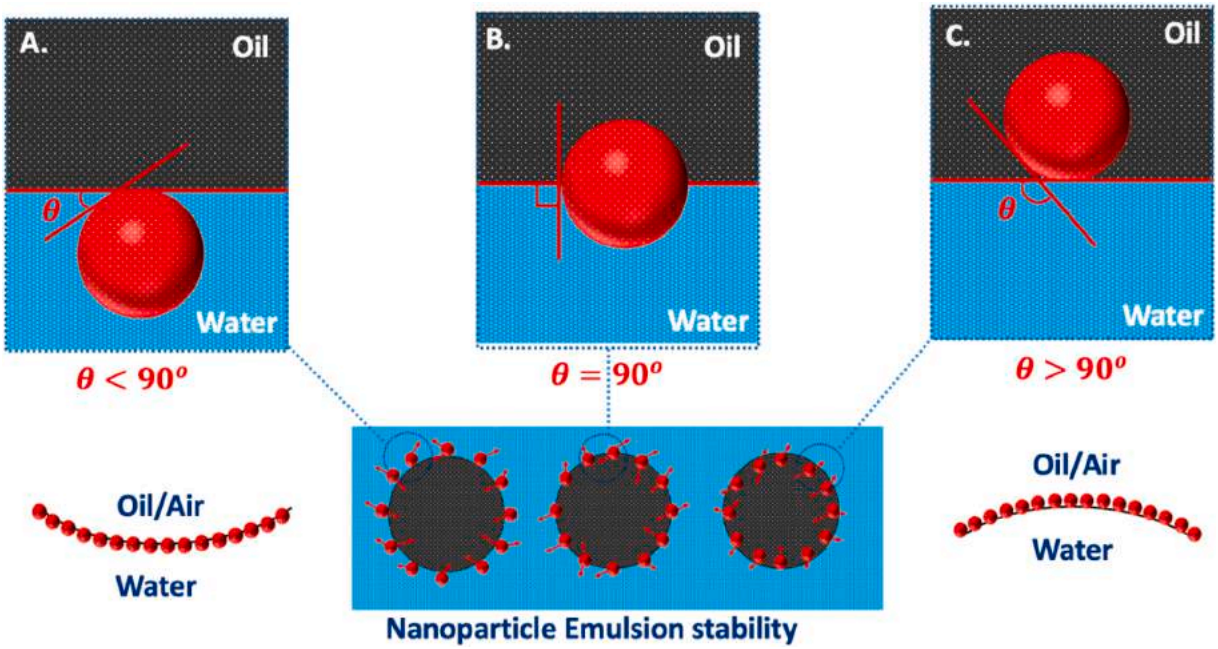

Fig. 11. Schematic representation of different NPs emulsions stability arrangements as per detachment energy model (a) hydrophilic particles, $\theta < 90°$ (b) hydrophilic/hydrophobic $\theta = 90°$ (c) hydrophobic particles, $\theta > 90°$ (Pal and Mandal, 2020).

literature. Despite numerous studies illustrating that IONPs can be used to prepare emulsions for EOR (Ingram et al., 2010; Zhou et al., 2011, 2012; Fan et al., 2016; Emrani & Nasr-El-Din, 2017; Prévot et al., 2017a, 2017b; Koroleva et al., 2019; Keran Li et al., 2020).

5.1.2. IFT reduction

At the molecular level, IFT is a phenomenon resulting from difference in energy between oil and water molecules at the fluid interface. In other words, it describes the energy required to make a unit area of interface between two immiscible liquids, thus taking the units of Joules per square metre or the equivalent Newtons per metre (Berry et al., 2015). IFT reduction deforms the sizes of trapped oil droplets to allow easy mobilization through pore throats. It also promotes the formation of in-situ emulsions which sweep, merge and carry along the oil droplets (Sheng, 2015). The IFT reduction of NPs has been a controversial point widely discussed in the literature. Researchers have continually argued that the interactions between oil and water molecules are merely influenced in the presence of NPs. Hence, NPs particles do not reduce IFT. Some studies have reported very little to non-significant change in the presence of SiO_2 (Pichot et al., 2012; Biswal et al., 2016; Jiang et al., 2017) and ZnO (Fereidooni Moghadam and Azizian, 2014; Moghadam and Azizian, 2014) whereas others have reported substantial change in the presence of SiO_2 (Agi et al., 2020d; Ngouangna et al., 2020; Wu et al., 2020), ZnO (Soleimani et al., 2018), aluminium oxide (Al_2O_3) (Gbadamosi et al., 2019b) nickel oxide (NiO) (Gomaa et al., 2018a) and Fe_3O_4 (El-hoshoudy et al., 2019; Pereira et al., 2020; Saien and Gorji, 2017). Studies carried out by Ruhland et al. (2013) investigating the surface activity and self-assembly behaviour of homogenous NPs and Janus particles with different geometries showed that the magnitude of IFT reduction is directly correlated to their adsorption at the oil-water interface. Similarly, Glaser et al. (2006) observed that the amphiphilicity nature of gold (Au) − Fe_3O_4 Janus NPs substantially decreased the IFT of oil and water compared to individual homogeneous Au and Fe_3O_4 NPs at comparable concentrations. Likewise, Khalil et al. (2019) observed that Fe_3O_4 coated with oleic acid (Fe_3O_4 @OA) further decreased the IFT of oil-water beyond that of homogenous Fe_3O_4. Owing to improved adsorption of the long hydrocarbon tail of OA, which allowed some part of the dispersed Fe_3O_4 @OA to transfer to the oil phase. He et al. (2020b) also illustrated that cellulose-coated Janus Fe_3O_4 of asymmetric surface wettability were more interracially active compared to homogeneous Fe_3O_4 of uniform surface modification. Hence, the extent of IFT reduction in the presence of Janus Fe_3O_4 was greater than that of homogeneous Fe_3O_4. Therefore, the plausible reason behind the dispersity in results is possibly the poor adsorption affinity of homogenous NPs and the difference in surface charge of the NPs which control their adsorption and packing behaviour at the interface. The mechanisms of IFT reduction dictates that NPs form a monolayer between the oil-water interfaces, and the extent of IFT reduction is a depends on the contact angle at the oil-water interfaces. Homogenous Fe_3O_4, which are hydrophilic, mostly reside in the water interface and rely on electrostatic adsorption, which is very week compared amphiphilicity (Sofla et al., 2019) (Fig. 12a) hence, the IFT reduction is minimal. Thenceforth, the magnitude of IFT reduction is improved by utilizing hydrophobic coatings to attain amphiphilicity (Fig. 12b). Furthermore, the synergy of IONPs and surfactants significantly improves the magnitude of IFT reduction beyond that observed for each component (Suleimanov et al., 2011; Biswal et al., 2016; Betancur et al., 2019) Surfactants are well known for their ability to substantially decrease IFT by replacing the molecules of oil and water at the interface. However, rock adsorption reduces surfactants efficiency and increases operation cost. NPs on the other hand, reduces surfactants adsorption and act as carriers to the oil-water interface while surfactants improve the hydrophobicity of NPs. The mechanism and effectiveness of the synergy between IONPs and surfactants primarily depends on the type of surfactant and dispersion/reservoir pH (Fig. 12c). Regarding the type of surfactant, positively charged cationic surfactant molecules are attracted and attach onto negatively charged IONPS. As a result, the NPs are more hydrophobic and move towards the oil-water interface. Presence of both IONPs and surfactants at the oil-water interface dramatically decreases IFT whereas repulsive forces between negatively charged anionic surfactants molecules and IONPs drives the surfactant molecules away from the bulk solution towards the oil-water interface. Thus, increasing the amount of free surfactant molecules at the oil-water interface. On the contrary, non-ionic surfactants which have no electrostatic charge, behave completely different, and the presences of | IONPs may retard the efficiency of these surfactants (Zargartalebi et al.,

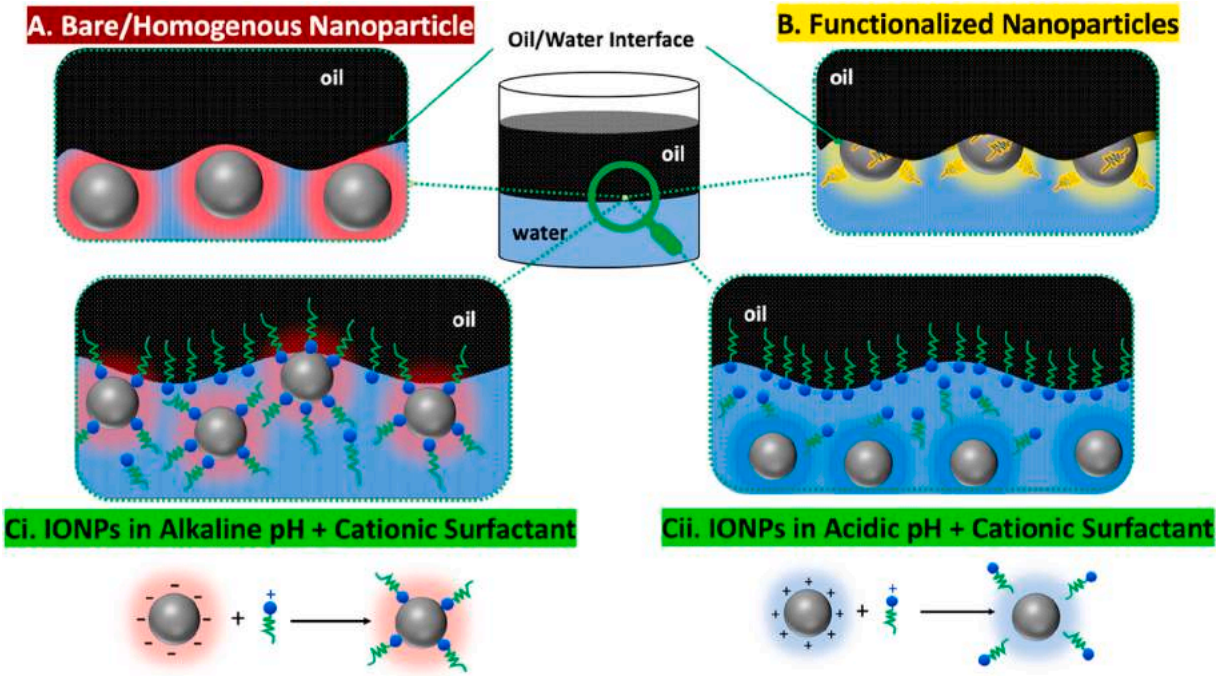

Fig. 12. Mechanism of IFT reduction in the presence of (a) bare IONPs weekly adsorbed at oil-water interface (b) functionalized IONPs strongly adsorbed at the oil-water interface (c.) synergy of surfactants and IONPs resulting in more reactivity at the oil-water interface. (ci) IONPs and surfactants attracted due to opposite electrostatic forces (cii) IONPs and surfactants repel due to same electrostatic forces (Saien and Gorji, 2017).

2014). The is because, both the surfactants and NPs compete to displace each other at the oil-water interface. Since the magnitude of surfactant IFT reduction is greater than that of IONPs, less non-ionic surfactants at the oil-water interface will yield less IFT reduction. To summarize, IONPs improves the effectiveness of cationic surfactants more than that of anionic surfactants in an alkaline medium while it decreases the effectiveness of non-ionic surfactants. Fig. 12 illustrates the mechanism of IFT reduction using bare IONPs, functionalized IONPs and the synergy of IONPs and surfactants in alkaline/acidic medium. Hence, pH influences the surface charge of IONPs and can change it from negative-neutral - positive. Thus, influencing the adsorption and orientation of surfactants at the O/W interface. Alkaline pH facilitates the adsorption of cationic surfactants onto the IONPs whereas acidic pH promotes the repulsion of cationic surfaces and vice versa. However, unlike the case of non-ionic surfactants and negative IONPs, at natural pH, the NPs have hydroxyl groups on their surface, which may form hydrogen bonds with the cationic surfactant molecules. Thereby, adsorbing the surfactants molecules (Saien and Gorji, 2017). Furthermore, the presence of salts, which decreases the electrostatic repulsion may lead to more adsorption or repulsion between the surfactants and NPs. Ahualli et al. (2011), observed that despite the repulsive charges between negative NPs and anionic surfactants, a small part of the surfactant molecules still adsorbs onto the surface of NPs in the presence of salts. Betancur et al. (2019) also observed that the method of adding salts, surfactants and NPs influence the degree of IFT reduction. According to their results, adding salts before surfactant reduces the formation of surfactant micelles and adsorption onto the surface of the NPs because the electrolytes interact with the surface charge of the NPs. Therefore, reducing the quantity of available electrolytes which facilities the formation of surfactant micelles. However, if the surfactants are added to the salt solution before the NPs, the electrolytes favour the formation of surfactant micelles which are then adsorbed onto the surface of the NPs.

5.1.3. *Wettability alteration*

Wettability alteration is considered the most prominent mechanism of NPs in EOR. Wettability alteration allows water to imbibe into the porous media to extract oil. Numerous investigations on the impact of wettability alteration using NPs can be found in literature. NPs are efficient wettability modifiers due to their high surface energy and free movement within the micrometre scale rock pores. Moreover, in the presence of NPs, the efficiency of other wetting agents such as surfactants, polymers and salt ions are also enhanced. The two possible underlying mechanisms leading to wettability alteration in the presence of NPs are: (i) nanoparticle adsorption on the solid surface, resulting to change in surface energy and reduced friction (Fig. 10d) (ii) the creation of a pressure gradient created in the vicinity of the three-phase contact line due to the solid-like ordering fluid 'wedge' (Fig. 10c) (Druetta et al., 2018). Regardless of the underlying mechanism, in order to modify wettability, the NPs must be adsorbed onto the rock surface (Hendraningrat and Torsæter, 2015; Al-Anssari et al., 2016). Hou et al. (2015,2019) illustrated various pathways leading to wettability alteration using ellipsometry, zeta potential and contact angle measurements. The results indicated that the primary underlying mechanisms for wettability alteration were ion-pair formation and adsorption of particles onto the rock surface through hydrogen bonding and hydrophobic interactions as well as electrostatic interactions. Thus, the hydrophilic nature and high surface energy of IONPs can alter wettability towards a more water-wetting state. Contact angle measurements and energy dispersive X-ray (EDX) analysis carried out by Izadi et al. (2019) showed that the presence of Fe_3O_4 improved the water wetness of carbonate rocks primarily through adsorption. The contact angle decreased from 160° to 114° and the EDX analysis showed that the surface of the treated rock samples consisted of Ca, Mg and Fe constituent materials, whereas those treated without Fe_3O_4 had only Ca and Mg (Fig. 13c). Similarly, Fourier transform infrared spectroscopy (FTIR) analysis and contact angle measurements carried out by Shalbafan et al. (2019) illustrated the wettability alteration and adsorption phenomena of Fe_3O_4 and Fe_3O_4 coated with either hydrophilic polymer or ionic surfactant (Ethylenediaminetetraacetic (EDTA) & Sodium Lauryl Sulfate (SLS). In comparison, the extent of wettability alteration and adsorption of SLS coated Fe_3O_4 was greater than that of EDTA coatings and

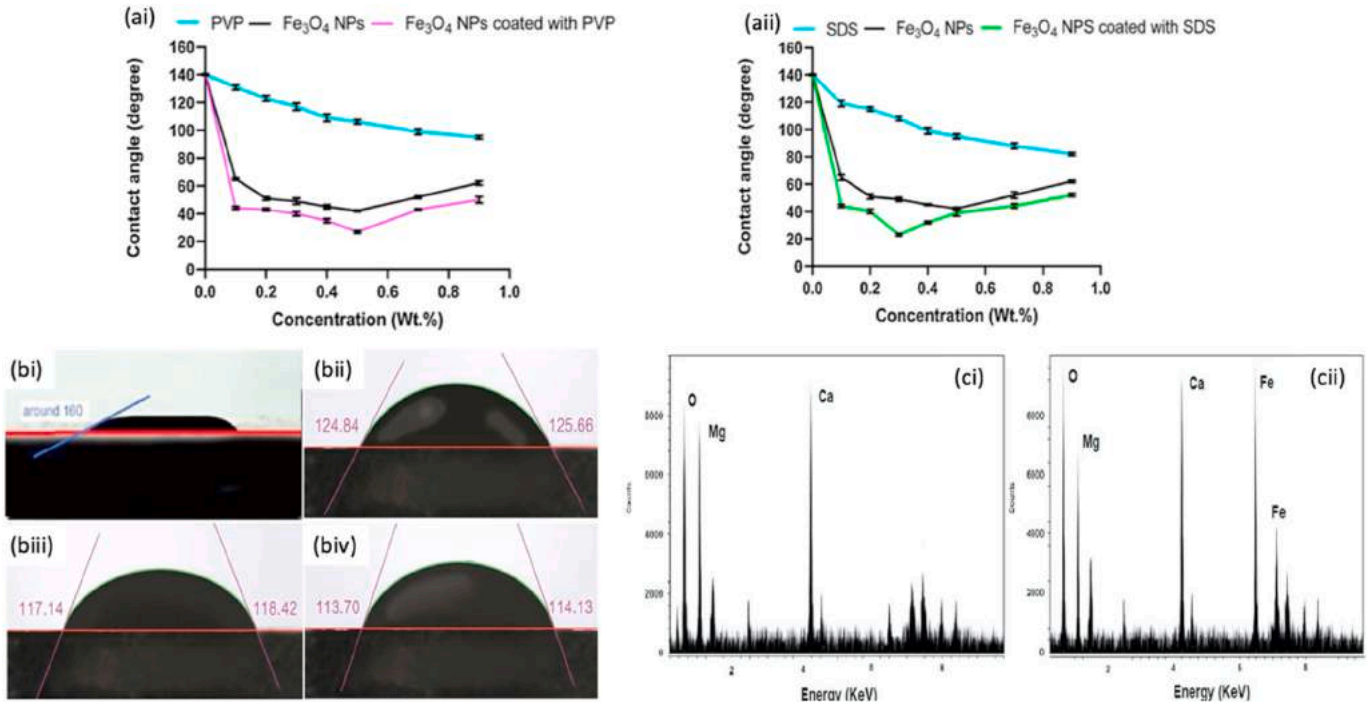

Fig. 13. Influence of Fe_3O_4 nanofluids on wettability alteration (a) contact angle versus Fe_3O_4 nanofluids with different concentrations (i) with PVP (ii) with SDS (Shalbafan et al., 2020a) (b) contact angle measurements(i) without nanofluid-oil wet (ii) – (iv) increasing Fe_3O_4 nanofluid concentration (c) EDX analysis of carbonated rock (i) without nanofluid (ii) treated with Fe_3O_4 nanofluid (Izadi et al., 2019).

homogeneous Fe_3O_4 at high concentrations. However, at low concentrations the EDTA coatings performed better. Nevertheless, at optimum concentrations under reservoir conditions, SLS coatings resulted in more oil recovery owing to better stability in the presence of brine. In addition, the authors observed that all the NPs reduced permeability and porosity in the following order EDTA coatings > SLS coatings > homogeneous Fe_3O_4. In a more recent study, the same authors (Shalbafan et al., 2020a) reinforced their findings using Fe_3O_4 with new coating agents (SDS) as an ionic surfactant and polyvinylpyrrolidone (PVP) as a hydrophilic polymer). SEM images showed adsorption of the particles, evidenced by significant change in the rugosity of the rock surface while ZP measurements showed increased surface charge due to particle adsorption. The rock surface charge increased from −3.39 mV to −24.5 mV and −29.6 Mv, respectively for PVP and SDS coatings. Both results suggested irreversible adsorption of Fe_3O_4. The findings were consistent with previous FTIR results (Shalbafan et al., 2019) and studies carried out by Nwidee et al. (2017). Fig. 13a and b shows the effect of different Fe_3O_4 nanofluids concentrations on contact angle. Notably, increasing contraction improved wettability alteration and the performance of SDS coating was better than that of PVP and homogeneous Fe_3O_4. Due to the higher positive charge density of the SDS coating, which increases adsorption onto the rock surface. Thus, changing the surface energy leading to wettability alteration (Francisco et al., 2020). Furthermore, surface roughness and spreading behaviour resulting from structural disjoining pressure contribute to wettability alteration. With regard to the spreading behaviour of NPs on the substrate, Wasan and Nikolov (2003) proposed that 2D structuring/layering of NPs in the form of a wedge film gave rise to structural disjoining pressure (a force normal to the interface) is also a mechanism responsible for the detachment of oil from the solid substrate. In simple words, the disjoining pressure is the pressure required to overcome oil adhesion, and the same pressure pushes the particles forward to occupy and expel oil from the rock pores. Therefore, structural disjoining pressure is driving force behind nanofluid spreading. Experimental studies and theoretical calculations have indicated that the structural disjoining pressure is substantially magnified by the injection pressure and higher near the tip of the wedge compared to bulk solution (Chengara et al., 2004; Wasan et al., 2011; Kondiparty et al., 2012; Liu et al., 2012). The positioning of the particles within the wedge is function of the overall entropy of the dispersion (Nazari Moghaddam et al., 2015). Thus, the structural disjoining pressure increases with increasing electrostatic repulsion. In conclusion, the literature shows that Fe_3O_4 nanofluids, both homogeneous and modified, are promising candidates for wettability alteration. However, it is worth noting that unlike in the case of IFT reduction and emulsion stability, where increased concentration increases adsorption and performance. The case of wettability alteration is different because increased concentration, will intensify adsorption, leading to reduced porosity and permeability. Which in turn affects the overall recovery of oil and quantity of recoverable particles resulting from irreversible adsorption on the solid substrate. More research should therefore be focused on efficient coatings with minimal adsorption.

5.1.4. Sweep efficiency improvement

EOR sweeping efficiency is judged by the mobility ratio (M) which is the mobility of fluid displacement (nanofluid) to oil displacement. Mathematically, it can be expressed as,

$$Mobility\ ratio = \frac{K_{rd}}{K_{ro}} \times \frac{\mu_o}{\mu_d} \tag{9}$$

whereas k_r is relative permeability, μ is viscosity. Subscript 'd' and 'o' are fluid and oil displacement, respectively. All parameters are in units of consistency. M greater than 1 implies that the mobility of the fluid displacement is higher than that of oil, an adverse event known as viscous fingering, resulting in poor oil recovery (Kamal et al., 2015; James G. Speight, 2016; Tengku Mohd et al., 2016) Albeit, thermal recovery techniques are commonly used for heavy oil processing, non-thermal recovery techniques are first considered due to their relatively low cost and technical simplicity. However, given the extremely high viscosity of heavy oil, it is difficult to obtain M of less than one even when the viscosity of the injection fluid is increased using polymers. Fe_3O_4 nanofluids have the ability to simultaneously increase the viscosity of the injection fluid and also minimise heavy oil viscosity with or

without steam stimulation. The reduction however, is higher with steam stimulation due to the stronger effect of aquathermolysis which is catalysed in the presence of metal particles (Farooqui et al., 2015). Moreover, using either EM waves or a magnetic field, the viscosity and displacement path of Fe_3O_4 nanofluids could be regulated and controlled. Hence, improving sweeping performance and overcoming limitations induced by reservoir heterogeneity or other factors (Bahiraei and Hangi, 2015; Malekzadeh et al., 2016; Shekhawat et al., 2016; Huang et al., 2018).

5.1.4.1. Improving displacing fluid viscosity. It has been well documented that the presence of particles, even at low concentrations, in dispersion fluid greatly increases the viscosity of the dispersion fluid by minimising the mobility of neighbouring fluid molecules in dispersion (Mishra et al., 2014; Bashirnezhad et al., 2016; Abdullah et al., 2020; Agi et al., 2020e). In most studies, water and ethylene glycol are the chosen base fluid (Bashirnezhad et al., 2016). Rheological studies investigating the behaviour of Fe_3O_4 nanofluids have shown that increasing particle loading increases fluid flow resistance, resulting in increased fluid viscosity, and the nanofluids may exhibit Newtonian or non-Newtonian behaviour (Sharma et al., 2016; Anu and Hemalatha, 2016; Bashirnezhad et al., 2016; Murshed and Estellé, 2017). Wang et al. (2016) demonstrated how the viscosity of water increased by 22.5% in the presences of Fe_3O_4 owing to the enhancement of the internal shear impact of the particles. Kazemzadeh et al. (2018) compared the viscosity increment of different nanofluids with that of seawater. According to the results, at 0.05 wt% particle concentration, the viscosity increment was in the following order: Sea water < SiO_2 < TiO_2 < Fe_3O_4 < Fe_3O_4/SiO_2, < TiO_2/SiO_2. Abareshi et al. (2011) documented that α-Fe_2O_3/glycerol nanofluids were non-Newtonian and the non-Newtonian characteristics of the nanofluids was more apparent at high concentrations when the amount of aggregation was higher. According to the authors, increasing concentration reduced the distance between the particles and trapped a large amount of glycerol between them, resulting in less mobilisation. Syam Sundar et al. (2013) reported that Fe_3O_4/water within the concentration range of range of 0–2 wt% displayed Newtonian behaviour. Likewise, Khalil et al. (2019) comparing the mobility ratio and viscosity increment of Fe_3O_4 nanofluids with different coatings observed that in most cases, the nanofluids had Newtonian behaviour whereas hydrophilic coatings exhibited higher viscosities compared to hydrophobic and hydrophilic−lipophilic coatings. Similar observations was reported by Zhang and Han (2018). Their study suggest that water molecules are easily adsorbed by hydrophilic molecules to form a water layer around the particles. Thereby, increasing their radius which causes high interfacial resistance and hinder their mobility in the base fluid. Though nanofluids are able to increase fluid viscosity, several studies suggest that the incremental viscosity of the nanofluids plays a weak role in EOR (Izadi et al., 2019). This may change, if the particles are used in conjunction with polymers (Ali et al., 2020a,b,c) or a magnetic field. Comparing the incremental viscosity of Fe_2O_3, TiO_2 and SiO_2 on polyacrylamide polymer solutions, Khan et al. (2018) observed that the incremental viscosity of Fe_2O_3 and TiO_2 were more prominent than that of SiO_2 due to the higher thermal conductivity of the metal oxides. TiO_2 and Fe_2O_3 increased the viscosity of the polymer solution by 83.3% and 64.3%, respectively. The study also showed that in the presence of salts, ion-dipole interaction between cations and oxygen atoms on the surface of the particles reduced the attack of cations on the polymer molecules and further increased the effectiveness of the polymer solution. With regard to magnetic field, studies have shown that the viscosity of Fe_3O_4 nanofluids can substantially be increased with a magnetic field because the viscosity of Fe_3O_4 nanofluids increases with increasing magnetic induction (Gontijo and Cunha, 2015; Cunha et al., 2016; Mohammadfam et al., 2020). A magnetic field changes the fluid rheology by inducing the formation of chain like structures called magneto-viscous effect. Wang et al. (2016) explained that the suspended particles follow the direction of a magnetic line and form chainlike structures which increases the flow resistance (Sun et al., 2020). Rangsanga and Sirisathitkul (2019) demonstrated how the presence of a small magnetic field of 142 OE improved the viscosity of Fe_3O_4 nanofluid fluid by 16.2%. Similarly, Malekzadeh et al. (2016) showed that the viscosity of Fe_3O_4 nanofluids increased by 20% and 175% for $\phi = 0.1$ vol% and $\phi =$ 1 vol%, using a magnetic field strength of 130 and 550 Gauss, respectively. Divandari et al. (2019) also demonstrated how the presence of a magnetic field improved the oil recovery of Fe_3O_4 @citric acid beyond that of polymer solutions due to higher shear viscosity of the nanofluids. Fig. 14 shows a comparison of flooding results between IONPs and polymer solutions in the presence of different magnetic fields.

5.1.4.2. Decreasing heavy oil viscosity. The research paradigm of using NPs in heavy oil reduction focuses on the removal of asphaltene and acting as a catalyst to break down the structure of the heavy oil (Fakher et al., 2018; Freitag, 2018; Xu et al., 2018; Struchkov et al., 2019). Asphalt is a homogenised solid product with a very high molecular weight that is mainly composed of carbon, hydrogen, nitrogen, oxygen, and sulphur molecules (Nwadinigwe et al., 2015; Mozaffari et al., 2018; Struchkov et al., 2019). Heavy oil contains a large amount of these asphalt molecules, which increases the viscosity of the oil, the asphalt molecules are also prone to aggregation and the creation of viscoelastic networks, which increases the oil viscosity. Such viscous heavy oil characteristics necessitates in-situ upgrading processes prior to extraction (Liu et al., 2019). The two prominent ways in which metals decrease heavy oil viscosity are exothermic chemical reactions and thermal conductivity enhancement. Exothermic chemical reactions are considered the driving energy behind catalytic activities while thermal conductivity enhancement improves heat transfer. Fe_3O_4 NPs mainly reduces heavy oil viscosity by reducing asphaltene interaction and restraining the formation of viscoelastic network (Betancur Camilo et al., 2016). Specifically, at low temperatures (<100 °C), Fe_3O_4 breaks down carbon -sulphur (C–S) bonds in asphaltene molecules (Nassar et al., 2015). The Breakdown of the C–S bonds reduces the average molecular weight and increases the aromatic and saturated groups of crude oil. Hascakir et al. (2008) demonstrated how micron iron powders decreased crude oil viscosity up to 88% when the polar components were broken down. Shokrlu and Babadagli (2010) stated that nano-sized Fe_3O_4 had higher viscosity reduction capabilities compared to micron sized Fe_3O_4 due to the larger specific surface area of NPs which resulted in more reactivity. Aristizábal-Fontal et al. (2018) reported that Fe_3O_4 NPs decreased the viscosity of heavy oil by up to 81%. According to their results, the Fe_3O_4 NPs easily adsorbed and split C–S asphalt molecules. Besides, the C–S breakdown catalytic effect of Fe_3O_4, researchers have also observed that other exothermic chemical reactions such as the rusting of Fe, formation of components like iron sulphide and chelate among others, may occur as the reaction proceeds. All these lead to further dissociation of chemical bonds in the oil component. For instance, studies carried out by Hasçakir et al. (2010) showed that exothermic chemical reactions such as the rusting of Fe produces local heat at the intermolecular level (Equation (10)) and according to Patel et al. (2018) the dissociation energy of asphaltene heteroatoms C–S, carbon-nitrogen (C–N), and carbon-oxygen (C–O) are 713, 750, and 1076 kJ/mol, respectively. Thus, the heat generated (1644 kJ) is sufficient to breakdown the C–N and C–O bonds of asphaltene molecules in crude oil.

$$4Fe_{(s)} + 3O_{2(g)} + xH_2O_{(l)} \rightarrow 2Fe_2O_3.xH_2O_{(s)} + \text{heat}\ \ (1644\text{kJ}) \quad (10)$$

At high temperatures (>100 °C), Fe_3O_4 aids in heat transfer and intensifies aquathermolysis. Aquathermolysis involves the application of specific temperature and pressure conditions to break down heavy oil molecular components. During aquathermolysis, several reactions such as pyrolyzing, hydrogenation and desulfurization take place (Li et al., 2019). Aquathermolysis reactions using water hydrolysis alone are

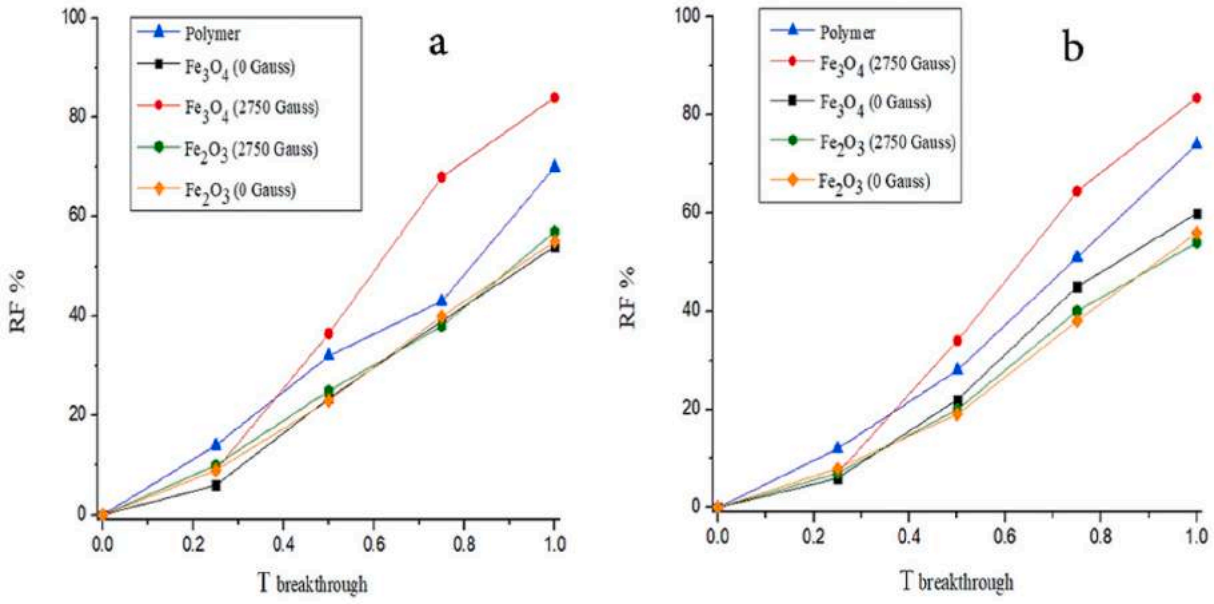

Fig. 14. Effect of polymer solution, Fe_2O_3 and Fe_3O_4 nanofluids on oil recovery factor a) heterogeneous micromodel and b) homogeneous micromodel. The presence of magnetic field improved the viscosity of Fe_3O_4 nanofluids resulting in incremental oil recovery beyond the reach of polymer solution (Divandari et al., 2019).

ineffective because asphalt heteroatoms interact with each other by means of hydrogen bonding or van der Waals forces and polymerize to form larger molecules (Iskandar et al., 2016a). Therefore, the presences of a catalyst is necessary. Hendraningrat et al. (2014) demonstrated the effectiveness Fe_3O_4 as catalysts. According to their results, the governing mechanism involved heat transfer associated with pyrolysis and catalytic bond fission. Lin et al. (2018) demonstrated the catalytic aquathermolysis behaviour of Fe_3O_4/zeolite NPs, in which the synthetic catalyst effectively decreased heavy oil viscosity by up to 85% through the breakdown of C–S asphalt bands and decomposition into smaller molecules. Similarly, Nugraha et al. (2013) showed that the viscosity of the heavy oil further decreased by 30% in the presence of Fe_3O_4 NPs during aquathermolysis. In aquathermolysis, Fe_3O_4 NPs serves as a hydrogen donor and aids in the transfer of hydrogen from steam to oil. This improves the hydrolysis of C–S bonds. Besides, the immediate viscosity reduction, it decreases viscosity regression. In the absence of sufficient hydrogen molecules, active chains which are produced as by-product of aquathermolysis can react with each other to create a high molecular weight chain leading to viscosity regression. But in the presence of sufficient hydrogen, the active chains will react with the hydrogen to produce a lower molecular weight chain (Iskandar et al., 2016a). Owing to the several physicochemical reactions that occur during viscosity reduction in the presence of Fe_3O_4 NPs, the influence on increasing particle concentration on viscosity reduction is still not clear in the literature. For instance, Gomaa et (2018b) and El-hoshoudy et al. (2019) observed that maximum viscosity reduction occurred at high concentrations due to improved catalytic activity. Hence, increasing concentrations improved the extent viscosity reduction. On the other hand, Afzal et al. (2014) and Shokrlu and Babadagli (2010) observed that maximum viscosity reduction occurred at low concentrations since the particles act as catalysts in the reactions. Hence, increasing concentrations reduces the extent of viscosity reduction, because the mechanism responsible for viscosity increment was more dominant. From a physicochemical point of view, it is reasonable to assume that at low concentrations the NPs might not be enough for catalytic reactions and at high concentrations, aggregation will dominate intermolecular and catalytic reactions resulting to increased viscosity. Therefore, maximum efficacy would be at an optimum concentration depending on particle size and/or asphalt molecules, as some studies suggest that the optimum concentration is related to the quantity of asphalt molecules in crude oil, while others suggest that it is a function of particle size and temperature (Shokrlu and Babadagli, 2014; Patel et al., 2018). Furthermore, Fe_3O_4 NPs reduce the total energy required for heat transfer and improve the efficiency of thermal recovery methods such as electrical/electromagnetic heating. The Low thermal conductivity of heavy oil limits the transfer of heat during thermal recovery methods. However, the presence of Fe_3O_4 NPs in oil increases the heat distribution due to high thermal conductivity of the particles. The small sizes of the NPs allow free movement, micro-convection and faster dispersion of heat. Moreover, the number of atoms on the surface of particles are very high compared to those in the inner surface so there are plenty of electrons available for heat transfer (Khatke et al., 2017; Tawfik, 2017) Researchers agree that increasing particle concentration and temperature improves the thermal enhancement of Fe_3O_4 NPs, leading to oil viscosity decrease (Sundar et al., 2014; Sarbolookzadeh Harandi et al., 2016; Jamilpanah et al., 2017; Hussain et al., 2020). However, materials with high thermal conductivity are not always effective in decreasing oil viscosity (Gu et al., 2013; Song et al., 2018). Therefore, it should not be considered as a decisive factor for oil viscosity reduction. All things being considered Fe_3O_4 NPs can facilitate heavy oil viscosity reduction in both low and high temperatures.

5.1.4.3. Preventing asphaltene precipitation. The precipitation of asphalt is a process in which asphalt molecules leave the oil as a solid particle. It occurs due to change in temperature, pressure and composition of crude oil during oil recovery. Asphaltene precipitation and deposition alters rock wettability, causes pore plugging, decreases effective permeability, and reduces oil recovery (Doryani et al., 2016; Shen and Sheng, 2018; Fakher et al., 2019). In some cases it may lead to formation damage (Taheri-Shakib et al., 2018). Accordingly, a solution to eliminate or reduce asphaltene precipitation is crucial for EOR. So far, experimental studies have shown that a significant amount of asphaltene can be adsorbed by Fe_3O_4 NPs within a short period of time (Nassar et al., 2011; Kazemzadeh et al., 2015; Khamarui et al., 2015). Asphaltene precipitation can therefore be minimized during oil recovery using IONPs. The robust absorbance ability Fe_3O_4 NPs is the result of unpaired electrons which promote electron pairing (Iskandar et al., 2016b). In multiple studies, Setoodeh et al. (2018a, b, 2020) compared the adsorption efficiency of Fe_3O_4 NPs having different coatings. The asphaltene adsorption of the coatings from the highest to the least was in the following

order: Fe_3O_4/polythiophene > Fe_3O_4/metal-organic framework > Fe_3O_4/Graphene oxide > Fe_3O_4/chitosan > Fe_3O_4 > Fe_3O_4/SiO_2. Shayan and Mirzayi (2015) also compared the asphaltene adsorption speed of maghemite (MNPs) and hematite (HNPs) nanofluids. The results indicated that the adsorption of asphalt onto HNPs was faster than that of MNPs, but the overall adsorption capacity of MNPs was higher than that of HNPs. The measured Gibbs free energies, entropies and enthalpies also showed that the adsorption of MNPs was endothermic while that of HNPs was exothermic.

5.2. Application of magnetic and electromagnetic waves in EOR

Eco-friendly techniques such as the application of magnetic fields and EM waves have been proposed for oil recovery enhancement. Magnetic fields and EM waves are introduced to magnetized water (MW), magnetic and/or dielectric nanofluids to improve oil recovery (Esmaeilnezhad et al., 2017; Kashif and Puspitasari, 2017). Albeit it has been established that EM waves and magnetic fields improve oil recovery by improving the sweeping efficiency (Yahya et al., 2012, 2014bib_Yahya_et_al_2012, 2014; Soleimani et al., 2016). More recently, studies have shown that additional oil recovery pathways such as wettability alteration, IFT reduction and breakthrough time are also enhanced in the presence of a magnetic field. The presence of a magnetic field not only improves oil recovery but also speed-up recovery process. Hosseini et al. (2019a, 2019b) investigated the effect of magnetic field on wettability alteration and IFT reduction. Their results showed that the presence of a magnetic field speed-up imbibition and substantially decreases the contact angle of water-wet and oil-wet carbonate rocks. Similarly, Amrouche et al. (2019, 2020) observed that the rate of spontaneous imbibition increased by about 8.5 times in the presence of a magnetic field. Streaming potential measurements indicated that dynamic change in surface potential was responsible for wettability alteration and water imbibition into the rock pores. In other words, the presence of magnetic field influenced the reservoir rock physicochemical properties and strengthen the electrostatic interactions between the nanofluids and rock surfaces. Based on their findings, the authors proposed a new parameter ΔT for disjoining pressure measurements. Wherein ΔT is time difference between droplet removal (initial time before the introduction of seawater, NPs, magnets or any EOR technique) and time required for removal due to disjoining pressure. In conclusion, magnetic fields in the presence of IONPs improves oil recovery by increasing nanofluid viscosity, decreasing oil viscosity and enhancing wettability alteration. The influence of IFT is negligible. EM waves on the other hand are effective in improving IFT reduction by creating a disturbance at the oil-water interface (Zaid et al., 2014; Esmaeilnezhad et al., 2018; Zhou et al., 2020). When IONPs are adsorbed at the O/W interface or localized in emulsion, and exposed to EM waves, the resultant particle movements displace the interface due to pressure waves, resulting to incremental oil recovery. Ryoo et al. (2012) explained that the interfacial displacement is caused by acoustic pressure waves produced in the rock pores containing the NPs at the oil-water interface. Thus, the EM waves effectiveness is highly dependent on interface particle adsorption. Table 4 shows a summary of viscosity enhancement, IFT reduction, and wettability alterations results leading to incremental oil recovery using IONPs.

5.3. Comparison of IONFs with other nanofluids

Despite the potential and favourable advantages of IONPs in EOR application, the literature is sparse. The plausible reason behind this is that a number of researchers suggest that the potential of its oil recovery is inferior to other NPs, especially SiO_2 (Haroun et al., 2012; Fakoya and Shah, 2017; Hassani et al., 2020). This review shows that the effectiveness of bare IONPs relative to other NPs is still arguable and cannot be fully established from the available literature. Firstly, they are only a few studies comparing the extent of IONPs oil recovery mechanism in

Table 4
Summary of viscosity enhancement, IFT reduction, and wettability alterations results leading to incremental oil recovery using IONPs.

IONPs	Conc.	Dispersant	Porous Medium	Nanofluid Viscosity or Oil Viscosity		IFT		Contact Angle		Oil Recovery	Author
				Before	After	Before	After	Before	After		
Fe_3O_4@ cetyltrimethyl ammonium bromide (CTAB)		NaCl + barium (Ba^{2+})	Calcium carbonate grains	–	–	30 mN/m	1 mN/m	90°	<30°	35%	Pereira et al. (2020)
Fe_3O_4 20–40 nm	1 wt%	NaCl 4 wt%	–	–	–	28 mN/m	17 mN/m	–	–	–	Divandari et al. (2020)
Fe_3O_4@SiO2@Xanthan	1500 ppm	DI water	Carbonate rocks	0.89 cp	1.93 cp	28.3 mN/m	8.6 mN/m	134°	34°	–	Ali et al. (2020a)
Fe_3O_4	0.05 wt%	Brine 11,000 ppm	Sandstone			40 mN/m	31 mN/m	–	–	–	Ali et al. (2020b)
Fe_3O_4@citrate -polymer 47 nm	400 ppm	Seawater	Sandstone	0.99 cp	1.08 cp	11.23 mN/m	7.92 mN/m	160°	114°	>25%	Izadi et al. (2019)
Fe_3O_4@ citric 20–26 nm	0.8 wt-2 wt%-	NaCl 5000 ppm	Micromodel	–	–	37.47 mN/m	16.71 mN/m	106°	41°	22%	Divandari et al. (2019)
Fe_2O_3 50 nm	1.0 wt %.	NaCl 35,000 ppm	Sandstone	9.00 cp	6.03 cp	37.9 mN/m	41%	–	–	19.6%	El-hoshoudy et al. (2019)
Fe_3O_4 @carbon 60 nm	100 mg L−1	2000 mg L−1surfactant	Sandstone	–	–	24.3 mN/m	1 × 10−4 mN/m	54°	10°	30%	Betancur et al. (2019)
Fe_3O_4@SiO_2 30 nm	0.05 wt%	Seawater	Carbonate sands	1.09 cp	1.19 cp	39 mN/m	17.5 mN/m	137°	40°	24%	Kazemzadeh et al. (2019)
Fe_3O_4 15–20 nm	0.05 wt%	Seawater	Carbonate sands	1.09 cp	1.13 cp	39 mN/m	21.2 mN/m	137°	75°	21%	Kazemzadeh et al. (2018)
Fe_3O_4 @ Chitosan	0.03 wt%	seawater	Sand pack	264 cp	161 cp	22.49 mN/m	14.47 mN/m	145°	90°	10.8%	Rezvani et al. (2018)
Fe_3O_4 40 nm	0.01 wt%	1-hexadecyl-3-methyl	–	–	–	50.5 mN/m	<1 mN/m	–	–	–	Saien and Hashemi (2018)
Fe_2O_3 5 nm	1.0 wt %	NaCl 35,000 ppm	Sandstone	6.42 cp	2.02 cp	47.9 mN/m	<20 mN/m	–	–	45%	Gomaa et al. (2018a, 2018b)
Fe_3O_4 <80 nm	0.8 wt %	5000 ppm NaCl	Sandstone	–	–	–	–	50.44°	29.7°	15.38%	Esmaeilnezhad et al. (2018)

the literature. Secondly, within the available literature, it is difficult to compare the performance of the NPs due to far too many other factors, such as experimental conditions, particle characteristics and dispersing fluids, among others. Thirdly, some of the experimental data and results from different researchers are not consistent and even conflict with each other. Nevertheless, we present a comparison of the effect of bare IONPs against other NPs used in the same studies. Joonaki and Ghanaatian (2014) observed that Fe_3O_4 dispersed in propanol had the lowest performance compared to Al_2O_3 and SiO_2. The same trend was observed in all three scenarios of flooding experiments carried out by the authors (brine followed by nanofluids; propanol followed by nanofluids & nanofluids from the initial stage). On the other hand, spontaneous imbibition experiments carried by Ogolo et al. (2012), showed that Fe_3O_4 dispersed in either DI water or brine performed better than Al_2O_3, SiO_2 treated with silane, Ni_2O_3, magnesium oxide (MgO), ZnO, zirconium oxide (ZrO_2) and tin oxide (SnO). However, in the same study using the same NPs, flooding experiments showed that Al_2O_3 outperformed Fe_3O_4 when dispersed in DI water but when dispersed in brine Al_2O_3, SiO_2 and Ni_2O_3 outperformed Fe_3O_4 in the order listed above. Using a micromodel, Kazemzadeh et al. (2019) observed that Fe_3O_4 dispersed in brine (Persian Gulf Water) outperformed SiO_2 by controlling asphaltene precipitation. Contrary to these observations, in another study, using a micromodel and heavy oil with asphaltenes, the same author (Kazemzadeh et al., 2015) observed that SiO_2 dispersed in brine performed better than Fe_3O_4 dispersed in brine. In a more recent study, Amrouche et al. (2020) observed that Fe_3O_4 dispersed in DI water or seawater outperformed Al_2O_3, similar and in contrast to the results observed by Ogolo using spontaneous imbibition in DI water and brine, respectively. A feasibility study conducted by Gomaa et al. (2018b) comparing the net cost of oil recovery for Al_2O_3, NiO, zeolite, SiO_2, Fe_2O_3, tungsten trioxide, and montmorillonite with the main variable being nanomaterial cost and concentration revealed that Fe_3O_4 was the most economical with the highest oil recovery amongst the selected nanomaterials. All things being considered; it seems reasonable to conclude that the performance of Fe_3O_4 depends on the dispersion fluid, type of oil and reservoir contact time. Fig. 15 shows a summary of the different results obtained in the same studies comparing Fe_3O_4 with other NPs. With regard to the potential application of Fe_3O_4 nanofluids for oil recovery, it can be concluded that Fe_3O_4 nanofluids are cost effective for EOR applications due to the following reasons. (i) Low synthesis cost when compared to other NPs with synthesis methods that require heat. Fe_3O_4 NPs can be synthesised at room temperature (Sharma et al., 2020) using inexpensive precursors (Srivastava et al., 2011). (ii) Easy modification routes (Wu et al., 2008a; 2015; Ali et al., 2016a,b) (iii) Suitable oil recovery, 5/7 of the comparison results showed that Fe_3O_4 had the highest oil recovery (Ogolo et al., 2012; Joonaki and Ghanaatian, 2014; Tarek, 2015; Gomaa et al., 2018a; Kazemzadeh et al., 2015, 2019bib_Kazemzadeh_et_al_2015, 2019; Amrouche et al., 2020). (iv) Multiple technological functionalities to improve oil recovery (Servin et al., 2016; Hosseini et al., 2019a,b; Khalil et al., 2019; Amrouche et al., 2020; Zhou et al., 2020) and (v) Recycling opportunities to save cost and environment (He et al., 2020a; Adewunmi et al., 2021; Jamsaz et al., 2021; khalilifard and Javadian, 2021).

6. Reservoir transportation and retention of IONPs

Despite the remarkable potential of IONFs in the petroleum industry, successful usage and recycling depends on their ability to mobilize oil from the point of injection to production wells. However, the physico-chemical interactions between the particles, sand (SiO_2) and rock grains rock grains can cause substantial retention and pore plugging in the smallest regions of the pore spaces. The mechanisms of particle retention in the porous media include reversible and irreversible adsorption to the rock-oil-water interfaces and straining attachment to the rock surfaces. Via particle collision and attachment to grain surfaces which are a function of chemical and physical characteristics of the particles and rock surfaces as well as the solution chemistry. However, the main retention mechanism of concern is irreversible attachment to the rock grain surfaces and straining. An irreversible process in which particles (or particle aggregates) are retained in the porous media at the pore throats that are too small to allow them to be transported. Leading to reduced permeability which may lead to harsh formation damage (Yuan et al., 2017). Rock grain surface retention can be predicated using a constant first-order attachment rate coefficient. However, when both the suspension and rock grain surfaces have repulsive forces, the predicted coefficients have been found to be underestimated. Thus, the DVLO is extensively used to interpret and predict the deposition and retention of particles by cellulating the interaction energies between the particles and rock surfaces (Gomez-Flores et al., 2020). Although, most studies use conventional methods to calculate particle concentration after

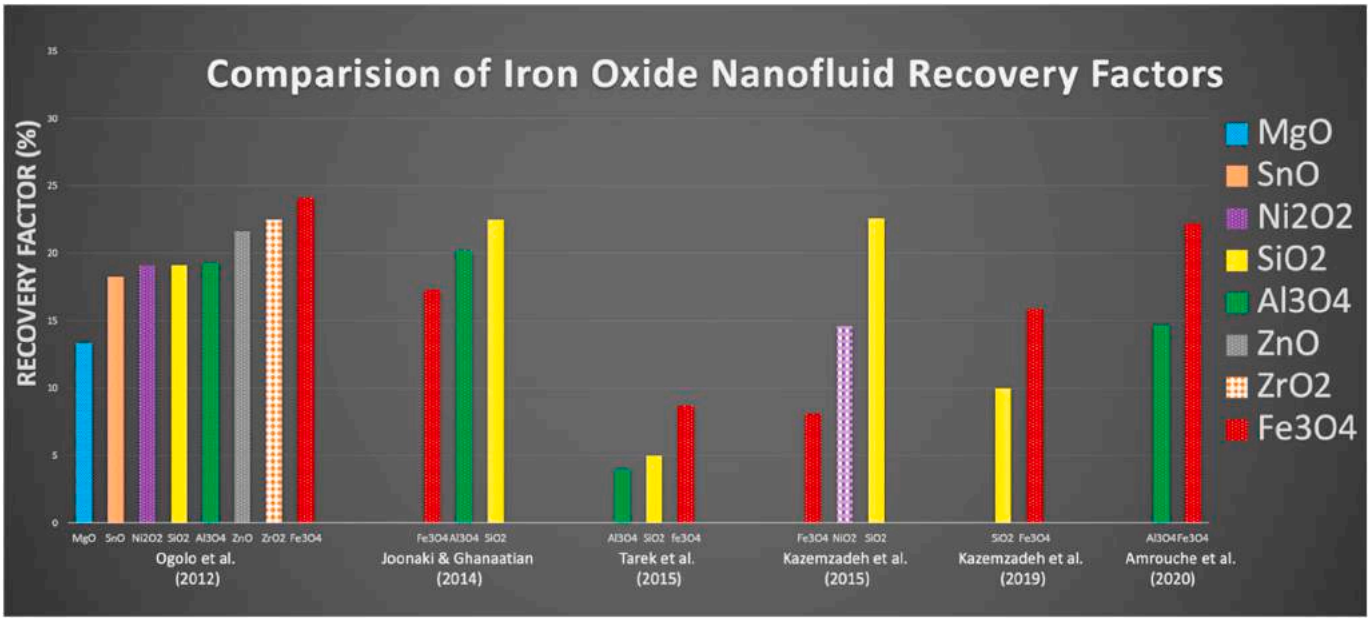

Fig. 15. Experimental results of the comparison between the recovery factor of IONPs and other NPs (Ogolo et al., 2012; Joonaki and Ghanaatian, 2014; Tarek, 2015; Kazemzadeh et al., 2015, 2019bib_Kazemzadeh_et_al_2015, 2019; Amrouche et al., 2020).

breakthrough (Yu et al., 2010; Esfandyari Bayat et al., 2015; Al-Anssari et al., 2017a). They often fail to predict transport measurements due to changes in particle deposition which can occur over the length of long reservoir travel time. These length dependant variations have significant scaling-up implications. Experimental studies carried out by Lakshmanan et al. (2015) to quantify the retention of Fe_3O_4 nanofluids using MRI surface interactions and DLVO theory showed that dispersion coefficient decreased with distance whereas deposition rate constants and fast deposition rate constants increased with distance. In other words, particle concentration decreases whereas deposition acceleration increases with reservoir travel time. Therefore, novel non-invasive laboratory techniques are required to fully understand and view the transport phenomena of nanofluids under reservoir conditions. Harsh reservoir conditions such as high pressure, high salinity (>1 M ion strength), the presence of divalent salts (Ca^{2+} and Mg^{2+}) and high temperatures (150 °C) also present unique challenges for the stabilization transportation and retention of nanofluids in the porous medium. Amongst the aforementioned parameters, salinity has the most devastating effect on the transport, retention and oil recovery system of IONFs compared to pressure and temperature (Khalil et al., 2019; Shalbafan et al., 2019, 2020abib_Shalbafan_et_al_2019bib_Shalbafan_et_al_2020a). Laboratory scale experiments show that the mobility of NPs increases with temperature while increasing salinity increases particle retention due to the screening effect of electrolytes (Al-Anssari et al., 2017b). IONFs cannot form stable dispersions in reservoir salinity without any functional groups and the hydrophilic nature of IONPs intensifies depositions and retention. Stabilized and hydrophobic treatment significantly improves mobility and reduces retention in the porous medium Therefore, surface treatment of IONPs is a necessity for reservoir applications. In most studies amina groups, polymers and citrate have been used to decrease retention. Yu et al. (2010) documented the transportation of Fe_3O_4@citrate NPs in sandstone and carbonate porous media. Experimenting with several pore volumes showed that there was very little retention (<5%) even at high concentration (10 wt%) and high salinity (3 wt% NaCl.). Citrate coating provided ample electrostatic repulsion between the particles and the negatively charged sandstone and carbonate porous media. Bagaria et al. (2013) documented low adsorption (<2.2 mg/m^2, <1.1% monolayer coverage) of Fe_3O_4 @ sulfonated copolymer on silica grains at high salinity of 8% wt% (NaCl) and 2% wt ($CaCl_2$). Izadi et al. (2019) reported stable transportation of Fe_3O_4 nanofluids at salinities of up to (256,000 ppm) and temperature (85 °C) without any aggregation. Due to citric acid and anionic polyelectrolyte polymer functionalization which imparted steric, electrostatic and electro steric stabilization. Park et al. (2014) compared the effectiveness of citric acid and PEG coatings in reducing particle retention on SiO_2 and carbonate rocks. According to their findings, the particle retention of PEG coatings was ~10% less than that of citric acid coatings. The recovery percentages of PEG coatings in SiO_2 sands below 10 mM salt concentrations were almost 100% in all pH conditions, while in calcium carbonate sands, the recovery percentages were around 10–30% in all pH and salt conditions. Fig. 16 illustrates the recovery percentage of citric acid and PEG coatings and the impact of reservoir chemistry (pH & salinity) on particle recovery. According to the results, the particle retention of Fe_3O_4 with PEG/citric acid coatings in the presence of reservoir salinity and/or calcium carbonate sands are still high. Likely, due to irreversible adsorption or sedimentation caused by NP instability.

7. Challenges and opportunities

Despite the extensive technological advances made in medical and biomedical applications utilizing IONPs, the technologies cannot be used directly in reservoir conditions. Unlike the human body, where temperature and salinity are almost constant, reservoir temperature and salinity are extreme. Consequently, the fundamental challenge which may hinder the application of IONPs in the petroleum industry is the limited inherent stability, where particle agglomeration can lead to loss

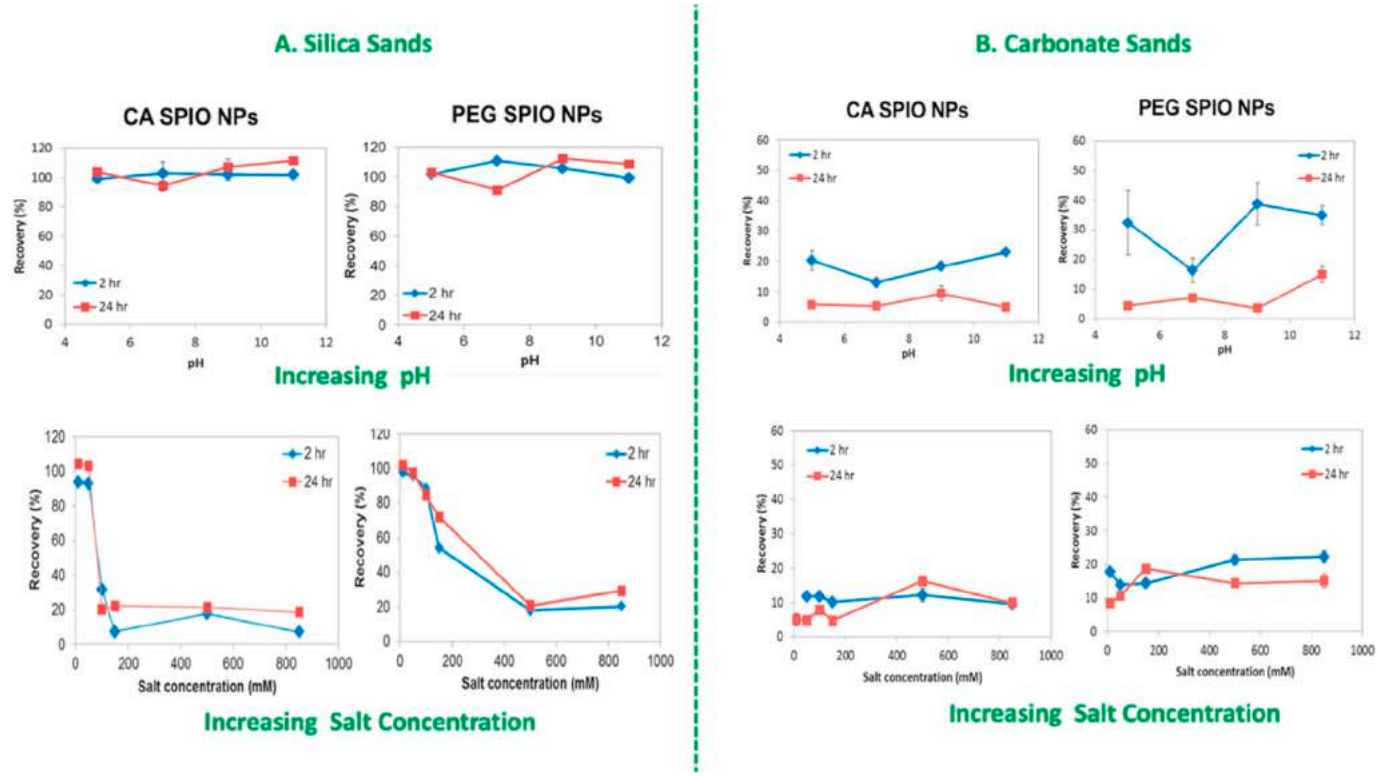

Fig. 16. (A) Recovery percentages of Fe_3O_4 coated with citric acid and PEG from SiO_2 sands after 2 and 24 h at various pH and salt concentrations (B) recovery percentages of Fe_3O_4 coated with citric acid and PEG from calcium carbonate sands after 2 and 24 h at various pH and salt concentrations. (concentration of salts = 10 mM at variable pH while pH = 7.5 at variable salt concertation) (Park et al., 2014).

of properties and transportability under reservoir conditions. The crucial pre-requisites to meet reservoir application are (i) IONPs should remain evenly distributed in the injected fluid without aggregates, (ii) IONPs should be able to propagate a long distance deep inside the reservoirs with minimal retention and (iii) IONPs should be applied to specific and desired locations in the reservoir, such as oil-water interfaces. The aforementioned requirements may be fulfilled by adding a specific coating of particular polymer, surfactant or SiO_2 which has demonstrated minimal retention. However, more research in particle retention models which considers adsorption due to reservoir travel time is needed to accurately predicate recoverability of IONPs in the reservoir. Other challenges that may also apply to IONPs are as follow:

1. **Controlling Physicochemical Properties and Storage:** Precise control of particle size, dispersion and surface coatings still appears to be a stumbling block that could lead to unfavourable physicochemical properties. In addition, bare Fe_3O_4 tends to oxidize easily in the air to form maghemite (γFe_2O_3) and therefore loses some magnetic properties. Long-term storage may also result in a loss of physicochemical properties. More research is needed on surface modification technology which will help in maintaining the physicochemical properties of NPs over long period of time.
2. **Economic Feasibility and Scalability**: Compared to bulk (micron scale) materials, NPs are costly to produce due to the relatively high embodied energy required to produce a unit mass of the material within the nanoscale domain (Ali et al., 2016; Alsaba et al., 2020). According to a study that examined the energy consumption and greenhouse gas emissions implications of producing nanomaterials, most nanomaterials had a relatively higher cost of production when compared to their bulk counterpart. Owing to the fact that production involves an energy-intensive synthesis process or an additional mechanical process to reduce particle size (Kim and Fthenakis, 2013). Therefore, the major cost of synthesizing IONPs can be linked to heat consumption. To that end, a study comparing the economics and scalability of producing IONPs suggested that co-precipitation and micro emulsion approaches are the most cost-effective methods for scalability (Augusto et al., 2020). These synthesis methods require a reaction temperature of 20–90 °C (Augusto et al., 2020). Precisely, the co-precipitation approach is a proven scalable method with reaction occurring at room temperature. Moreover, in EOR applications, magnets have similar benefits with chemicals and the presence of a magnetic field considerably decreases the quantity of IONPs required. In addition, the recycling opportunity and ability to simultaneously incorporate more than one function into the NPs suggest it is a cost-effective choice (Servin et al., 2016; Amrouche et al., 2020; Adewunmi et al., 2021)
3. **Health and Safety:** NPs can surreptitiously enter into the environment through water, soil, or air and certain toxicities have been associated with these NPs. Therefore, basic knowledge of their toxicity and effects is a prerequisite for handling nanomaterials. The same manner exposure to fine particulate matter (PM2.5, particles with a diameter of less than 2.5 μm) can infiltrate the lung, irritate and corrode the alveolar wall, consequently impairing lung function (Xing et al., 2016). Nanomaterials inhaled can effortlessly reach deep into the lungs, bloodstream and other sites in the human body including the liver, heart, or tissues and exert reactivity as toxicology effects (Khan et al., 2019). Moreover, their small sizes facilitate translocation of active chemical species from organismal barriers such as the skin, lung, body tissues and organs causing irreversible oxidative stress, organelle damage, asthma, and cancer (Jeevanandam et al., 2018; Khan et al., 2019). Studies comparing the effects of submicron sized and nanosized Fe_3O_4 show that the small sizes and large surface area of the NPs generally induce greater neurotoxicity to the nervous system compared to submicron sized particles (Wang et al., 2008; Zhu et al., 2008). Therefore, their small size and high reactivity, could be potential lethal factors unusual in micron-sized counter parts. Research advancements which have reported acute toxic effects of IONPs in living systems suggest that it is dose dependent (Nations et al., 2011; Jeevanandam et al., 2018; Vidya and Chitra, 2019). It was reported that small doses of iron on a typical male adult may not cause iron-related toxicity because the adult human has an entire body iron reserve of about 4000 mg. However, large doses may cause an increase in plasmatic iron concentration as a result of the surpassed transferrin iron binding capacity, resulting in oxidative stress and a variety of toxicities, including cardiac and hepatic toxicity (Reddy et al., 2012). On the other, in aquatic systems, especially microbes and invertebrates, exposure to as low as 1 mg/L concentrations have been reported to cause haematological and biochemical growth deficits (Saravanan and R Suganya, 2011; Nations et al., 2011). Likewise, exposure to high concentrations of up 1000 mg/L was reported to induce developmental and growth abnormalities but no mortality (Li et al., 2009). Therefore, from a toxicological standpoint, IONPs are considered toxic. However, relative to other magnetic NPs, (Fe_3O_4 & γFe_2O_3), have garnered a lot of interest, especially in medical and pharmaceutical areas because of their least toxicity and biological compatibility. Therefore, they are employed in a variety of biological applications, including protein immobilisation, MRI, thermal therapy, and drug administration (Reddy et al., 2012; Shokrollahi, 2013; Ulbrich et al., 2016; Natarajan et al., 2019).
4. **Field Trials:** Most oilfield nanotechnology studies are based on potential applications using numerical simulation and laboratory experiments. There has been no field trail for the application of IONPs in EOR, and only a few field trials using other NPs have been reported (Hassani et al., 2020). Synergy between researchers and oil cooperation is therefore recommended in order to facilitate field trials and the advancement of nanotechnology in the oil and gas industry.

8. Conclusions

In this review, critical information on the properties, formulation and application of IONPs in oil recovery is depicted. The oil recovery mechanism of IONPs were discussed in detail and compared with other NPs. The results offer prospects for field application and the drawbacks opened opportunities for research. From the findings of this review the resulting conclusions were made.

1. The bottom-up approach offers superior control and flexibility. Likewise, co-precipitation is the ideal method for oil recovery applications of IOPNs owing to its simplicity, minimal energy requirement, and ease of large-scale reproducibility.
2. The growth process determines the final size, particle distribution and shape of the IONPs. Hence, to attain monodispersed particles, nucleation should be avoided during the period of growth.
3. Experimental results indicate that the mechanism of IFT reduction dictates that IONPs form a monolayer between the oil-water interfaces, and the contact angle at the oil-water interface determines the degree of IFT reduction.
4. Literature review shows that unlike in IFT reduction and emulsion stability, where increased concentration increases adsorption and performance, in wettability alteration increased concentration, intensify adsorption, leading to reduced porosity, permeability and overall oil recovery.
5. Salinity has the most devastating effect on the transport, retention and oil recovery system of IONFs compared to pressure and temperature. Hence, for stable dispersion of IONPs in reservoir salinity surface treatment of IONPs is a necessity for reservoir condition applications.
6. It can be concluded from this study that the high recovery rate of IONPs makes it economically feasible and has potentials for oil field applications.

Declaration of competing interest

The authors declare that they have no known competing financial interests or personal relationships that could have appeared to influence the work reported in this paper.

Acknowledgement

This work was supported by Ministry of Higher Education (MOHE), Malaysia (Q.J130000.3551.07G12; R.J130000.7851.5F030; Q.J1300003551.06G68; R.J1300007351.4B545).

References

Abareshi, M., Sajjadi, S.H., Zebarjad, S.M., Goharshadi, E.K., 2011. Fabrication, characterization, and measurement of viscosity of α-Fe2O3-glycerol nanofluids. J. Mol. Liq. 163 (1), 27–32. https://doi.org/10.1016/j.molliq.2011.07.007.

Abdullah, A.M., Chowdhury, A.R., Yang, Y., Vasquez, H., Moore, H.J., Parsons, J.G., Lozano, K., Gutierrez, J.J., Martirosyan, K.S., Uddin, M.J., 2020. Tailoring the viscosity of water and ethylene glycol based TiO2 nanofluids. J. Mol. Liq. 297, 111982. https://doi.org/10.1016/j.molliq.2019.111982. Elsevier B.V.

Adewunmi, A.A., Kamal, M.S., 2018. April 23). Assessment of Fly Ash as a Potential Demulsifier for Highly Stable Water-In-Crude Oil Emulsion Produced in the Petroleum Industry. Society of Petroleum Engineers - SPE Kingdom of Saudi Arabia Annual Technical Symposium and Exhibition 2018. https://doi.org/10.2118/192364-ms. SATS 2018.

Adewunmi, A.A., Kamal, M.S., Solling, T.I., 2021. Application of magnetic nanoparticles in demulsification: a review on synthesis, performance, recyclability, and challenges. J. Petrol. Sci. Eng. 196, 107680. https://doi.org/10.1016/j.petrol.2020.107680. July 2020.

Afzal, S., Nikookar, M., Ehsani, M.R., Roayaei, E., 2014. An experimental investigation of the catalytic effect of Fe2O3 nanoparticle on steam injection process of an Iranian reservoir. Iranian J. Oil Gas Sci. Technol. 3 (2), 27–36. https://doi.org/10.22050/ijogst.2014.6033.

Agi, A., Junin, R., Gbadamosi, A., 2018. Mechanism governing nanoparticle flow behaviour in porous media: insight for enhanced oil recovery applications. Int. Nano Lett. 8 (2), 49–77. https://doi.org/10.1007/s40089-018-0237-3.

Agi, A., Junin, R., Abbas, A., Gbadamosi, A., Azli, N.B., 2020a. Effect of dynamic spreading and the disperse phase of crystalline starch nanoparticles in enhancing oil recovery at reservoir condition of a typical sarawak oil field. Appl. Nanosci. 10 (1), 263–279. https://doi.org/10.1007/s13204-019-01102-5.

Agi, A., Junin, R., Abdullah, M.O., Jaafar, M.Z., Arsad, A., Wan Sulaiman, W.R., Norddin, M.N.A.M., Abdurrahman, M., Abbas, A., Gbadamosi, A., Azli, N.B., 2020b. Application of polymeric nanofluid in enhancing oil recovery at reservoir condition. J. Petrol. Sci. Eng. 194 (June), 107476. https://doi.org/10.1016/j.petrol.2020.107476.

Agi, A., Junin, R., Arsad, A., Abbas, A., Gbadamosi, A., Azli, N.B., Oseh, J., 2020c. Ultrasound-assisted weak-acid hydrolysis of crystalline starch nanoparticles for chemical enhanced oil recovery. Int. J. Biol. Macromol. 148, 1251–1271. https://doi.org/10.1016/j.ijbiomac.2019.10.099.

Agi, A., Junin, R., Gbadamosi, A., Manan, M., Jaafar, M.Z., Abdullah, M.O., Arsad, A., Azli, N.B., Abdurrahman, M., Yakasai, F., 2020d. Comparing natural and synthetic polymeric nanofluids in a mid-permeability sandstone reservoir condition. J. Mol. Liq. 317, 113947. https://doi.org/10.1016/j.molliq.2020.113947.

Agi, A., Junin, R., Jaafar, M.Z., Mohsin, R., Arsad, A., Gbadamosi, A., Fung, C.K., Gbonhinbor, J., 2020e. Synthesis and application of rice husk silica nanoparticles for chemical enhanced oil recovery. J. Mater. Res. Technol. 9 (6), 13054–13066. https://doi.org/10.1016/j.jmrt.2020.08.112.

Agi, A., Junin, R., Jaafar, M.Z., Sidek, M.A., Yakasai, F., Gbadamosi, A., Oseh, J., 2021. Formulation of bionanomaterials: a review of particle design towards oil recovery applications. J. Ind. Eng. Chem. https://doi.org/10.1016/j.jiec.2021.03.032.

Ahmed, S., Elraies, K.A., 2018. Microemulsion in enhanced oil recovery. In: Science and Technology behind Nanoemulsions. InTech. https://doi.org/10.5772/intechopen.75778.

Ahmed, N., Alam, M.S., Salam, M.A., 2020a. Experimental analysis of drilling fluid prepared by mixing iron (III) oxide nanoparticles with a KCl–Glycol–PHPA polymer-based mud used in drilling operation. J. Petrol. Exploration Production Technol. 10 (8), 3389–3397. https://doi.org/10.1007/S13202-020-00933-1, 2020 10:8.

Ahmed, N., Alam, M.S., Salam, M.A., 2020b. Experimental analysis of drilling fluid prepared by mixing iron (III) oxide nanoparticles with a KCl–Glycol–PHPA polymer-based mud used in drilling operation. J. Petrol. Exploration Production Technol. 10 (8), 3389–3397. https://doi.org/10.1007/s13202-020-00933-1.

Ahualli, S., Iglesias, G.R., Wachter, W., Dulle, M., Minami, D., Glatter, O., 2011. Adsorption of anionic and cationic surfactants on anionic colloids: supercharging and destabilization. Langmuir 27 (15), 9182–9192. https://doi.org/10.1021/la201242d.

Al-Anssari, S., Barifcani, A., Wang, S., Maxim, L., Iglauer, S., 2016. Wettability alteration of oil-wet carbonate by silica nanofluid. J. Colloid Interface Sci. 461, 435–442. https://doi.org/10.1016/j.jcis.2015.09.051.

Al-Anssari, S., Nwidee, L.N., Ali, M., Sangwai, J.S., Wang, S., Barifcani, A., Iglauer, S., 2017a. Retention of silica nanoparticles in limestone porous media. In: Society of Petroleum Engineers - SPE/IATMI Asia Pacific Oil and Gas Conference and Exhibition 2017, 2017-January. https://doi.org/10.2118/186253-ms.

Al-Anssari, S., Nwidee, L.N., Ali, M., Sangwai, J.S., Wang, S., Barifcani, A., Iglauer, S., 2017b. Retention of silica nanoparticles in limestone porous media. Society of Petroleum Engineers - SPE/IATMI Asia Pacific Oil and Gas Conference and Exhibition 2017, 2017-Janua. https://doi.org/10.2118/186253-ms.

Al-Shehri, A.A., Ellis, E.S., Servin, J.M.F., Kosynkin, D.V., Kanj, M.Y., Schmidt, H.K., 2013. Illuminating the reservoir: magnetic nanomappers. *SPE Middle East Oil and gas Show and conference*. MEOS, Proceedings 3, 2180–2189. https://doi.org/10.2118/164461-ms.

Al-Yasiri, M., W. A.-S.-A. J. of N. R., 2015. undefined. (2015). How the drilling fluids can be made more efficient by using nanomaterials. Citeseer 3 (3), 41–45. https://doi.org/10.11648/j.nano.20150303.12.

Ali, N., Zhang, B., Zhang, H., Li, W., Zaman, W., Tian, L., Zhang, Q., 2015a. Novel Janus magnetic micro particle synthesis and its applications as a demulsifier for breaking heavy crude oil and water emulsion. Fuel 141, 258–267. https://doi.org/10.1016/j.fuel.2014.10.026.

Ali, N., Zhang, B., Zhang, H., Zaman, W., Li, X., Li, W., Zhang, Q., 2015b. Interfacially active and magnetically responsive composite nanoparticles with raspberry like structure; synthesis and its applications for heavy crude oil/water separation. Colloid. Surface. Physicochem. Eng. Aspect. 472, 38–49. https://doi.org/10.1016/j.colsurfa.2015.01.087.

Ali, A., Zafar, H., Zia, M., Haq, I. ul, Phull, A.R., Ali, J.S., Hussain, A., 2016a. Synthesis, characterization, applications, and challenges of iron oxide nanoparticles. Nanotechnol. Sci. Appl. 9, 49–67. https://doi.org/10.2147/NSA.S99986.

Ali, A., Zafar, H., Zia, M., ul Haq, I., Phull, A.R., Ali, J.S., Hussain, A., 2016b. Synthesis, characterization, applications, and challenges of iron oxide nanoparticles. In: Nanotechnology, Science and Applications, vol. 9. Dove Press, pp. 49–67. https://doi.org/10.2147/NSA.S99986.

Ali, S., Khan, S.A., Eastoe, J., Hussaini, S.R., Morsy, M.A., Yamani, Z.H., 2018. Synthesis, characterization, and relaxometry studies of hydrophilic and hydrophobic superparamagnetic Fe3O4 nanoparticles for oil reservoir applications. Colloid. Surface. Physicochem. Eng. Aspect. 543, 133–143. https://doi.org/10.1016/j.colsurfa.2018.02.002.

Ali, A.M., Yahya, N., Qureshi, S., 2020a. Interactions of ferro-nanoparticles (hematite and magnetite) with reservoir sandstone: implications for surface adsorption and interfacial tension reduction. Petrol. Sci. 17 (4), 1037–1055. https://doi.org/10.1007/s12182-019-00409-w.

Ali, H., Soleimani, H., Yahya, N., Khodapanah, L., Sabet, M., Demiral, B.M.R., Hussain, T., Adebayo, L.L., 2020b. Enhanced oil recovery by using electromagnetic-assisted nanofluids: a review. J. Mol. Liq. 309, 113095. https://doi.org/10.1016/j.molliq.2020.113095. Elsevier B.V.

Ali, J., Manshad, A.K., Imani, I., Sajadi, S.M., Keshavarz, A., 2020c. Greenly synthesized magnetite@SiO2@Xanthan nanocomposites and its application in enhanced oil recovery: IFT reduction and wettability alteration. Arabian J. Sci. Eng. 1–11. https://doi.org/10.1007/s13369-020-04377-x.

Alnarabiji, M.S., Husein, M.M., 2020. Application of bare nanoparticle-based nanofluids in enhanced oil recovery. Fuel 267, 117262. https://doi.org/10.1016/j.fuel.2020.117262. November 2019.

Alsaba, M.T., Al Dushaishi, M.F., Abbas, A.K., 2020. A comprehensive review of nanoparticles applications in the oil and gas industry. J. Petrol. Exploration Production Technol. 10 (Issue 4), 1389–1399. https://doi.org/10.1007/s13202-019-00825-z. Springer.

Alvi, M.A.A., Belayneh, M., Bandyopadhyay, S., Minde, M.W., 2020. Effect of iron oxide nanoparticles on the properties of water-based drilling fluids. Energies 13 (24), 6718. https://doi.org/10.3390/en13246718.

Alvi, M.A.A., Belayneh, M., Fjelde, K.K., Saasen, A., Bandyopadhyay, S., 2021. Effect of hydrophobic iron oxide nanoparticles on the properties of oil-based drilling fluid. J. Energy Resour. Technol. 143 (4) https://doi.org/10.1115/1.4048231.

Amrouche, Farida, Gomari, S.R., Islam, M., Donglai, X., 2019. New insights into the application of a magnetic field to enhance oil recovery from oil-wet carbonate reservoirs. Energy Fuel. 33 (11), 10602–10610. https://doi.org/10.1021/acs.energyfuels.9b02296.

Amrouche, F., Gomari, S.R., Islam, M., Xu, D., 2020. Effect of magnetic field on physiochemical properties of carbonate reservoirs 2020 (1), 1–5. https://doi.org/10.3997/2214-4609.202010986.

Amrouche, Farida, Gomari, S.R., Islam, M., Donglai, X., 2020. A novel hybrid technique to enhance oil production from oil-wet carbonate reservoirs by combining a magnetic field with alumina and iron oxide nanoparticles. J. Clean. Prod. xxxx, 124891. https://doi.org/10.1016/j.jclepro.2020.124891.

An, C., Yan, B., Alfi, M., Mi, L., Killough, J.E., Heidari, Z., 2017. Estimating spatial distribution of natural fractures by changing NMR T2 relaxation with magnetic nanoparticles. J. Petrol. Sci. Eng. 157, 273–287. https://doi.org/10.1016/j.petrol.2017.07.030.

Anu, K., Hemalatha, J., 2016. Viscosity studies of water based magnetite nanofluids. AIP Conference Proceedings 1731, 050148. https://doi.org/10.1063/1.4947802.

Arias, L.S., Pessan, J.P., Vieira, A.P.M., De Lima, T.M.T., Delbem, A.C.B., Monteiro, D.R., 2018. Iron oxide nanoparticles for biomedical applications: a perspective on synthesis, drugs, antimicrobial activity, and toxicity. Antibiotics 7 (Issue 2). https://doi.org/10.3390/antibiotics7020046. MDPI AG.

Aristizábal-Fontal, J.E., Cortés, F.B., Franco, C.A., 2018. Viscosity reduction of extra heavy crude oil by magnetite nanoparticle-based ferrofluids. Adsorpt. Sci. Technol. 36 (1–2), 23–45. https://doi.org/10.1177/0263617417704309.

Atta, A.M., Abdullah, M.M.S., Al-Lohedan, H.A., Ezzat, A.O., 2018. Demulsification of heavy crude oil using new nonionic cardanol surfactants. J. Mol. Liq. 252, 311–320. https://doi.org/10.1016/j.molliq.2017.12.154.

Augusto, P.A., Castelo-Grande, T., Vargas, D., Pascual, A., Hernández, L., Estevez, A.M., Barbosa, D., 2020. Upscale design, process development, and economic analysis of industrial plants for nanomagnetic particle production for environmental and biomedical use. Materials 13 (11). https://doi.org/10.3390/ma13112477.

Aurand, K., 2017. Enhanced Oil Recovery Using Silica Nanoparticles: an Experimental Evaluation of Oil Production, Recovery Mechanisms and Nanofluid Stability.

Aval, S.F., Akbarzadeh, A., Yamchi, M.R., Zarghami, F., Nejati-Koshki, K., Zarghami, N., 2016. Gene silencing effect of SiRNA-magnetic modified with biodegradable copolymer nanoparticles on hTERT gene expression in lung cancer cell line. *Artificial Cells*. Nanomed. Biotechnol. 44 (1), 188–193. https://doi.org/10.3109/21691401.2014.934456.

Bagaria, H.G., Neilson, B.M., Worthen, A.J., Xue, Z., Yoon, K.Y., Cheng, V., Lee, J.H., Velagala, S., Huh, C., Bryant, S.L., Bielawski, C.W., Johnston, K.P., 2013. Adsorption of iron oxide nanoclusters stabilized with sulfonated copolymers on silica in concentrated NaCl and CaCl2 brine. J. Colloid Interface Sci. 398, 217–226. https://doi.org/10.1016/j.jcis.2013.01.056.

Bahiraei, M., Hangi, M., 2015. Flow and heat transfer characteristics of magnetic nanofluids: a review. J. Magn. Magn Mater. 374, 125–138. https://doi.org/10.1016/j.jmmm.2014.08.004.

Bakhteeva, I.A., Medvedeva, I.V., Uimin, M.A., Byzov, I.V., Zhakov, S.V., Yermakov, A.E., Shchegoleva, N.N., 2016. Magnetic sedimentation and aggregation of Fe3O4@SiO2 nanoparticles in water medium. Separ. Purif. Technol. 159, 35–42. https://doi.org/10.1016/j.seppur.2015.12.043.

Bandyopadhyay, S., 2016. Smart and Multifunctional Core-Shell Nanoparticles (NPs) for Drug Delivery.

Barry, M.M., Jung, Y., Lee, J.K., Phuoc, T.X., Chyu, M.K., 2015. Fluid filtration and rheological properties of nanoparticle additive and intercalated clay hybrid bentonite drilling fluids. J. Petrol. Sci. Eng. 127, 338–346. https://doi.org/10.1016/J.PETROL.2015.01.012.

Bashirnezhad, K., Bazri, S., Safaei, M.R., Goodarzi, M., Dahari, M., Mahian, O., Dalkiliça, A.S., Wongwises, S., 2016. Viscosity of nanofluids: a review of recent experimental studies. Int. Commun. Heat Mass Tran. 73, 114–123. https://doi.org/10.1016/j.icheatmasstransfer.2016.02.005.

Berry, J.D., Neeson, M.J., Dagastine, R.R., Chan, D.Y.C., Tabor, R.F., 2015. Measurement of surface and interfacial tension using pendant drop tensiometry. J. Colloid Interface Sci. 454, 226–237. https://doi.org/10.1016/j.jcis.2015.05.012. Academic Press Inc.

Betancur Camilo, A., Cortés, Farid B., F, S., 2016. Magnetite-silica nanoparticles with A core-shell structure for inhibiting the formation damage caused by the precipitation/deposition of asphaltene. In: Asphaltenes Fundamentals, Applications and Future Developments, vol. 21, pp. 95–96. Issue 3.

Betancur, Stefanía, Carrasco-Marín, F., Pérez-Cadenas, A.F., Franco, C.A., Jiménez, J., Manrique, E.J., Quintero, H., Cortés, F.B., 2019. Effect of magnetic iron core-carbon shell nanoparticles in chemical enhanced oil recovery for ultralow interfacial tension region. Energy Fuel. 33 (5), 4158–4168. https://doi.org/10.1021/acs.energyfuels.9b00426.

Betancur, Stefania, Giraldo, L.J., Carrasco-Marín, F., Riazi, M., Manrique, E.J., Quintero, H., García, H.A., Franco-Ariza, C.A., Cortéscortés, F.B., 2019. Importance of the Nanofluid Preparation for Ultra-low Interfacial Tension in Enhanced Oil Recovery Based on Surfactant− Nanoparticle−Brine System Interaction. https://doi.org/10.1021/acsomega.9b02372.

Binks, B.P., Yin, D., 2016. Pickering emulsions stabilized by hydrophilic nanoparticles:: in situ surface modification by oil. Soft Matter 12 (32), 6858–6867. https://doi.org/10.1039/c6sm01214k.

Biswal, N.R., Rangera, N., Singh, J.K., 2016. Effect of different surfactants on the interfacial behavior of the n-hexane-water system in the presence of silica nanoparticles. J. Phys. Chem. B 120 (29), 7265–7274. https://doi.org/10.1021/acs.jpcb.6b03763.

Boul, P.J., Ajayan, P.M., 2020. Nanotechnology research and development in upstream oil and gas. Energy Technol. 8 (1), 1901216. https://doi.org/10.1002/ENTE.201901216.

Camargo, P.H.C., Rodrigues, T.S., da Silva, A.G.M., Wang, J., 2015. Controlled synthesis: nucleation and growth in solution. In: Metallic Nanostructures: from Controlled Synthesis to Applications. Springer International Publishing, pp. 49–74. https://doi.org/10.1007/978-3-319-11304-3_2.

Campos, E.A., Pinto, D.V.B.S., de Oliveira, J.I.S., Mattos, E. da C., Dutra, R. de C.L., 2015. Synthesis, characterization and applications of iron oxide nanoparticles - a short review. J. Aero. Technol. Manag. 7 (3), 267–276. https://doi.org/10.5028/jatm.v7i3.471.

Cardona, L., Arias-Madrid, D., Cortés, F.B., Lopera, S.H., Franco, C.A., 2018. Heavy Oil Upgrading and Enhanced Recovery in a Steam Injection Process Assisted by NiO-And PdO-Functionalized SiO 2 Nanoparticulated Catalysts. Mdpi.Com. https://doi.org/10.3390/catal8040132.

Chakraborty, S., Panigrahi, P.K., 2020. Stability of nano fluid : a review. Appl. Therm. Eng. 174 (April).

Chang, J., Waclawik, E.R., 2014. Colloidal semiconductor nanocrystals: controlled synthesis and surface chemistry in organic media. RSC Adv. 4 (45), 23505–23527. https://doi.org/10.1039/c4ra02684e. Royal Society of Chemistry.

Cheng, K., Chi, L., Heidari, Z., 2014. Improved assessment of pore-size distribution and pore connectivity in multiple-porosity systems using superparamagnetic iron oxide nanoparticles and nmr measurements. Proceedings - SPE Annual Technical Conference and Exhibition 4, 2885–2899. https://doi.org/10.2118/170792-ms.

Chengara, A., Nikolov, A.D., Wasan, D.T., Trokhymchuk, A., Henderson, D., 2004. Spreading of nanofluids driven by the structural disjoining pressure gradient. J. Colloid Interface Sci. 280 (1), 192–201. https://doi.org/10.1016/j.jcis.2004.07.005.

Chi, L., Cheng, K., Heidari, Z., 2016a. Improved assessment of interconnected porosity in multiple-porosity rocks by use of nanoparticle contrast agents and nuclear-magnetic-resonance relaxation measurements. SPE Reservoir Eval. Eng. 19 (1), 95–107. https://doi.org/10.2118/170792-pa.

Chi, L., Cheng, K., Heidari, Z., 2016b. Improved assessment of interconnected porosity in multiple-porosity rocks by use of nanoparticle contrast agents and nuclear-magnetic-resonance relaxation measurements. SPE Reservoir Eval. Eng. 19 (1), 95–107. https://doi.org/10.2118/170792-pa.

Cid, A., 2018. Synthesis of NPs by microemulsion method. In: Microemulsion - a Chemical Nanoreactor [Working Title]. IntechOpen. https://doi.org/10.5772/intechopen.80633.

Cotin, G., Piant, S., Mertz, D., Felder-Flesch, D., Begin-Colin, S., 2018. Iron oxide nanoparticles for biomedical applications: synthesis, functionalization, and application. In: Iron Oxide Nanoparticles for Biomedical Applications. Elsevier, pp. 43–88. https://doi.org/10.1016/b978-0-08-101925-2.00002-4.

Cunha, F.R., Rosa, A.P., Dias, N.J., 2016. Rheology of a very dilute magnetic suspension with micro-structures of nanoparticles. J. Magn. Magn Mater. 397, 266–274. https://doi.org/10.1016/j.jmmm.2015.08.039.

Dennis, C.L., Ivkov, R., 2013. Physics of heat generation using magnetic nanoparticles for hyperthermia. Int. J. Hyperther. 29 (8), 715–729. https://doi.org/10.3109/02656736.2013.836758. Informa Healthcare.

Dey, P., Izake, E.L., 2015. Magnetic nanoparticles boosting the osmotic efficiency of a polymeric FO draw agent: effect of polymer conformation. Desalination 373, 79–85. https://doi.org/10.1016/j.desal.2015.07.010.

Dheyab, M.A., Aziz, A.A., Jameel, M.S., Noqta, O.A., Khaniabadi, P.M., Mehrdel, B., 2020. Simple rapid stabilization method through citric acid modification for magnetite nanoparticles. Sci. Rep. 10 (1), 1–8. https://doi.org/10.1038/s41598-020-67869-8.

Divandari, H., Hemmati-Sarapardeh, A., Schaffie, M., Ranjbar, M., 2019. Integrating synthesized citric acid-coated magnetite nanoparticles with magnetic fields for enhanced oil recovery: experimental study and mechanistic understanding. J. Petrol. Sci. Eng. 174 (September 2018), 425–436. https://doi.org/10.1016/j.petrol.2018.11.037.

Divandari, H., Hemmati-Sarapardeh, A., Schaffie, M., Ranjbar, M., 2020. Integrating functionalized magnetite nanoparticles with low salinity water and surfactant solution: interfacial tension study. Fuel 281. https://doi.org/10.1016/j.fuel.2020.118641. November 2019.

Dolai, J., Mandal, K., Jana, N.R., 2021. Nanoparticle size effects in biomedical applications. ACS Appl. Nano Mater. https://doi.org/10.1021/ACSANM.1C00987 acsanm.1c00987.

Doryani, H., Malayeri, M.R., Riazi, M., 2016. Visualization of asphaltene precipitation and deposition in a uniformly patterned glass micromodel. Fuel 182, 613–622. https://doi.org/10.1016/j.fuel.2016.06.004.

Druetta, P., Raffa, P., Picchioni, F., 2018. Plenty of room at the bottom: nanotechnology as solution to an old issue in enhanced oil recovery. Appl. Sci. 8 (Issue 12) https://doi.org/10.3390/app8122596.

El-hoshoudy, A.N., Gomaa, S., Taha, M., 2019. Improving oil recovery using Fe2O3 nanoparticles flooding. Petrol. Coal. 61 (4), 798–807.

Eltoum, H., Yang, Y.L., Hou, J.R., 2020. The effect of nanoparticles on reservoir wettability alteration: a critical review. In: Petroleum Science, vol. 1. China University of Petroleum Beijing. https://doi.org/10.1007/s12182-020-00496-0, 3.

Emrani, A.S., Nasr-El-Din, H.A., 2017. Stabilizing CO2 foam by use of nanoparticles. SPE J. 22 (2), 494–504. https://doi.org/10.2118/174254-PA.

Esfandyari Bayat, A., Junin, R., Shamshirband, S., Tong Chong, W., 2015. Transport and retention of engineered Al2 O3, TiO2, and SiO2 nanoparticles through various sedimentary rocks. Sci. Rep. 5 (1), 1–12. https://doi.org/10.1038/srep14264.

Esmaeilnezhad, E., Choi, H.J., Schaffie, M., Gholizadeh, M., Ranjbar, M., 2017. Characteristics and applications of magnetized water as a green technology. J. Clean. Prod. 161, 908–921. https://doi.org/10.1016/j.jclepro.2017.05.166. Elsevier Ltd.

Esmaeilnezhad, E., Van, S. Le, Chon, B.H., Choi, H.J., Schaffie, M., Gholizadeh, M., Ranjbar, M., 2018. An experimental study on enhanced oil recovery utilizing nanoparticle ferrofluid through the application of a magnetic field. J. Ind. Eng. Chem. 58, 319–327. https://doi.org/10.1016/j.jiec.2017.09.044.

Ewis, D., Benamor, A., Ba-Abbad, M.M., Nasser, M., El-Naas, M., Qiblawey, H., 2020. Removal of oil content from oil-water emulsions using iron oxide/bentonite nano adsorbents. J. Water Proc. Eng. 38 https://doi.org/10.1016/j.jwpe.2020.101583.

Fakher, S., Imqam, A., Wanas, E., 2018, December 10. Investigating the viscosity reduction of ultra-heavy crude oil using hydrocarbon soluble low molecular weight compounds to improve oil production and transportation. In: SPE International Heavy Oil Conference and Exhibition. https://doi.org/10.2118/193677-MS.

Fakher, S., Ahdaya, M., Elturki, M., Imqam, A., 2019. Critical review of asphaltene properties and factors impacting its stability in crude oil. In: Journal of Petroleum Exploration and Production Technology. Springer, pp. 1–18. https://doi.org/10.1007/s13202-019-00811-5.

Fakoya, M.F., Shah, S.N., 2017. Emergence of nanotechnology in the oil and gas industry: emphasis on the application of silica nanoparticles. Petroleum 3 (4), 391–405. https://doi.org/10.1016/j.petlm.2017.03.001.

Fan, Y., Guo, R., Shi, X., Allen, S., Cao, Z., Baker, J.R., Wang, S.H., 2016. Modified nanoemulsions with iron oxide for magnetic resonance imaging. Nanomaterials 6 (12). https://doi.org/10.3390/nano6120223.

Faraji, M., Yamini, Y., Rezaee, M., 2010. Magnetic nanoparticles: synthesis, stabilization, functionalization, characterization, and applications. J. Iran. Chem. Soc. 7 (1), 1–37. https://doi.org/10.1007/BF03245856.

Farooqui, J., Babadagli, T., Li, H.A., 2015. Improvement of the recovery factor using nano-metal particles at the late stages of cyclic steam stimulation. In: Society of

Petroleum Engineers - SPE Canada Heavy Oil Technical Conference 2015. CHOC, pp. 601–617. https://doi.org/10.2118/174478-ms, 2015.
Faudzi, F.N.M., Hamzah, A.A., 2021. Nanoparticle in composite material. In: Nanoparticles in Analytical and Medical Devices. Elsevier, pp. 71–82. https://doi.org/10.1016/b978-0-12-821163-2.00005-4.
Fereidooni Moghadam, T., Azizian, S., 2014. Effect of ZnO nanoparticle and hexadecyltrimethylammonium bromide on the dynamic and equilibrium oil–water interfacial tension. J. Phys. Chem. B 118 (6), 1527–1534. https://doi.org/10.1021/jp4106986.
Foroozesh, J., Kumar, S., 2020. Nanoparticles behaviors in porous media: application to enhanced oil recovery. J. Mol. Liq. 316 https://doi.org/10.1016/j.molliq.2020.113876.
Foroughi, F., Hassanzadeh-Tabrizi, S.A., Bigham, A., 2016. In situ microemulsion synthesis of hydroxyapatite-MgFe2O4 nanocomposite as a magnetic drug delivery system. Mater. Sci. Eng. C 68, 774–779. https://doi.org/10.1016/J.MSEC.2016.07.028.
Francisco, A.D., Grasseschi, D., Nascimento, R.S.V., 2020. Wettability alteration of oil-wet carbonate rocks by chitosan derivatives for application in enhanced oil recovery. J. Appl. Polym. Sci. 50098 https://doi.org/10.1002/app.50098.
Freitag, N.P., 2018. Similarity of the effect of different dissolved gases on heavy-oil viscosity. SPE Reservoir Eval. Eng. 21 (3), 747–756. https://doi.org/10.2118/189456-pa.
Frimpong, R.A., Hilt, J.Z., 2010. Magnetic nanoparticles in biomedicine: synthesis, functionalization and applications 1401–1414. https://doi.org/10.2217/NNM.10.114. Https://Doi.Org/10.2217/Nnm.10.114, 5(9).
Gautam, R.K., Gautam, P.K., Banerjee, S., Soni, S., Singh, S.K., Chattopadhyaya, M.C., 2015. Removal of Ni(II) by magnetic nanoparticles. J. Mol. Liq. 204, 60–69. https://doi.org/10.1016/j.molliq.2015.01.038.
Gbadamosi, A.O., Junin, R., Manan, M.A., Yekeen, N., Agi, A., Oseh, J.O., 2018. Recent advances and prospects in polymeric nanofluids application for enhanced oil recovery. J. Ind. Eng. Chem. 66, 1–19. https://doi.org/10.1016/j.jiec.2018.05.020. Korean Society of Industrial Engineering Chemistry.
Gbadamosi, A.O., Junin, R., Manan, M.A., Agi, A., Oseh, J.O., Usman, J., 2019a. Effect of aluminium oxide nanoparticles on oilfield polyacrylamide: rheology, interfacial tension, wettability and oil displacement studies. J. Mol. Liq. 296 https://doi.org/10.1016/j.molliq.2019.111863.
Gbadamosi, A.O., Junin, R., Manan, M.A., Agi, A., Yusuff, A.S., 2019b. An overview of chemical enhanced oil recovery: recent advances and prospects. In: International Nano Letters, vol. 9. Springer Berlin Heidelberg. https://doi.org/10.1007/s40089-019-0272-8. Issue 3.
Giustini, A.J., Petryk, A.A., Cassim, S.M., Tate, J.A., Baker, I., Hoopes, P.J., 2010. Magnetic nanoparticle hyperthermia in cancer treatment. Nano LIFE 17–32. https://doi.org/10.1142/s1793984410000067, 01(01n02).
Glaser, N., Adams, D.J., Böker, A., Krausch, G., 2006. Janus particles at liquid-liquid interfaces. Langmuir 22 (12), 5227–5229. https://doi.org/10.1021/la060693i.
Gomaa, S., Taha, M., An, E.-H., 2018a. Investigating the effect of different nanoparticles on the interfacial tension investigating the effect of different nanoparticles on the interfacial tension reduction. November, 0–7. https://doi.org/10.23880/ppej-16000176.
Gomaa, S., Taha, M., An, E., 2018b. Investigating the effect of different nanofluids types on crude oil viscosity. Petrol. Petrochem. Eng. J. 2 (7), 1–6. https://doi.org/10.23880/ppej-16000177.
Gomez-Flores, A., Bradford, S.A., Hwang, G., Choi, S., Tong, M., Kim, H., 2020. Shape and orientation of bare silica particles influence their deposition under intermediate ionic strength: a study with QCM–D and DLVO theory. Colloid. Surface. Physicochem. Eng. Aspect. 599, 124921. https://doi.org/10.1016/j.colsurfa.2020.124921.
Gontijo, R.G., Cunha, F.R., 2015. Dynamic numerical simulations of magnetically interacting suspensions in creeping flow. Powder Technol. 279, 146–165. https://doi.org/10.1016/j.powtec.2015.03.033.
Gu, B., Hou, B., Lu, Z., Wang, Z., Chen, S., 2013. Thermal conductivity of nanofluids containing high aspect ratio fillers. Int. J. Heat Mass Tran. 64, 108–114. https://doi.org/10.1016/j.ijheatmasstransfer.2013.03.080.
Guan, B.H., Khalid, M.H.M., Matraji, H.H., Chuan, L.K., Soleimani, H., 2014. An evaluation of iron oxide nanofluids in enhanced oil recovery application 1621, 600–604. https://doi.org/10.1063/1.4898529.
Guselnikova, O., Barras, A., Addad, A., Sviridova, E., Szunerits, S., Postnikov, P., Boukherroub, R., 2020. Magnetic polyurethane sponge for efficient oil adsorption and separation of oil from oil-in-water emulsions. Separ. Purif. Technol. 240, 116627. https://doi.org/10.1016/J.SEPPUR.2020.116627.
Haroun, M., Ansari, A., Al Kindy, N., Sayed, N.A., Ali, B., Sarma, H., 2012. Smart nano-EOR process for Abu Dhabi carbonate reservoirs. In: Society of Petroleum Engineers - Abu Dhabi International Petroleum Exhibition and Conference 2012, ADIPEC 2012 - Sustainable Energy Growth: People, Responsibility, and Innovation, vol. 5, pp. 3610–3622. https://doi.org/10.2118/162386-ms.
Hasany, S., Ahmed, I., Rajan, J., Nanotechnol, A.R.-N., 2012. Systematic review of the preparation techniques of iron oxide magnetic nanoparticles. undefined. (2011). Researchgate.Net 2012 (6), 148–158. https://doi.org/10.5923/j.nn.20120206.01.
Hascakir, B., Babadagli, T., Akin, S., 2008. Experimental and numerical modeling of heavy-oil recovery by electrical heating. In: Society of Petroleum Engineers - International Thermal Operations and Heavy Oil Symposium, ITOHOS 2008 - "Heavy Oil: Integrating the Pieces, vol. 2, pp. 755–768. https://doi.org/10.2118/117669-ms.
Hassani, S.S., Daraee, M., Sobat, Z., 2020. Advanced development in upstream of petroleum industry using nanotechnology. Chin. J. Chem. Eng. 28 (6), 1483–1491. https://doi.org/10.1016/j.cjche.2020.02.030.
Hassanjani-Roshan, A., Vaezi, M.R., Shokuhfar, A., Rajabali, Z., 2011. Synthesis of iron oxide nanoparticles via sonochemical method and their characterization. Particuology 9 (1), 95–99. https://doi.org/10.1016/j.partic.2010.05.013.
Hasçakir, B., Babadagli, T., Akin, S., 2010. Field-scale analysis of heavy-oil recovery by electrical heating. SPE Reservoir Eval. Eng. 13 (1), 131–142. https://doi.org/10.2118/117669-PA.
He, S., Liang, L., Zeng, Y., Ding, Y., Lin, Y., Liu, X., 2016. The influence of water-based drilling fluid on mechanical property of shale and the wellbore stability. Petroleum 2 (1), 61–66. https://doi.org/10.1016/J.PETLM.2015.12.002.
He, X., Liang, C., Liu, Q., Xu, Z., 2019a. Magnetically responsive Janus nanoparticles synthesized using cellulosic materials for enhanced phase separation in oily wastewaters and water-in-crude oil emulsions. Chem. Eng. J. 378 https://doi.org/10.1016/j.cej.2019.122045.
He, X., Liang, C., Liu, Q., Xu, Z., 2019b. Magnetically responsive Janus nanoparticles synthesized using cellulosic materials for enhanced phase separation in oily wastewaters and water-in-crude oil emulsions. Chem. Eng. J. 378, 122045. https://doi.org/10.1016/J.CEJ.2019.122045.
He, X., Liang, C., Liu, Q., Xu, Z., 2019c. Magnetically responsive Janus nanoparticles synthesized using cellulosic materials for enhanced phase separation in oily wastewaters and water-in-crude oil emulsions. Chem. Eng. J. 378, 122045. https://doi.org/10.1016/j.cej.2019.122045.
He, X., Liu, Q., Xu, Z., 2020a. Treatment of oily wastewaters using magnetic Janus nanoparticles of asymmetric surface wettability. J. Colloid Interface Sci. 568, 207–220. https://doi.org/10.1016/J.JCIS.2020.02.019.
He, X., Liu, Q., Xu, Z., 2020b. Cellulose-coated magnetic janus nanoparticles for dewatering of crude oil emulsions. Chem. Eng. Sci. 116215 https://doi.org/10.1016/j.ces.2020.116215.
Hendraningrat, L., Torsæter, O., 2015. Metal oxide-based nanoparticles: revealing their potential to enhance oil recovery in different wettability systems. Appl. Nanosci. 5 (2), 181–199. https://doi.org/10.1007/s13204-014-0305-6.
Hendraningrat, L., Souraki, Y., Torsæter, O., 2014. Experimental investigation of decalin and metal nanoparticles-assisted bitumen upgrading during catalytic aquathermolysis. Soc. Petrol. Eng. European Unconventional Res. Conf. Exhibition 2014: Unlocking European Potential 2, 1235–1245. https://doi.org/10.2118/167807-ms.
Hernández-Hernández, A.A., Aguirre-Álvarez, G., Cariño-Cortés, R., Mendoza-Huizar, L. H., Jiménez-Alvarado, R., 2020. Iron oxide nanoparticles: synthesis, functionalization, and applications in diagnosis and treatment of cancer, 11. In: Chemical Papers, vol. 74, pp. 3809–3824. https://doi.org/10.1007/s11696-020-01229-8. Springer.
Hosseini, H., Apourvari, S.N., Schaffie, M., 2019a. Wettability alteration of carbonate rocks via magnetic fields application. J. Petrol. Sci. Eng. 172, 280–287. https://doi.org/10.1016/j.petrol.2018.08.022.
Hosseini, H., Hosseini, H., Jalili, M., Norouzi Apourvari, S., Schaffie, M., Ranjbar, M., 2019b. Static adsorption and interfacial tension of Sodium dodecyl sulfate via magnetic field application. J. Petrol. Sci. Eng. 178, 205–215. https://doi.org/10.1016/j.petrol.2019.03.040.
Hou, B.F., Wang, Y.F., Huang, Y., 2015. Mechanism and influencing factors of wettability alteration of water-wet sandstone surface by CTAB. J. Dispersion Sci. Technol. 36 (11), 1587–1594. https://doi.org/10.1080/01932691.2014.981338.
Hou, B., Jia, R., Fu, M., Huang, Y., Wang, Y., 2019. Mechanism of wettability alteration of an oil-wet sandstone surface by a novel cationic gemini surfactant. Energy Fuel. 33 (5), 4062–4069. https://doi.org/10.1021/acs.energyfuels.9b00304.
Hu, Z., Nourafkan, E., Gao, H., Wen, D., 2017. This is a repository copy of Microemulsions stabilized by in-situ synthesized nanoparticles for enhanced oil recovery. In: Microemulsions Stabilized by In-Situ Synthesized Nanoparticles 1 for Enhanced Oil Recovery. https://doi.org/10.1016/j.fuel.2017.08.004.
Huang, T., Yao, J., Huang, Z., Xie, H., Zhang, J., Liu, J., 2018. Laboratory investigation of ferrofluid flooding for oil recovery. Zhongguo Shiyou Daxue Xuebao (Ziran Kexue Ban)/Journal of China University of Petroleum (Edition of Natural Science) 42 (1), 99–104. https://doi.org/10.3969/j.issn.1673-5005.2018.01.012.
Huh, C., Milner, B., Nizamidin, N., G, A., P, E., 2014. Hydrophobic paramagnetic nanoparticles as intelligent crude oil tracers. In: Google Patents. https://patents.google.com/patent/US20150050356A1/en.
Hussain, S., Mottahir Alam, M., Imran, M., Zouli, N., Aziz, A., Irshad, K., Haider, M., Khan, A., 2020. Fe3O4 nanoparticles decorated multi-walled carbon nanotubes based magnetic nanofluid for heat transfer application. Mater. Lett. 274, 128043. https://doi.org/10.1016/j.matlet.2020.128043.
Ingram, D.R., Kotsmar, C., Yoon, K.Y., Shao, S., Huh, C., Bryant, S.L., Milner, T.E., Johnston, K.P., 2010. Superparamagnetic nanoclusters coated with oleic acid bilayers for stabilization of emulsions of water and oil at low concentration. J. Colloid Interface Sci. 351 (1), 225–232. https://doi.org/10.1016/j.jcis.2010.06.048.
Iqbal, M., Lyon, B.A., Ureña-Benavides, E.E., Moaseri, E., Fei, Y., McFadden, C., Javier, K. J., Ellison, C.J., Pennell, K.D., Johnston, K.P., 2017. High temperature stability and low adsorption of sub-100 nm magnetite nanoparticles grafted with sulfonated copolymers on Berea sandstone in high salinity brine. Colloid. Surface. Physicochem. Eng. Aspect. 520, 257–267. https://doi.org/10.1016/j.colsurfa.2017.01.080.
Iskandar, F., Dwinanto, E., Abdullah, M., Khairurrijal, Muraza, O., 2016a. Viscosity reduction of heavy oil using nanocatalyst in aquathermolysis reaction. In: KONA Powder and Particle Journal, vol. 2016. Hosokawa Powder Technology Foundation, pp. 3–16. https://doi.org/10.14356/kona.2016005, 33.
Iskandar, F., Dwinanto, E., Abdullah, M., Khairurrijal, Muraza, O., 2016b. Viscosity reduction of heavy oil using nanocatalyst in aquathermolysis reaction. KONA Powder Particle J. 2016 (33), 3–16. https://doi.org/10.14356/kona.2016005.

Izadi, N., Koochi, M.M., Amrollahi, A., Pourkhalil, M., 2019. Investigation of functionalized polyelectrolyte polymer-coated Fe3O4 nanoparticles stabilized in high salinity brine at high temperatures as an EOR agent. J. Petrol. Sci. Eng. 178, 1079–1091. https://doi.org/10.1016/j.petrol.2019.01.074.

Jagadeesh Babu, V., Kiran, S.K., Ramakrishna, S., Babu, V.J., 2018. Merum Sireesha A Review on Nanomaterial Revolution in Oil and Gas Industry for EOR (Enhanced Oil Recovery) Methods. https://doi.org/10.31031/RDMS.2018.04.000579.

James G Speight, 2016. Introduction to enhanced recovery methods for heavy oil and tar sands. In: Introduction to Enhanced Recovery Methods for Heavy Oil and Tar Sands. Elsevier. https://doi.org/10.1016/c2014-0-01296-8.

Jamilpanah, P., Pahlavanzadeh, H., Kheradmand, A., 2017. Thermal conductivity, viscosity, and electrical conductivity of iron oxide with a cloud fractal structure. Heat and Mass Transfer/Waerme- Und Stoffuebertragung 53 (4), 1343–1354. https://doi.org/10.1007/s00231-016-1891-5.

Jamsaz, A., Goharshadi, E.K., Barras, A., Ifires, M., Szunerits, S., Boukherroub, R., 2021. Magnetically driven superhydrophobic/superoleophilic graphene-based polyurethane sponge for highly efficient oil/water separation and demulsification. Separ. Purif. Technol. 274, 118931. https://doi.org/10.1016/J.SEPPUR.2021.118931.

Jeevanandam, J., Barhoum, A., Chan, Y.S., Dufresne, A., Danquah, M.K., 2018. Review on nanoparticles and nanostructured materials: history, sources, toxicity and regulations. Beilstein J. Nanotechnol. 9 (Issue 1), 1050–1074. https://doi.org/10.3762/bjnano.9.98. Beilstein-Institut.

Jiang, R., Li, K., Horne, R., 2017. A mechanism study of wettability and interfacial tension for EOR using silica nanoparticles. Proceedings - SPE Annual Technical Conference and Exhibition 1–17. https://doi.org/10.2118/187096-ms, 0.

Jolivet, J.P., Chanéac, C., Tronc, E., 2004. Iron oxide chemistry. From molecular clusters to extended solid networks. Chem. Commun. 4 (5), 477–483. https://doi.org/10.1039/b304532n.

Joonaki, E., Ghanaatian, S., 2014. The application of nanofluids for enhanced oil recovery: effects on interfacial tension and coreflooding process. Petrol. Sci. Technol. 32 (21), 2599–2607. https://doi.org/10.1080/10916466.2013.855228.

Jorge, M.J., Nilson, M.C., Aracely, H.R., Machuca-Martínez, F., 2019. Data on the removal of metals (Cr3+, Cr6+, Cd2+, Cu2+, Ni2+, Zn2+) from aqueous solution by adsorption using magnetite particles from electrochemical synthesis. Data in Brief 24, 103956. https://doi.org/10.1016/j.dib.2019.103956.

J Sheng, J., 2011. Modern Chemical Enhanced Oil Recovery: Theory and Practice - James J. Sheng - Google Books. https://books.google.com.my/books?hl=en&lr=&id=etgfFzWrIosC&oi=fnd&pg=PP2&ots=GzP66fcxe&sig=LjQ3g0CRq8ljPlInk72QSTvfgNw&redir_esc=y#v=onepage&q&f=false.

Kamal, M.S., Sultan, A.S., Al-Mubaiyedh, U.A., Hussein, I.A., Feng, Y., 2015. Rheological properties of thermoviscosifying polymers in high-temperature and high-salinity environments. Can. J. Chem. Eng. 93 (7), 1194–1200. https://doi.org/10.1002/cjce.22204.

Kamal, M.S., Adewunmi, A.A., Sultan, A.S., Al-Hamad, M.F., Mehmood, U., 2017. Recent advances in nanoparticles enhanced oil recovery: rheology, interfacial tension, oil recovery, and wettability alteration. J. Nanomater. 1–15. https://doi.org/10.1155/2017/2473175, 2017.

Kashchiev, D., van Rosmalen, G.M., 2003. Review: nucleation in solutions revisited. Cryst. Res. Technol. 38 (78), 555–574. https://doi.org/10.1002/crat.200310070.

Kashif, M., Puspitasari, P., 2017. Optimum conditions for EOR using nanofluids subjected to EM waves. J. Mech. Eng. Sci. Technol. 1 (1), 15–23. https://doi.org/10.17977/um016v1i12017p015.

Kayani, Z.N., Arshad, S., Riaz, S., Naseem, S., 2014. Synthesis of iron oxide nanoparticles by sol-gel technique and their characterization. IEEE Trans. Magn. 50 (8) https://doi.org/10.1109/TMAG.2014.2313763.

Kazemzadeh, Y., Eshraghi, S.E., Kazemi, K., Sourani, S., Mehrabi, M., Ahmadi, Y., 2015. Behavior of asphaltene adsorption onto the metal oxide nanoparticle surface and its effect on heavy oil recovery. Ind. Eng. Chem. Res. 54 (1), 233–239. https://doi.org/10.1021/ie503797g.

Kazemzadeh, Y., Sharifi, M., Riazi, M., Rezvani, H., Tabaei, M., 2018. Potential effects of metal oxide/SiO 2 nanocomposites in EOR processes at different pressures. Colloid. Surface. Physicochem. Eng. Aspect. 559 (August), 372–384. https://doi.org/10.1016/j.colsurfa.2018.09.068.

Kazemzadeh, Y., Dehdari, B., Etemadan, Z., Riazi, M., Sharifi, M., 2019. Experimental investigation into Fe3O4/SiO2 nanoparticle performance and comparison with other nanofluids in enhanced oil recovery. Petrol. Sci. 16 (3), 578–590. https://doi.org/10.1007/s12182-019-0314-x.

Kenouche, S., Larionova, J., Bezzi, N., Guari, Y., Bertin, N., Zanca, M., Lartigue, L., Cieslak, M., Godin, C., Morrot, G., Goze-Bac, C., 2014. NMR investigation of functionalized magnetic nanoparticles Fe3O4 as T1-T2 contrast agents. Powder Technol. 255, 60–65. https://doi.org/10.1016/j.powtec.2013.07.038.

Khalil, M., Aulia, G., Budianto, E., Mohamed Jan, B., Habib, S.H., Amir, Z., Abdul Patah, M.F., 2019. Surface-functionalized superparamagnetic nanoparticles (SPNs) for enhanced oil recovery: effects of surface modifiers and their architectures. ACS Omega. https://doi.org/10.1021/acsomega.9b03174.

khalilifard, M., Javadian, S., 2021. Magnetic superhydrophobic polyurethane sponge loaded with Fe3O4@oleic acid@graphene oxide as high performance adsorbent oil from water. Chem. Eng. J. 408, 127369. https://doi.org/10.1016/J.CEJ.2020.127369.

Khamarui, S., Saima, Y., Laha, R.M., Ghosh, S., Maiti, D.K., 2015. Functionalised MnVI-nanoparticles: an advanced high-valent magnetic catalyst. Sci. Rep. 5 (1), 1–8. https://doi.org/10.1038/srep08636.

Khan, M.B., Khoker, F., Husain, M., Ahmed, M., Anwer, S., 2018. Academ J Polym Sci Effects of Nanoparticles on Rheological Behavior of Polyacrylamide Related to Enhance Oil Recovery, vol. 1. https://doi.org/10.19080/AJOP.2018.01.555573.

Khan, I., Saeed, K., Khan, I., 2019. Nanoparticles: properties, applications and toxicities. Arabian J. Chem. 12 (7), 908–931. https://doi.org/10.1016/j.arabjc.2017.05.011. Elsevier B.V.

Kharisov, B.I., Rasika Dias, H.V., Kharissova, O.V., Manuel Jiménez-Pérez, V., Olvera Pérez, B., Muñoz Flores, B., 2012. Iron-containing nanomaterials: synthesis, properties, and environmental applications. RSC Adv. 2 (25), 9325–9358. https://doi.org/10.1039/c2ra20812a.

Khatke, L., Rathi, M., Bhanavase, V.L., Patil, A.J., 2017. Effect of Nanoparticle Size on Heat Transfer Intensification. http://www.ijritcc.org.

Kim, H.C., Fthenakis, V., 2013. Life cycle energy and climate change implications of nanotechnologies: a Critical Review. J. Ind. Ecol. 17 (4), 528–541. https://doi.org/10.1111/J.1530-9290.2012.00538.X.

Kim, I., Worthen, A.J., Lotfollahi, M., Johnston, K.P., Dicarlo, D.A., Huh, C., 2017. Nanoparticle-stabilized emulsions for improved mobility control for adverse-mobility waterflooding. In: IOR NORWAY 2017 - 19th European Symposium on Improved Oil Recovery: Sustainable IOR in a Low Oil Price World. https://doi.org/10.3997/2214-4609.201700314.

Kim, C., Lee, J., Schmucker, D., Fortner, J.D., 2020a. Highly stable superparamagnetic iron oxide nanoparticles as functional draw solutes for osmotically driven water transport. Npj Clean Water 3 (1), 1–6. https://doi.org/10.1038/s41545-020-0055-9.

Kim, C., Lee, J., Schmucker, D., Fortner, J.D., 2020b. Highly stable superparamagnetic iron oxide nanoparticles as functional draw solutes for osmotically driven water transport. Npj Clean Water 1–6. https://doi.org/10.1038/s41545-020-0055-9, 2020 3:1, 3(1).

Ko, S., Kim, E.S., Park, S., Daigle, H., Milner, T.E., Huh, C., Bennetzen, M.V., Geremia, G. A., 2016. Oil droplet removal from produced water using nanoparticles and their magnetic separation. In: Proceedings - SPE Annual Technical Conference and Exhibition, 2016-Janua. https://doi.org/10.2118/181893-ms.

Ko, S., Kim, E.S., Park, S., Daigle, H., Milner, T.E., Huh, C., Bennetzen, M.V., Geremia, G. A., 2017. Amine functionalized magnetic nanoparticles for removal of oil droplets from produced water and accelerated magnetic separation. J. Nanoparticle Res. 19 (4), 1–14. https://doi.org/10.1007/s11051-017-3826-6.

Kondiparty, K., Nikolov, A.D., Wasan, D., Liu, K.L., 2012. Dynamic spreading of nanofluids on solids. part I: Experimental. Langmuir 28 (41), 14618–14623. https://doi.org/10.1021/la3027013.

Koroleva, M., Bidanov, D., Yurtov, E., 2019. Emulsions stabilized with mixed SiO2 and Fe3O4 nanoparticles: mechanisms of stabilization and long-term stability. Phys. Chem. Chem. Phys. 21 (3), 1536–1545. https://doi.org/10.1039/c8cp05292a.

Kothari, N., Raina, B., Chandak, K.B., Iyer, V., Mahajan, H.P., 2010. *Application of Ferrofluids for Enhanced Surfactant Flooding in IOR*. 1–7. https://doi.org/10.2118/131272-ms.

Krahne, R., Morello, G., Figuerola, A., George, C., Deka, S., Manna, L., 2011. Physical properties of elongated inorganic nanoparticles. Phys. Rep. 501, 75–221. https://doi.org/10.1016/j.physrep.2011.01.001. Issues 3–5.

Kudr, J., Haddad, Y., Richtera, L., Heger, Z., Nanomaterials, M.C.-, 2017. Magnetic Nanoparticles: from Design and Synthesis to Real World Applications. undefined. (2017). Mdpi.Com. https://doi.org/10.3390/nano7090243.

Kumar, N., Mandal, A., 2020. Experimental investigation of PEG 6000/tween 40/SiO2 NPs stabilized nanoemulsion properties: a versatile oil recovery approach. J. Mol. Liq. https://doi.org/10.1016/j.molliq.2020.114087, 114087.

Kumar, N., Gaur, T., Mandal, A., 2017. Characterization of SPN Pickering emulsions for application in enhanced oil recovery. J. Ind. Eng. Chem. 54, 304–315. https://doi.org/10.1016/j.jiec.2017.06.005.

Kumar, G., Kakati, A., Mani, E., Sangwai, J.S., 2020. Stability of nanoparticle stabilized oil-in-water Pickering emulsion under high pressure and high temperature conditions: comparison with surfactant stabilized oil-in-water emulsion. J. Dispersion Sci. Technol. 1–14. https://doi.org/10.1080/01932691.2020.1730888.

Lakshmanan, S., Holmes, W.M., Sloan, W.T., Phoenix, V.R., 2015. Nanoparticle transport in saturated porous medium using magnetic resonance imaging. Chem. Eng. J. 266, 156–162. https://doi.org/10.1016/j.cej.2014.12.076.

Laurent, S., Forge, D., Port, M., Roch, A., Robic, C., Vander Elst, L., Muller, R.N., 2008. Magnetic iron oxide nanoparticles: synthesis, stabilization, vectorization, physicochemical characterizations and biological applications. Chem. Rev. 108 (6), 2064–2110. https://doi.org/10.1021/cr068445e.

Li, H., Zhou, Q., Wu, Y., Fu, J., Wang, T., Jiang, G., 2009. Effects of waterborne nano-iron on medaka (Oryzias latipes): antioxidant enzymatic activity, lipid peroxidation and histopathology. Ecotoxicol. Environ. Saf. 72 (3), 684–692. https://doi.org/10.1016/J.ECOENV.2008.09.027.

Li, Kewen, Wang, D., Jiang, S., 2018. Review on enhanced oil recovery by nanofluids. Oil Gas Sci. Technol. 73 https://doi.org/10.1051/ogst/2018052.

Li, C., Huang, W., Zhou, C., Chen, Y., 2019. Advances on the transition-metal based catalysts for aquathermolysis upgrading of heavy crude oil. Fuel 257, 115779. https://doi.org/10.1016/j.fuel.2019.115779. Elsevier Ltd.

Li, Keran, Xie, L., Wang, B., Yan, J., Tang, H., Zhou, D., 2020. Mechanistic investigation of surfactant-free emulsion polymerization using magnetite nanoparticles modified by citric acid as stabilizers. Langmuir 36 (28), 8290–8300. https://doi.org/10.1021/acs.langmuir.0c01493.

Liang, J., Du, N., Song, S., Hou, W., 2015. Magnetic demulsification of diluted crude oil-in-water nanoemulsions using oleic acid-coated magnetite nanoparticles. Colloid. Surface. Physicochem. Eng. Aspect. 466, 197–202. https://doi.org/10.1016/J.COLSURFA.2014.11.050.

Liang, C., He, X., Liu, Q., Xu, Z., 2018. Adsorption-based synthesis of magnetically responsive and interfacially active composite nanoparticles for dewatering of water-in-diluted bitumen emulsions. Energy Fuel. 32 (8), 8078–8089. https://doi.org/10.1021/ACS.ENERGYFUELS.8B01187.

Lim, J.K., Yeap, S.P., Leow, C.H., Toh, P.Y., Low, S.C., 2014. Magnetophoresis of iron oxide nanoparticles at low field gradient: the role of shape anisotropy. J. Colloid Interface Sci. 421, 170–177. https://doi.org/10.1016/j.jcis.2014.01.044.

Lin, D., Feng, X., Wu, Y., Ding, B., Lu, T., Liu, Y., Chen, X., Chen, D., Yang, C., 2018. Insights into the synergy between recyclable magnetic Fe 3 O 4 and zeolite for catalytic aquathermolysis of heavy crude oil. Appl. Surf. Sci. 456, 140–146. https://doi.org/10.1016/j.apsusc.2018.06.069.

Liu, K.L., Kondiparty, K., Nikolov, A.D., Wasan, D., 2012. Dynamic spreading of nanofluids on solids part II: Modeling. Langmuir 28 (47), 16274–16284. https://doi.org/10.1021/la302702g.

Liu, Z., Wang, H., Blackbourn, G., Feng, M.A., Zhengjun, H.E., Wen, Z., Wang, Z., Yang, Z., Luan, T., Zhenzhen, W.U., 2019. Heavy oils and oil sands: global distribution and resource assessment. Acta Geol. Sin. 93 (Issue 1), 199–212. https://doi.org/10.1111/1755-6724.13778. Wiley-Blackwell Publishing Asia.

Lü, T., Qi, D., Zhang, D., Lin, S., Mao, Y., Zhao, H., 2018. Facile synthesis of N-(aminoethyl)-aminopropyl functionalized core-shell magnetic nanoparticles for emulsified oil-water separation. J. Alloys Compd. 769, 858–865. https://doi.org/10.1016/J.JALLCOM.2018.08.071.

Macnae, J., 2017. Superparamagnetism in ground and airborne electromagnetics: geometrical and physical controls. Geophysics 82 (6), E347–E356. https://doi.org/10.1190/GEO2017-0223.1.

Mahmoud, O., Nasr-El-Din, H.A., 2020. Formation-damage assessment and filter-cake characterization of Ca-bentonite fluids enhanced with nanoparticles. SPE Drill. Complet. https://doi.org/10.2118/191155-pa.

Mahmoud, O., Nasr-El-din, H.A., Vryzas, Z., Kelessidis, V.C., 2018. Using ferric oxide and silica nanoparticles to develop modified calcium bentonite drilling fluids. SPE Drill. Complet. 33 (1), 12–26. https://doi.org/10.2118/178949-pa.

Majidi, S., Sehrig, F.Z., Farkhani, S.M., Goloujeh, M.S., Akbarzadeh, A., 2016. Current methods for synthesis of magnetic nanoparticles. Issue 2. In: Artificial Cells, Nanomedicine and Biotechnology, vol. 44. Taylor & Francis, pp. 722–734. https://doi.org/10.3109/21691401.2014.982802.

Malekzadeh, A., Pouranfard, A.R., Hatami, N., Kazemnejad Banari, A., Rahimi, M.R., 2016. Experimental investigations on the viscosity of magnetic nanofluids under the influence of temperature, volume fractions of nanoparticles and external magnetic field. J. Appl. Fluid Mech. 9 (2), 693–697. https://doi.org/10.18869/acadpub.jafm.68.225.24022.

Medvedeva, I., Uimin, M., Yermakov, A., Mysik, A., Byzov, I., Nabokova, T., Gaviko, V., Shchegoleva, N., Zhakov, S., Tsurin, V., Linnikov, O., Rodina, I., Platonov, V., Osipov, V., 2012. Sedimentation of Fe 3O 4 nanosized magnetic particles in water solution enhanced in a gradient magnetic field. J. Nanoparticle Res. 14 (3) https://doi.org/10.1007/s11051-012-0740-9.

Mi, T., Cai, Y., Wang, Q., Habibul, N., Ma, X., Su, Z., Wu, W., 2020. Synthesis of Fe3O4 nanocomposites for efficient separation of ultra-small oil droplets from hexadecane-water emulsions. RSC Adv. 10 (17), 10309–10314. https://doi.org/10.1039/d0ra01044h.

Mishra, P.C., Mukherjee, S., Nayak, S.K., Panda, A., 2014. A brief review on viscosity of nanofluids. Int. Nano Lett. 4 (4), 109–120. https://doi.org/10.1007/s40089-014-0126-3.

Mitchell, J., Staniland, J., Fordham, E., 2013. Paramagnetic doping agents in magnetic resonance studies of oil recovery. Petrophysics 54 (4), 349–367. https://www.onepetro.org/journal-paper/SPWLA-2013-v54n4-A3.

Moghadam, T.F., Azizian, S., 2014. Effect of ZnO nanoparticles on the interfacial behavior of anionic surfactant at liquid/liquid interfaces. Colloid. Surface. Physicochem. Eng. Aspect. 457 (1), 333–339. https://doi.org/10.1016/j.colsurfa.2014.06.009.

Mohammadfam, Y., Zeinali Heris, S., Khazini, L., 2020. Experimental Investigation of Fe3O4/hydraulic oil magnetic nanofluids rheological properties and performance in the presence of magnetic field. Tribol. Int. 142, 105995. https://doi.org/10.1016/j.triboint.2019.105995.

Mohammed, A.S., 2017. Effect of temperature on the rheological properties with shear stress limit of iron oxide nanoparticle modified bentonite drilling muds. Egyptian J. Petrol. 26 (3), 791–802. https://doi.org/10.1016/j.ejpe.2016.10.018.

Moore, T.L., Rodriguez-Lorenzo, L., Hirsch, V., Balog, S., Urban, D., Jud, C., Rothen-Rutishauser, B., Lattuada, M., Petri-Fink, A., 2015. Nanoparticle colloidal stability in cell culture media and impact on cellular interactions. Chem. Soc. Rev. 44 (17), 6287–6305. https://doi.org/10.1039/c4cs00487f.

Moura, H.M., Unterlass, M.M., 2020. Biogenic metal oxides. Biomimetics 5 (Issue 2). https://doi.org/10.3390/BIOMIMETICS5020029. MDPI Multidisciplinary Digital Publishing Institute.

Mozaffari, S., Li, W., Thompson, C., Ivanov, S., Seifert, S., Lee, B., Kovarik, L., Karim, A. M., 2018. Ligand-mediated nucleation and growth of palladium metal nanoparticles. JoVE. https://doi.org/10.3791/57667, 2018(136), e57667.

Murshed, S.M.S., Estellé, P., 2017. A state of the art review on viscosity of nanofluids. In: Renewable and Sustainable Energy Reviews, vol. 76. Elsevier Ltd, pp. 1134–1152. https://doi.org/10.1016/j.rser.2017.03.113.

Na, Y., Yang, S., Lee, S., 2014. Evaluation of citrate-coated magnetic nanoparticles as draw solute for forward osmosis. Desalination 347, 34–42. https://doi.org/10.1016/j.desal.2014.04.032.

Naghizadeh, A., Azin, R., Osfouri, S., Fatehi, R., 2020. Wettability alteration of calcite and dolomite carbonates using silica nanoparticles coated with fluorine groups. J. Petrol. Sci. Eng. 188, 106915. https://doi.org/10.1016/j.petrol.2020.106915.

Najafi, A., Nematipour, K., 2017. Synthesis and magnetic properties evaluation of monosized FeCo alloy nanoparticles through microemulsion method. J. Supercond. Nov. Magnetism 30 (9), 2647–2653. https://doi.org/10.1007/S10948-017-4052-2, 2017 30:9.

Nassar, N.N., Hassan, A., Pereira-Almao, P., 2011. Metal oxide nanoparticles for asphaltene adsorption and oxidation. Energy Fuel. 25 (3), 1017–1023. https://doi.org/10.1021/ef101230g.

Nassar, N.N., Betancur, S., Acevedo, S., Franco, C.A., Cortés, F.B., 2015. Development of a population balance model to describe the influence of shear and nanoparticles on the aggregation and fragmentation of asphaltene aggregates. Ind. Eng. Chem. Res. 54 (33), 8201–8211. https://doi.org/10.1021/acs.iecr.5b02075.

Natarajan, S., Harini, K., Gajula, G.P., Sarmento, B., Neves-Petersen, M.T., Thiagarajan, V., 2019. Multifunctional magnetic iron oxide nanoparticles: diverse synthetic approaches, surface modifications, cytotoxicity towards biomedical and industrial applications. BMC Materials 1 (1), 1–22. https://doi.org/10.1186/s42833-019-0002-6.

Nations, S., Wages, M., Cañas, J.E., Maul, J., Theodorakis, C., Cobb, G.P., 2011. Acute effects of Fe2O3, TiO2, ZnO and CuO nanomaterials on Xenopus laevis. Chemosphere 83 (8), 1053–1061. https://doi.org/10.1016/J.CHEMOSPHERE.2011.01.061.

Nazari Moghaddam, R., Bahramian, A., Fakhroueian, Z., Karimi, A., Arya, S., 2015. Comparative study of using nanoparticles for enhanced oil recovery: wettability alteration of carbonate rocks. Energy Fuel. 29 (4), 2111–2119. https://doi.org/10.1021/ef5024719.

Negin, C., Ali, S., Xie, Q., 2016. Application of nanotechnology for enhancing oil recovery – a review. Petroleum 2 (Issue 4), 324–333. https://doi.org/10.1016/j.petlm.2016.10.002. KeAi Communications Co.

Ngouangna, E.N., Manan, M.A., Oseh, J.O., Norddin, M.N.A.M., Agi, A., Gbadamosi, A. O., 2020. Influence of (3–Aminopropyl) triethoxysilane on silica nanoparticle for enhanced oil recovery. J. Mol. Liq. 315, 113740. https://doi.org/10.1016/j.molliq.2020.113740.

Nguyen, T.P., Le, U.T.P., Ngo, K.T., Pham, K.D., Dinh, L.X., 2016. Synthesis of polymer-coated magnetic nanoparticles from red mud waste for enhanced oil recovery in offshore reservoirs. J. Electron. Mater. 45 (7), 3801–3808. https://doi.org/10.1007/s11664-016-4513-6.

Nikiforov, V.N., Koksharov, Y.A., Polyakov, S.N., Malakho, A.P., Volkov, A.V., Moskvina, M.A., Khomutov, G.B., Irkhin, V.Y., 2013. Magnetism and Verwey transition in magnetite nanoparticles in thin polymer film. J. Alloys Compd. 569, 58–61. https://doi.org/10.1016/j.jallcom.2013.02.059.

Nugraha, M.I., Noorlaily, P., Abdullah, M., Khairurrijal, Iskandara, F., 2013. Synthesis of NixFe3-xO4 nanoparticles by microwave-assisted coprecipitation and their application on viscosity reduction of heavy oil. Mater. Sci. Forum 737, 204–208. https://doi.org/10.4028/www.scientific.net/MSF.737.204.

Nwadinigwe, C.A., Anigbogu, I.V., Ujam, O.T., 2015. Studies on precipitation performance of n-heptane and n-pentane/n-heptane on C7 and C5/C7 asphaltenes and maltenes from 350 °C atmospheric residuum of three Nigerian light crudes. J. Petrol. Exploration Production Technol. 5 (4), 403–407. https://doi.org/10.1007/s13202-014-0150-x.

Nwidee, L.N., Lebedev, M., Barifcani, A., Sarmadivaleh, M., Iglauer, S., 2017. Wettability alteration of oil-wet limestone using surfactant-nanoparticle formulation. J. Colloid Interface Sci. 504, 334–345. https://doi.org/10.1016/j.jcis.2017.04.078.

Ogolo, N.A., Olafuyi, O.A., Onyekonwu, M.O., 2012. Enhanced oil recovery using nanoparticles. In: Society of Petroleum Engineers - SPE Saudi Arabia Section Technical Symposium and Exhibition 2012, pp. 276–284. https://doi.org/10.2118/160847-ms.

Oseh, J.O., Mohd Norddin, M.N.A., Ismail, I., Gbadamosi, A.O., Agi, A., Mohammed, H. N., 2019. A novel approach to enhance rheological and filtration properties of water–based mud using polypropylene–silica nanocomposite. J. Petrol. Sci. Eng. 181 https://doi.org/10.1016/j.petrol.2019.106264.

Oseh, J.O., Mohd Norddin, M.N.A., Ismail, I., Gbadamosi, A.O., Agi, A., Ismail, A.R., 2020a. Study of cuttings lifting with different annular velocities using partially hydrolyzed polyacrylamide and enriched polypropylene–nanosilica composite in deviated and horizontal wells. Appl. Nanosci. 10 (3), 971–993. https://doi.org/10.1007/s13204-019-01163-6.

Oseh, J.O., Mohd Norddin, M.N.A., Ismail, I., Gbadamosi, A.O., Agi, A., Ismail, A.R., 2020b. Experimental investigation of cuttings transportation in deviated and horizontal wellbores using polypropylene–nanosilica composite drilling mud. J. Petrol. Sci. Eng. 189 https://doi.org/10.1016/j.petrol.2020.106958.

Oseh, J.O., Norddin, M.N.A.M., Ismail, I., Agi, A., Gbadamosi, A.O., Ismail, A.R., Manoger, P., Ravichandran, K., 2020c. Synergistic application of polypropylene and silica nanoparticle modified by (3-Aminopropyl) triethoxysilane for cuttings transport. In: Journal of King Saud University - Engineering Sciences. https://doi.org/10.1016/J.JKSUES.2020.10.007.

Oseh, J.O., Norddin, M.N.A.M., Ismail, I., Gbadamosi, A.O., Agi, A., Ismail, A.R., Manoger, P., Ravichandran, K., 2020d. Enhanced cuttings transport efficiency of water-based muds using (3–Aminopropyl) triethoxysilane on polypropylene-nanosilica composite. Arabian J. Chem. 13 (8), 6904–6920. https://doi.org/10.1016/J.ARABJC.2020.07.004.

Oseh, J.O., Norddin, M.N.A.M., Muhamad, H.N., Ismail, I., Gbadamosi, A.O., Agi, A., Ismail, A.R., Blkoor, S.O., 2020e. Influence of (3–Aminopropyl) triethoxysilane on entrapped polypropylene at nanosilica composite for shale swelling and hydration inhibition. J. Petrol. Sci. Eng. 194 https://doi.org/10.1016/j.petrol.2020.107560.

Ozel, F., Kockar, H., Karaagac, O., 2015. Growth of iron oxide nanoparticles by hydrothermal process: effect of reaction parameters on the nanoparticle size. J. Supercond. Nov. Magnetism 28 (3), 823–829. https://doi.org/10.1007/s10948-014-2707-9.

Pal, N., Mandal, A., 2020. Oil recovery mechanisms of Pickering nanoemulsions stabilized by surfactant-polymer-nanoparticle assemblies: a versatile surface energies' approach. Fuel 276, 118138. https://doi.org/10.1016/j.fuel.2020.118138.

Pal, N., Kumar, N., Mandal, A., 2019. Stabilization of dispersed oil droplets in nanoemulsions by synergistic effects of the gemini surfactant, PHPA polymer, and silica nanoparticle [Research-article]. Langmuir 35 (7), 2655–2667. https://doi.org/10.1021/acs.langmuir.8b03364.

Park, Y.C., Paulsen, J., Nap, R.J., Whitaker, R.D., Mathiyazhagan, V., Song, Y.Q., Hürlimann, M., Szleifer, I., Wong, J.Y., 2014. Adsorption of superparamagnetic iron oxide nanoparticles on silica and calcium carbonate sand. Langmuir 30 (3), 784–792. https://doi.org/10.1021/la404387t.

Patel, H., Shah, S., Ahmed, R., 2018. Effects of nanoparticles and temperature on heavy oil viscosity. J. Petrol. Sci. Eng. https://doi.org/10.1016/j.petrol.2018.04.069.

Pei, H.H., Zhang, G.C., Ge, J.J., Zhang, J., Zhang, Q., Fu, L.P., 2015. Investigation of nanoparticle and surfactant stabilized emulsion to enhance oil recovery in waterflooded heavy oil reservoirs. In: Society of Petroleum Engineers - SPE Canada Heavy Oil Technical Conference 2015. CHOC, pp. 666–676. https://doi.org/10.2118/174488-ms, 2015.

Peng, J., Liu, Q., Xu, Z., Masliyah, J., 2012. Novel magnetic demulsifier for water removal from diluted bitumen emulsion. Energy Fuel. 26 (5), 2705–2710. https://doi.org/10.1021/ef2014259.

Peng, K., Xiong, Y., Lu, L., Liu, J., Huang, X., 2018. Recyclable functional magnetic nanoparticles for fast demulsification of waste metalworking emulsions driven by electrostatic interactions. ACS Sustain. Chem. Eng. 6 (8), 9682–9690. https://doi.org/10.1021/ACSSUSCHEMENG.8B00499.

Pereira, M.L.D.O., Maia, K.C.B., Silva, W.C., Leite, A.C., Francisco, A.D.D.S., Vasconcelos, T.L., Nascimento, R.S.V., Grasseschi, D., 2020. Fe3O4Nanoparticles as surfactant carriers for enhanced oil recovery and scale prevention. ACS Appl. Nano Mater. 3 (6), 5762–5772. https://doi.org/10.1021/acsanm.0c00939.

Pichot, R., Spyropoulos, F., Norton, I.T., 2012. Competitive adsorption of surfactants and hydrophilic silica particles at the oil-water interface: interfacial tension and contact angle studies. J. Colloid Interface Sci. 377 (1), 396–405. https://doi.org/10.1016/j.jcis.2012.01.065.

Pilapil, B.K., Jahandideh, H., Bryant, S.L., Trifkovic, M., 2016. Stabilization of oil-in-water emulsions with noninterfacially adsorbed particles. Langmuir 32 (28), 7109–7116. https://doi.org/10.1021/acs.langmuir.6b00873.

Prathna, Sharma, S.K., Kennedy, M., 2017. Arsenic and fluoride removal by iron oxide and iron oxide/alumina nanocomposites: a comparison. Proceedings of the World Congress on New Technologies 1–4. https://doi.org/10.11159/icnfa17.118.

Prévot, G., Kauss, T., Lorenzato, C., Gaubert, A., Larivière, M., Baillet, J., Laroche-Traineau, J., Jacobin-Valat, M.J., Adumeau, L., Mornet, S., Barthélémy, P., Duonor-Cérutti, M., Clofent-Sanchez, G., Crauste-Manciet, S., 2017a. Iron oxide core oil-in-water nanoemulsion as tracer for atherosclerosis MPI and MRI imaging. Int. J. Pharm. 532 (2), 669–676. https://doi.org/10.1016/j.ijpharm.2017.09.010.

Prévot, G., Mornet, S., Lorenzato, C., Kauss, T., Adumeau, L., Gaubert, A., Baillet, J., Barthélémy, P., Clofent-Sanchez, G., Crauste-Manciet, S., 2017b. Data on iron oxide core oil-in-water nanoemulsions for atherosclerosis imaging. Data in Brief 15, 876–881. https://doi.org/10.1016/j.dib.2017.10.059.

Prigiobbe, V., Ko, S., Wang, Q., Huh, C., Bryant, S.L., Bennetzen, M.V., 2015. Magnetic nanoparticles for efficient removal of oilfield contaminants: modeling of magnetic separation and validation. Proceedings - SPE International Symposium on Oilfield Chemistry 2, 1093–1104. https://doi.org/10.2118/173786-ms.

Punia, P., Bharti, M.K., Chalia, S., Dhar, R., Ravelo, B., Thakur, P., Thakur, A., 2020. Recent advances in synthesis, characterization, and applications of nanoparticles for contaminated water treatment- A review. In: Ceramics International. Elsevier Ltd. https://doi.org/10.1016/j.ceramint.2020.09.050.

Rahmani, A.R., Athey, A., Chen, J., Wilt, M., 2013a. Sensitivity of Dipole Magnetic Tomography to Magnetic Nanoparticle Injectates. Society of Exploration Geophysicists International Exposition and 83rd Annual Meeting, pp. 571–575. https://doi.org/10.1190/segam2013-0142.1. SEG 2013: Expanding Geophysical Frontiers.

Rahmani, A.R., Bryant, S., Huh, C., Athey, A., Ahmadian, M., Chen, J., Wilt, M., 2013b. Crosswell magnetic sensing of superparamagnetic nanoparticles for subsurface applications. Proceedings - SPE Annual Technical Conference and Exhibition 1, 861–876. https://doi.org/10.2118/166140-ms.

Rahmani, A.R., Athey, A.E., Chen, J., Wilt, M.J., 2014. Sensitivity of dipole magnetic tomography to magnetic nanoparticle injectates. J. Appl. Geophys. 103, 199–214. https://doi.org/10.1016/j.jappgeo.2014.01.019.

Rahmani, A.R., Bryant, S., Huh, C., Athey, A., Ahmadian, M., Chen, J., Wilt, M., 2015. Crosswell magnetic sensing of superparamagnetic nanoparticles for subsurface applications. SPE J. 20 (5), 1067–1082. https://doi.org/10.2118/166140-PA.

Rangsanga, P., Sirisathitkul, C., 2019. Magnetoviscosity and wettability of magnetic fluids containing magnetite nanocubes. In: Jurnal Tribologi, vol. 22.

Reddy, L.H., Arias, J.L., Nicolas, J., Couvreur, P., 2012. Magnetic nanoparticles: design and characterization, toxicity and biocompatibility, pharmaceutical and biomedical applications. Issue 11. In: Chemical Reviews, vol. 112. American Chemical Society, pp. 5818–5878. https://doi.org/10.1021/cr300068p.

Rezvani, H., Riazi, M., Tabaei, M., Kazemzadeh, Y., Sharifi, M., 2018. Experimental investigation of interfacial properties in the EOR mechanisms by the novel synthesized Fe3O4@Chitosan nanocomposites. Colloid. Surface. Physicochem. Eng. Aspect. 544 (November 2017), 15–27. https://doi.org/10.1016/j.colsurfa.2018.02.012.

Rezvani, H., Kazemzadeh, Y., Sharifi, M., Riazi, M., Shojaei, S., 2019. A new insight into Fe3O4-based nanocomposites for adsorption of asphaltene at the oil/water interface: an experimental interfacial study. J. Petrol. Sci. Eng. 177, 786–797. https://doi.org/10.1016/j.petrol.2019.02.077.

Rochelle, M., Cornell, U.S., 2006. The Iron Oxides: Structure, Properties, Reactions, Occurrences and Uses, 2nd, Completely Revised and Extended, Edition.

Ruhland, T.M., Gröschel, A.H., Ballard, N., Skelhon, T.S., Walther, A., Müller, A.H.E., Bon, S.A.F., 2013. Influence of janus particle shape on their interfacial behavior at liquid-liquid interfaces. Langmuir 29 (5), 1388–1394. https://doi.org/10.1021/la3048642.

Ryoo, S., Rahmani, A.R., Yoon, K.Y., Prodanović, M., Kotsmar, C., Milner, T.E., Johnston, K.P., Bryant, S.L., Huh, C., 2012. Theoretical and experimental investigation of the motion of multiphase fluids containing paramagnetic nanoparticles in porous media. J. Petrol. Sci. Eng. 81, 129–144. https://doi.org/10.1016/j.petrol.2011.11.008.

Safaei, A., Esmaeilzadeh, F., Sardarian, A., Mousavi, S.M., Wang, X., 2020. Experimental investigation of wettability alteration of carbonate gas-condensate reservoirs from oil-wetting to gas-wetting using Fe3O4 nanoparticles coated with Poly (vinyl alcohol), (PVA) or Hydroxyapatite (HAp). J. Petrol. Sci. Eng. 184, 106530. https://doi.org/10.1016/j.petrol.2019.106530.

Sagala, F., Hethnawi, A., Nassar, N.N., 2020. Hydroxyl-functionalized silicate-based nanofluids for enhanced oil recovery. Fuel 269 (January), 117462. https://doi.org/10.1016/j.fuel.2020.117462.

Saien, J., Gorji, A.M., 2017. Simultaneous adsorption of CTAB surfactant and magnetite nanoparticles on the interfacial tension of n-hexane–water. J. Mol. Liq. 242, 1027–1034. https://doi.org/10.1016/j.molliq.2017.07.115.

Saien, J., Hashemi, S., 2018. Long chain imidazolium ionic liquid and magnetite nanoparticle interactions at the oil/water interface. J. Petrol. Sci. Eng. 160, 363–371. https://doi.org/10.1016/j.petrol.2017.10.057.

Sangaiya, P., Jayaprakash, R., 2018. A review on iron oxide nanoparticles and their biomedical applications. Issue 11. In: Journal of Superconductivity and Novel Magnetism, vol. 31. Springer New York LLC, pp. 3397–3413. https://doi.org/10.1007/s10948-018-4841-2.

Saravanan, M., R Suganya, M.R., 2011. Toxicity of iron oxide nanoparticles to Indian major carp, Labeo rohita on haematological, biochemical, ionoregulatory and enzymological alterations. In: 8th International Symposium on Recent Advances in Environmental Health Research. Jackson, MS, USA. Sep.1.https://scholar.google.com/scholar?q=Saravanan+M,+Suganya+R,+Ramesh+M+(2011)+Toxicity+of+iron+oxide+nanoparticles+to+Indian+major+carp,++Labeo+rohita++on+haematological,+biochemical,+ionoregulatory+and+enzymological+alterations.+8th+International+Symposiu.

Sarbolookzadeh Harandi, S., Karimipour, A., Afrand, M., Akbari, M., D'Orazio, A., 2016. An experimental study on thermal conductivity of F-MWCNTs-Fe3O4/EG hybrid nanofluid: effects of temperature and concentration. Int. Commun. Heat Mass Tran. 76, 171–177. https://doi.org/10.1016/j.icheatmasstransfer.2016.05.029.

Servin, Jesus Manuel Felix, 2018, October 19. Monitoring water flood front movement by propagating high frequency pulses through subsurface transmission lines. In: Society of Petroleum Engineers - SPE Asia Pacific Oil and Gas Conference and Exhibition 2018. APOGCE. https://doi.org/10.2118/191874-MS, 2018.

Servin, Jesus M.Felix, Schmidt, H.K., Ellis, E.S., 2016. Improved saturation mapping using planar tranmission lines and magnetic agents. In: Proceedings - SPE Annual Technical Conference and Exhibition. https://doi.org/10.2118/181343-ms, 2016-Janua.

Setoodeh, N., Darvishi, P., Esmaeilzadeh, F., 2018a. Adsorption of asphaltene from crude oil by applying polythiophene coating on Fe3O4 nanoparticles. J. Dispersion Sci. Technol. 39 (4), 578–588. https://doi.org/10.1080/01932691.2017.1339607.

Setoodeh, N., Darvishi, P., Lashanizadegan, A., 2018b. Enhancing of asphaltene adsorption onto Fe3O4 nanoparticles coated with metal-organic framework Mil-101 (Cr) for the inhibition of asphaltene precipitation. J. Dispersion Sci. Technol. 39 (3), 452–459. https://doi.org/10.1080/01932691.2017.1326310.

Setoodeh, N., Darvishi, P., Lashanizadegan, A., Esmaeilzadeh, F., 2020. A comparative study for evaluating the performance of five coatings applied on Fe3O4 nanoparticles for inhibition of asphaltene precipitation from crude oil. J. Dispersion Sci. Technol. 41 (11), 1616–1632. https://doi.org/10.1080/01932691.2019.1634581.

Shaker, S., Zafarian, S., et al., 2013. undefined. (2013). Preparation and characterization of magnetite nanoparticles by Sol-Gel method for water treatment. Researchgate.Net 2. https://www.researchgate.net/profile/Shilpachakra-Chidurala/publication/299453397_Synthesis_of_Magnetite_Nanoparticles_by_Sol-Gel_Method_for_Environmental_Applications/links/5d3aad994585153e59222b95/Synthesis-of-Magnetite-Nanoparticles-by-Sol-Gel-Method-for-Environmental-Applications.pdf.

Shalbafan, M., Esmaeilzadeh, F., Safaei, A., XiaopoWang, 2019. Experimental investigation of wettability alteration and oil recovery enhance in carbonate reservoirs using iron oxide nanoparticles coated with EDTA or SLS. J. Petrol. Sci. Eng. 180, 559–568. https://doi.org/10.1016/j.petrol.2019.05.085.

Shalbafan, M., Esmaeilzadeh, F., Vakili-Nezhaad, G.R., 2020a. Enhanced oil recovery by wettability alteration using iron oxide nanoparticles covered with PVP or SDS. Colloid. Surface. Physicochem. Eng. Aspect. 607, 125509. https://doi.org/10.1016/j.colsurfa.2020.125509.

Shalbafan, M., Esmaeilzadeh, F., Vakili-Nezhaad, G.R., 2020b. Enhanced oil recovery by wettability alteration using iron oxide nanoparticles covered with PVP or SDS. Colloid. Surface. Physicochem. Eng. Aspect. 607, 125509. https://doi.org/10.1016/j.colsurfa.2020.125509.

ShamsiJazeyi, H., Verduzco, R., Hirasaki, G.J., 2014. Reducing adsorption of anionic surfactant for enhanced oil recovery: Part I. Competitive adsorption mechanism. Colloid. Surface. Physicochem. Eng. Aspect. 453 (1), 162–167. https://doi.org/10.1016/j.colsurfa.2013.10.042.

Sharma, A.K., Tiwari, A.K., Dixit, A.R., 2016. Rheological behaviour of nanofluids: a review. In: Renewable and Sustainable Energy Reviews, vol. 53, pp. 779–791. https://doi.org/10.1016/j.rser.2015.09.033.

Sharma, A., Foppen, J.W., Banerjee, A., Bachhar, N., Bandyopadhyay, S., 2020. Magnetic Nanoparticles to Unique DNA Tracers-Effect of Functionalization on Physico-Chemical Properties. https://doi.org/10.21203/rs.3.rs-84463/v1.

Shayan, N.N., Mirzayi, B., 2015. Adsorption and removal of asphaltene using synthesized maghemite and hematite nanoparticles. Energy Fuel. 29 (3), 1397–1406. https://doi.org/10.1021/ef502494d.

Shehzad, F., Hussein, I.A., Kamal, M.S., Ahmad, W., Sultan, A.S., Nasser, M.S., 2018. Polymeric surfactants and emerging alternatives used in the demulsification of produced water: a review. In: Polymer Reviews, vol. 58. Taylor & Francis, pp. 63–101. https://doi.org/10.1080/15583724.2017.1340308. Issue 1.

Shekhawat, D.S., Aggarwal, A., Agarwal, S., Imtiaz, M.D., 2016. Magnetic Recovery-Injecting Newly Designed Magnetic Fracturing Fluid with Applied Magnetic Field for EOR. *Society of Petroleum Engineers - SPE Asia Pacific Hydraulic Fracturing Conference*. https://doi.org/10.2118/181853-ms.

Shen, Z., Sheng, J.J., 2018. Experimental and numerical study of permeability reduction caused by asphaltene precipitation and deposition during CO2 huff and puff injection in Eagle Ford shale. Fuel 211, 432–445. https://doi.org/10.1016/j.fuel.2017.09.047.

Shen, L., Li, B., Qiao, Y., 2018. Fe3O4 nanoparticles in targeted drug/gene delivery systems, 2018 Materials 11, 324. https://doi.org/10.3390/MA11020324. Page 324, S(2).

Sheng, J.J., 2015. Status of surfactant EOR technology. Petroleum 1 (Issue 2), 97–105. https://doi.org/10.1016/j.petlm.2015.07.003. KeAi Communications Co.

Shokrlu, Y. Hamedi, Babadagli, T., 2010. Effects of nano sized metals on viscosity reduction of heavy oil/bitumen during thermal applications. Society of Petroleum Engineers - Canadian Unconventional Resources and International Petroleum Conference 3 (Omole 1999), 1587–1596, 2010.

Shokrlu, Yousef Hamedi, Babadagli, T., 2014. Viscosity reduction of heavy oil/bitumen using micro- and nano-metal particles during aqueous and non-aqueous thermal applications. J. Petrol. Sci. Eng. 119, 210–220. https://doi.org/10.1016/j.petrol.2014.05.012.

Shokrollahi, H., 2013. Structure, synthetic methods, magnetic properties and biomedical applications of ferrofluids. Mater. Sci. Eng. C 33 (5), 2476–2487. https://doi.org/10.1016/J.MSEC.2013.03.028.

Sikiru, S., Rostami, A., Soleimani, H., Yahya, N., Afeez, Y., Aliu, O., Yusuf, J.Y., Oladosu, T.L., 2020. Graphene: outlook in the enhance oil recovery (EOR). J. Mol. Liq. xxxx, 114519. https://doi.org/10.1016/j.molliq.2020.114519.

Simonsen, G., Strand, M., Øye, G., 2018. Potential applications of magnetic nanoparticles within separation in the petroleum industry. J. Petrol. Sci. Eng. 165 (February), 488–495. https://doi.org/10.1016/j.petrol.2018.02.048.

Soares, P.I.P., Lochte, F., Echeverria, C., Pereira, L.C.J., T Coutinho, J., Ferreira, I.M.M., Novo, C.M.M., Borges, J.P.M.R., 2015. Thermal and magnetic properties of iron oxide colloids: influence of surfactants. Nanotechnology 26 (42), 425704. https://doi.org/10.1088/0957-4484/26/42/425704.

Soares, P.I.P., Laia, C.A.T., Carvalho, A., Pereira, L.C.J., Coutinho, J.T., Ferreira, I.M.M., Novo, C.M.M., Borges, J.P., 2016. Iron oxide nanoparticles stabilized with a bilayer of oleic acid for magnetic hyperthermia and MRI applications. Appl. Surf. Sci. 383, 240–247. https://doi.org/10.1016/j.apsusc.2016.04.181.

Soares, S.F., Fernandes, T., Trindade, T., Daniel-Da-Silva, A.L., 2019. Trimethyl chitosan/siloxane-hybrid coated Fe3O4 nanoparticles for the uptake of sulfamethoxazole from water. Molecules 24 (10). https://doi.org/10.3390/molecules24101958.

Sofla, S.J.D., James, L.A., Zhang, Y., 2019. Understanding the behavior of H+-protected silica nanoparticles at the oil-water interface for enhanced oil recovery (EOR) applications. J. Mol. Liq. 274, 98–114. https://doi.org/10.1016/j.molliq.2018.09.049.

Soleimani, H., Latiff, N.R.A., Yahya, N., Sabet, M., Khodapanah, L., Kozlowski, G., Chuan, L.K., Guan, B.H., 2016. Synthesis and characterization of yttrium iron Garnet (YIG) Nanoparticles activated by electromagnetic wave in enhanced oil recovery. J. Nano Res. 38, 40–46. https://doi.org/10.4028/www.scientific.net/JNanoR.38.40.

Soleimani, H., Baig, M.K., Yahya, N., Khodapanah, L., Sabet, M., Demiral, B.M.R., Burda, M., 2018. Synthesis of ZnO nanoparticles for oil–water interfacial tension reduction in enhanced oil recovery. Appl. Phys. Mater. Sci. Process 124 (2). https://doi.org/10.1007/s00339-017-1510-4, 0.

Song, D., Jing, D., Ma, W., Zhang, X., 2018. High thermal conductivity of nanoparticles not necessarily contributing more to nanofluids. Appl. Phys. Lett. 113 (22), 223104. https://doi.org/10.1063/1.5055058.

Srivastava, V., Singh, P., Weng, C., Sharma, Y., 2011. Economically viable synthesis of Fe3O4 nanoparticles and their characterization. Pol. J. Chem. Technol. 13 (2), 1–5. https://doi.org/10.2478/V10026-011-0015-8.

Srivastava, S., Usmani, Z., Atanasov, A.G., Singh, V.K., Singh, N.P., Abdel-Azeem, A.M., Prasad, R., Gupta, G., Sharma, M., Bhargava, A., 2020. Biological nanofactories: using living forms for metal nanoparticle synthesis. Mini Rev. Med. Chem. 21 (2), 245–265. https://doi.org/10.2174/1389557520999201116163012.

Stojanović, Z., Otoničar, M., Lee, J., Stevanović, M.M., Hwang, M.P., Lee, K.H., Choi, J., Uskoković, D., 2013. The solvothermal synthesis of magnetic iron oxide nanocrystals and the preparation of hybrid poly(l-lactide)-polyethyleneimine magnetic particles. Colloids Surf. B Biointerfaces 109, 236–243. https://doi.org/10.1016/j.colsurfb.2013.03.053.

Struchkov, I.A., Rogachev, M.K., Kalinin, E.S., Roschin, P.V., 2019. Laboratory investigation of asphaltene-induced formation damage. J. Petrol. Exploration Production Technol. 9 (2), 1443–1455. https://doi.org/10.1007/s13202-018-0539-z.

Suleimanov, B.A., Ismailov, F.S., Veliyev, E.F., 2011. Nanofluid for enhanced oil recovery. J. Petrol. Sci. Eng. 78 (2), 431–437. https://doi.org/10.1016/j.petrol.2011.06.014.

Sun, X., Zhang, Y., Chen, G., Gai, Z., 2017. Application of nanoparticles in enhanced oil recovery: a critical review of recent progress. Energies 10 (3). https://doi.org/10.3390/en10030345.

Sun, B., Guo, Y., Yang, D., Li, H., 2020. The effect of constant magnetic field on convective heat transfer of Fe3O4/water magnetic nanofluid in horizontal circular tubes. Appl. Therm. Eng. 171, 114920. https://doi.org/10.1016/j.applthermaleng.2020.114920.

Sundar, L.S., Singh, M.K., Sousa, A.C.M., 2014. Enhanced heat transfer and friction factor of MWCNT-Fe3O4/water hybrid nanofluids. Int. Commun. Heat Mass Tran. 52, 73–83. https://doi.org/10.1016/j.icheatmasstransfer.2014.01.012.

Syam Sundar, L., Singh, M.K., Sousa, A.C.M., 2013. Investigation of thermal conductivity and viscosity of Fe3O4 nanofluid for heat transfer applications. Int. Commun. Heat Mass Tran. 44, 7–14. https://doi.org/10.1016/j.icheatmasstransfer.2013.02.014.

Taheri-Shakib, J., Shekarifard, A., Naderi, H., 2018. Experimental investigation of the asphaltene deposition in porous media: accounting for the microwave and ultrasonic effects. J. Petrol. Sci. Eng. 163, 453–462. https://doi.org/10.1016/j.petrol.2018.01.017.

Tarek, M., 2015. Investigating nano-fluid mixture effects to enhance oil recovery. https://doi.org/10.2118/178739-stu.

Tawfik, M.M., 2017. Experimental studies of nanofluid thermal conductivity enhancement and applications: a review. In: Renewable and Sustainable Energy Reviews, vol. 75. Elsevier Ltd, pp. 1239–1253. https://doi.org/10.1016/j.rser.2016.11.111.

Tengku Mohd, T.A., Baco, J., Bakar, N.F.A., Jaafar, M.Z., 2016. Effects of particle shape and size on nanofluid properties for potential Enhanced Oil Recovery (EOR). MATEC Web of Conferences 69, 1–6. https://doi.org/10.1051/matecconf/20166903006.

Thanh, N.T.K., Maclean, N., Mahiddine, S., 2014. Mechanisms of nucleation and growth of nanoparticles in solution, 15. In: Chemical Reviews, vol. 114. American Chemical Society, pp. 7610–7630. https://doi.org/10.1021/cr400544s.

Udoetok I, A., Wilson, L.D., Headley J, V., 2016. Stabilization of pickering emulsions by iron oxide nano-particles (Fe3O4 NPs). Adv. Mater. Sci. 1 (2) https://doi.org/10.15761/AMS.1000107.

Ulbrich, K., Holá, K., Šubr, V., Bakandritsos, A., Tuček, J., Zbořil, R., 2016. Targeted drug delivery with polymers and magnetic nanoparticles: covalent and noncovalent approaches, release control, and clinical studies. Chem. Rev. 116 (9), 5338–5431. https://doi.org/10.1021/ACS.CHEMREV.5B00589.

Unni, M., Uhl, A.M., Savliwala, S., Savitzky, B.H., Dhavalikar, R., Garraud, N., Arnold, D. P., Kourkoutis, L.F., Andrew, J.S., Rinaldi, C., 2017. Thermal decomposition synthesis of iron oxide nanoparticles with diminished magnetic dead layer by controlled addition of oxygen. ACS Nano 11 (2), 2284–2303. https://doi.org/10.1021/acsnano.7b00609.

Urenã-Benavides, E.E., Lin, E.L., Foster, E.L., Xue, Z., Ortiz, M.R., Fei, Y., Larsen, E.S., Kmetz, A.A., Lyon, B.A., Moaseri, E., Bielawski, C.W., Pennell, K.D., Ellison, C.J., Johnston, K.P., 2016. Low adsorption of magnetite nanoparticles with uniform polyelectrolyte coatings in concentrated brine on model silica and sandstone. Ind. Eng. Chem. Res. 55 (6), 1522–1532. https://doi.org/10.1021/acs.iecr.5b03279.

Vallabani, N.V.S., Singh, S., 2018. Recent advances and future prospects of iron oxide nanoparticles in biomedicine and diagnostics. In: 3 Biotech, vol. 8. Springer Verlag, p. 279. https://doi.org/10.1007/s13205-018-1286-z. Issue 6.

Vidya, P.V., Chitra, K.C., 2019. Irreversible histopathological modifications induced by iron oxide nanoparticles in the fish, Oreochromis mossambicus (peters, 1852). Biol. Forum An Int. J. 11 (1). https://www.researchgate.net/publication/331345329.

Vipulanandan, C., Mohammed, A., 2020. Magnetic field strength and temperature effects on the behavior of oil well cement slurry modified with iron oxide nanoparticles and quantified with vipulanandan models. J. Test. Eval. 48 (6), 20180107. https://doi.org/10.1520/JTE20180107.

Vipulanandan, C., Krishnamoorti, R., Mohammed, A., Boncan, V., Narvaez, G., Hughes, B., Head, B., Pappas, J.M., 2015. Iron nanoparticle modified smart cement for real time monitoring of ultra deepwater oil well cementing applications. Proceedings of the Annual Offshore Technology Conference 3, 2216–2231. https://doi.org/10.4043/25842-ms.

Vipulanandan, C., Mohammed, A., Samuel, R.G., 2017. Smart bentonite drilling muds modified with iron oxide nanoparticles & characterized based on the electrical resistivity & rheological properties with varying magnetic field strengths & temperatures. Proceedings of the Annual Offshore Technology Conference 5, 3613–3630. https://doi.org/10.4043/27626-ms.

Vipulanandan, C., Maddi, A.R., Ganpatye, A.S., 2018. Smart spacer fluid modified with iron oxide nanoparticles for in-situ property enhancement was developed for cleaning oil based drilling fluids and characterized using the vipulanandan rheological model. Proceedings of the Annual Offshore Technology Conference 6, 4586–4605. https://doi.org/10.4043/28886-ms.

Vryzas, Z., Zaspalis, V., Nalbantian, L., Mahmoud, O., Nasr-El-Din, H.A., Kelessidis, V.C., 2016. A Comprehensive Approach for the Development of New Magnetite Nanoparticles Giving Smart Drilling Fluids with Superior Properties for HP/HT Applications. https://doi.org/10.2523/IPTC-18731-MS.

Vryzas, Zisis, Mahmoud, O., Nasr-El-Din, H., Zaspalis, V., Kelessidis, V.C., 2016. Incorporation of Fe3O4 nanoparticles as drilling fluid additives for improved drilling operations. Proceedings of the International Conference on Offshore Mechanics and Arctic Engineering - OMAE 8. https://doi.org/10.1115/OMAE2016-54071.

Vryzas, Zisis, Kelessidis, V.C., Bowman, M.B.J., Nalbantian, L., Zaspalis, V., Mahmoud, O., Nasr-El-Din, H.A., 2017. Smart magnetic drilling fluid with in-situ rheological controllability using Fe3O4 nanoparticles. In: SPE Middle East Oil and Gas Show and Conference, MEOS, Proceedings, 2017-March, pp. 2558–2569. https://doi.org/10.2118/183906-ms.

Wai, M.M., Khe, C.S., Yau, X.H., Liu, W.W., Sokkalingam, R., Jumbri, K., Lwin, N., 2019. Optimization and characterization of magnetite-reduced graphene oxide

nanocomposites for demulsification of crude oil in water emulsion. RSC Adv. 9 (41), 24003–24014. https://doi.org/10.1039/c9ra03304a.
Wang, B., Feng, W., Zhu, M., Wang, Y., Wang, M., Gu, Y., Ouyang, H., Wang, H., Li, M., Zhao, Y., Chai, Z., Wang, H., 2008. Neurotoxicity of low-dose repeatedly intranasal instillation of nano- and submicron-sized ferric oxide particles in mice. J. Nanoparticle Res. 11 (1), 41–53. https://doi.org/10.1007/S11051-008-9452-6, 2008 11:1.
Wang, Q., Prigiobbe, V., Huh, C., Bryant, S.L., Bennetzen, M.V., Mogensen, K., 2014. Removal of divalent cations from brine using selective adsorption onto magnetic nanoparticles. In: Society of Petroleum Engineers - International Petroleum Technology Conference 2014, IPTC 2014 - Innovation and Collaboration: Keys to Affordable Energy, vol. 2, pp. 1753–1764. https://doi.org/10.2523/iptc-17901-ms.
Wang, L., Wang, Y., Yan, X., Wang, X., Feng, B., 2016. Investigation on viscosity of Fe3O4 nanofluid under magnetic field. Int. Commun. Heat Mass Tran. 72, 23–28. https://doi.org/10.1016/j.icheatmasstransfer.2016.01.013.
Wanna, Y., Chindaduang, A., Tumcharern, G., Phromyothin, D., Porntheerapat, S., Nukeaw, J., Hofmann, H., Pratontep, S., 2016. Efficiency of SPIONs functionalized with polyethylene glycol bis(amine) for heavy metal removal. J. Magn. Magn Mater. 414, 32–37. https://doi.org/10.1016/j.jmmm.2016.04.064.
Wasan, D.T., Nikolov, A.D., 2003. Spreading of nanofluids on solids. Nature 423 (6936), 156–159. https://doi.org/10.1038/nature01591.
Wasan, D., Nikolov, A., Kondiparty, K., 2011. The wetting and spreading of nanofluids on solids: role of the structural disjoining pressure. Curr. Opin. Colloid Interface Sci. 16 (4), 344–349. https://doi.org/10.1016/j.cocis.2011.02.001.
Wu, W., He, Q., Jiang, C., 2008. Magnetic iron oxide nanoparticles: synthesis and surface functionalization strategies. Nanoscale Res. Lett. 3 (11), 397–415. https://doi.org/10.1007/s11671-008-9174-9.
Wu, W., Jiang, C., Roy, V.A.L., 2015. Recent progress in magnetic iron oxide-semiconductor composite nanomaterials as promising photocatalysts. Nanoscale 7 (1), 38–58. https://doi.org/10.1039/c4nr04244a. Royal Society of Chemistry.
Wu, W., Wu, Z., Yu, T., Jiang, C., Kim, W.S., 2015a. Recent progress on magnetic iron oxide nanoparticles: synthesis, surface functional strategies and biomedical applications. Issue 2. In: Science and Technology of Advanced Materials, vol. 16. Institute of Physics Publishing, 023501. https://doi.org/10.1088/1468-6996/16/2/023501.
Wu, W., Wu, Z., Yu, T., Jiang, C., Kim, W.S., 2015b. Recent progress on magnetic iron oxide nanoparticles: synthesis, surface functional strategies and biomedical applications. Issue 2. In: Science and Technology of Advanced Materials, vol. 16. Institute of Physics Publishing. https://doi.org/10.1088/1468-6996/16/2/023501.
Wu, W., Jiang, C.Z., Roy, V.A.L., 2016. Designed synthesis and surface engineering strategies of magnetic iron oxide nanoparticles for biomedical applications. Nanoscale 8 (47), 19421–19474. https://doi.org/10.1039/c6nr07542h.
Wu, H., Gao, K., Lu, Y., Meng, Z., Gou, C., Li, Z., Yang, M., Qu, M., Liu, T., Hou, J., Kang, W., 2020. Silica-based amphiphilic Janus nanofluid with improved interfacial properties for enhanced oil recovery. Colloid. Surface. Physicochem. Eng. Aspect. 586, 124162. https://doi.org/10.1016/j.colsurfa.2019.124162.
Xi, K., Cao, Y., Haile, B.G., Zhu, R., Jahren, J., Bjørlykke, K., Zhang, X., Hellevang, H., 2016. How does the pore-throat size control the reservoir quality and oiliness of tight sandstones? The case of the Lower Cretaceous Quantou Formation in the southern Songliao Basin, China. Mar. Petrol. Geol. 76, 1–15. https://doi.org/10.1016/j.marpetgeo.2016.05.001.
Xing, Y.-F., Xu, Y.-H., Shi, M.-H., Lian, Y.-X., 2016. The impact of PM2.5 on the human respiratory system. J. Thorac. Dis. 8 (1), E69. https://doi.org/10.3978/J.ISSN.2072-1439.2016.01.19.
Xiong, Y., Huang, X., Lu, B., Wu, B., Lu, L., Liu, J., Peng, K., 2020. Acceleration of floc-water separation and floc reduction with magnetic nanoparticles during demulsification of complex waste cutting emulsions. J. Environ. Sci. 89, 80–89. https://doi.org/10.1016/J.JES.2019.10.011.
Xu, Y., Ayala-Orozco, C., Wong, M.S., 2018. Heavy oil viscosity reduction using iron III para-toluenesulfonate hexahydrate. In: SPE Western Regional Meeting Proceedings. https://doi.org/10.2118/190020-ms.
Yahya, N., Kashif, M., Nasir, N., Akhtar, M.N., Yusof, N.M., 2012. Cobalt ferrite nanoparticles: an innovative approach for enhanced oil recovery application. J. Nano Res. 17, 115–126. https://doi.org/10.4028/www.scientific.net/JNanoR.17.115.
Yahya, N., Kashif, M., Shafie, A., Solemani, H., Zaid, H.M., Latiff, N.R.A., 2014. Improved oil recovery by high magnetic flux density subjected to iron oxide nanofluids. J. Nano Res. 26, 89–99. https://doi.org/10.4028/www.scientific.net/JNanoR.26.89.
Yahya, N., Ali, A.M., Wahaab, F.A., Sikiru, S., 2020. Spectroscopic analysis of the adsorption of carbon based nanoparticles on reservoir sandstones. J. Mater. Res. Technol. https://doi.org/10.1016/j.jmrt.2020.02.058.
Yakasai, F., Jaafar, M.Z., Bandyopadhyay, S., Agi, A., 2021. Current developments and future outlook in nanofluid flooding: a comprehensive review of various parameters influencing oil recovery mechanisms. J. Ind. Eng. Chem. 93, 138–162. https://doi.org/10.1016/j.jiec.2020.10.017.
Yamashita, K., Okada, S., Sawada, H., 2019. Preparation of fluoroalkyl end-capped vinyltrimethoxysilane oligomeric silica/magnetite composites – application to separation of oil and water. Colloid. Surface. Physicochem. Eng. Aspect. 581, 123668. https://doi.org/10.1016/J.COLSURFA.2019.123668.
Yekeen, N., Padmanabhan, E., Syed, A.H., Sevoo, T., Kanesen, K., 2020. Synergistic influence of nanoparticles and surfactants on interfacial tension reduction, wettability alteration and stabilization of oil-in-water emulsion. J. Petrol. Sci. Eng. 186, 106779. https://doi.org/10.1016/j.petrol.2019.106779.
Yu, H., Kotsmar, C., Yoon, K.Y., Ingram, D.R., Johnston, K.P., Bryant, S.L., Huh, C., 2010. Transport and retention of aqueous dispersions of paramagnetic nanoparticles in reservoir rocks. Proceedings - SPE Symposium on Improved Oil Recovery 2, 1027–1047. https://doi.org/10.2523/129887-ms.
Yu, J., Ge, Y., Cai, X., 2016. The desulfurization of magnetite ore by flotation with a mixture of xanthate and dixanthogen. Minerals 6 (3), 70. https://doi.org/10.3390/min6030070.
Yu, T., Halouane, F., Mathias, D., Barras, A., Wang, Z., Lv, A., Lu, S., Xu, W., Meziane, D., Tiercelin, N., Szunerits, S., Boukherroub, R., 2020. Preparation of magnetic, superhydrophobic/superoleophilic polyurethane sponge: separation of oil/water mixture and demulsification. Chem. Eng. J. 384, 123339. https://doi.org/10.1016/J.CEJ.2019.123339.
Yuan, B., Wang, W., Moghanloo, R.G., Su, Y., Wang, K., Jiang, M., 2017. Permeability reduction of berea cores owing to nanoparticle adsorption onto the pore surface: mechanistic modeling and experimental work. Energy Fuel. 31 (1), 795–804. https://doi.org/10.1021/acs.energyfuels.6b02108.
Yusoff, A.H.M., Salimi, M.N., Jamlos, M.F., 2018. A review: synthetic strategy control of magnetite nanoparticles production. Adv. Nano Res. 6 (1), 1–19. https://doi.org/10.12989/anr.2018.6.1.001.
Zaid, H.M., Latiff, N.R.A., Yahya, N., Soleimani, H., Shafie, A., 2014. Application of electromagnetic waves and dielectric nanoparticles in enhanced oil recovery. J. Nano Res. 26, 135–142. https://doi.org/10.4028/www.scientific.net/JNanoR.26.135.
Zargartalebi, M., Barati, N., Kharrat, R., 2014. Influences of hydrophilic and hydrophobic silica nanoparticles on anionic surfactant properties: interfacial and adsorption behaviors. J. Petrol. Sci. Eng. 119, 36–43. https://doi.org/10.1016/j.petrol.2014.04.010.
Zhang, B., Daigle, H., 2017. Oil-soluble contrast agents for NMR. In: SPWLA 58th Annual Logging Symposium. Society of Petrophysicists and Well-Log Analysts, p. 12 (https://doi.org/).
Zhang, S., Han, X., 2018. Effect of different surface modified nanoparticles on viscosity of nanofluids. Adv. Mech. Eng. 10 (2) https://doi.org/10.1177/1687814018762011, 168781401876201.
Zhang, Z., Wang, Z., He, S., Wang, C., Jin, M., Yin, Y., 2015. Redox reaction induced Ostwald ripening for size- and shape-focusing of palladium nanocrystals. Chem. Sci. 6 (9), 5197–5203. https://doi.org/10.1039/c5sc01787d.
Zhao, X., Shi, Y., Wang, T., Cai, Y., Jiang, G., 2008. Preparation of silica-magnetite nanoparticle mixed hemimicelle sorbents for extraction of several typical phenolic compounds from environmental water samples. J. Chromatogr. A 1188 (2), 140–147. https://doi.org/10.1016/j.chroma.2008.02.069.
Zhou, J., Qiao, X., Binks, B.P., Sun, K., Bai, M., Li, Y., Liu, Y., 2011. Magnetic pickering emulsions stabilized by Fe 3O 4 nanoparticles. Langmuir 27 (7), 3308–3316. https://doi.org/10.1021/la1036844.
Zhou, J., Wang, L., Qiao, X., Binks, B.P., Sun, K., 2012. Pickering emulsions stabilized by surface-modified Fe 3O 4 nanoparticles. J. Colloid Interface Sci. 367 (1), 213–224. https://doi.org/10.1016/j.jcis.2011.11.001.
Zhou, K., Zhou, X., Liu, J., Huang, Z., 2020. Application of magnetic nanoparticles in petroleum industry: a review. J. Petrol. Sci. Eng. 188, 106943. https://doi.org/10.1016/j.petrol.2020.106943.
Zhu, M.T., Feng, W.Y., Wang, B., Wang, T.C., Gu, Y.Q., Wang, M., Wang, Y., Ouyang, H., Zhao, Y.L., Chai, Z.F., 2008. Comparative study of pulmonary responses to nano- and submicron-sized ferric oxide in rats. Toxicology 247 (2–3), 102–111. https://doi.org/10.1016/j.tox.2008.02.011.
Zhu, C., Ko, S., Daigle, H., Zhang, B., 2018. NMR relaxation of surface-functionalized Fe304 nanoparticles. Petrophysics 59 (3), 407–417. https://doi.org/10.30632/PJV59N3-2018a8.
Zolfaghari, R., Fakhru'l-Razi, A., Abdullah, L.C., Elnashaie, S.S.E.H., Pendashteh, A., 2016. Demulsification techniques of water-in-oil and oil-in-water emulsions in petroleum industry. In: Separation and Purification Technology, vol. 170, pp. 377–407. https://doi.org/10.1016/j.seppur.2016.06.026.